AQUEOUS ELECTRON INITIATED DESTRUCTION OF PER- AND POLYFLUOROALKYL SUBSTANCES IN AQUEOUS MEDIA BY ULTRAVIOLET-LIGHT ACTIVATED SULFITE/IODIDE SYSTEM

DESTRUCTION AQUEUSE INITIÉE PAR ÉLECTRONS DE SUBSTANCES PER- ET POLYFLUOROALKYLE DANS DES MILIEUX AQUEUX PAR UN SYSTÈME SULFITE/IODURE ACTIVÉ PAR LA LUMIÈRE ULTRAVIOLETTE

A thesis submitted to the Division of Graduate Studies of

the Royal Military College of Canada

by

Natalia Maria O'Connor, B.Sc. Biology

In Partial Fulfillment of the Requirements for the Degree of Master of Applied Science

January 2024

Acknowledgements

First and foremost, I would like to thank my supervisors Dr. Kela Weber, Dr. Iris Koch and Dr. Kevin Mumford. This work would not have been possible without your guidance and mentorship. I am grateful for your support during the past two years as this work has evolved.

I would like to especially thank David Patch for his mentorship and support throughout every step of the journey. I am grateful for the unwavering support.

Thank you to Dr. Jennifer Scott for providing understanding into the mechanisms of this work.

To all at the Environmental Sciences Group who have helped me along the way I thank you, it has been a pleasure to gain valuable experience working with numerous talented and knowledgeable individuals.

I would like to thank Dr. Michael Bentel for providing deeper understanding pertaining to the roles of reactive species.

Thank you to Diana Noble and Taylor Veerecken for their invaluable assistance in the laboratory.

To my friends and family, I could not have made it through these past couple of years without your understanding and presence in my life.

Abstract

Per- and polyfluoroalkyl substances (PFAS) are a large class of synthetic aliphatic organofluorine compounds that are ubiquitous, recalcitrant, and linked to a growing number of toxicological effects. Characterized by their high proportion of carbon fluorine bonds, they all share a common perfluoroalkyl moiety CnF_2n. This structure lends PFAS many desirable properties, such as hydrophobicity, oiliphobicity, tensioactivity and high stability. PFAS were first manufactured in the 1930s and due to their desirable properties, they have found widespread usage in commercial and industrial applications. Commercial products such as makeup, fast food packaging, and textiles left in landfills leach PFAS into the environment. Massive quantities of PFAS are directly applied to the environment using aqueous film forming foam (AFFF) to extinguish fires. With the escalating global concern over PFAS contamination in water sources, there is a pressing need for technologies capable of complete mineralization of PFAS compounds, measured by both the loss of initial PFAS and quantitative recovery of resulting fluoride ions.

The overarching goal of this thesis was to develop an aqueous remediation technology capable of completely destroying PFAS that is efficient, cost-effective and has the potential to be scaled up to larger treatment volumes. This study investigated the efficacy of sulfite and iodide in a bicarbonate-buffered alkaline system, activated by ultraviolet (UV) light, for the destruction of PFAS. The UV/sulfite/iodide (UV/S+I) system creates a reductive environment by generating aqueous electrons that facilitate PFAS degradation. The extent of degradation and defluorination was examined for perfluorooctane sulfonic acid (PFOS), perfluorooctanoic acid (PFOA), 6:2 fluorotelomer sulfonic acid (6:2 FTS), and perfluorobutane sulfonic acid (PFBS).

Initial experiments employing the UV/S+I system achieved 100% degradation and over 90% defluorination for PFOS, PFOA, and 6:2 FTS, while incomplete degradation of PFBS was observed. Characterization of transformation products confirmed cleavage of carbon-carbon (C-C), carbon-sulfur (C-S), and carbon-fluorine (C-F) bonds resulting from aqueous electron attack. Based on an enhanced mechanistic understanding, a series of optimization experiments was conducted with the goal of achieving complete degradation of PFBS. The optimized protocol involved higher initial sulfite concentration and periodic addition of additional sulfite during UV-activation, resulting in 99.9% destruction and complete quantitative defluorination of PFBS.

Further investigations were undertaken to enhance understanding of the UV/S+I system for remediating PFAS in complex matrices. PFOS and 6:2 FTS solutions were supplemented with varying amounts of radical scavengers: butyl carbitol, isopropanol, methanol, and nitrate. These scavengers were chosen based on their relevance; butyl carbitol is commonly found in AFFF, methanol is the standard solvent for extracting PFAS from matrices, and nitrates are often present in water sources. Increasing concentrations of these scavengers resulted in reduced degradation and defluorination of PFOS and 6:2 FTS, though to varying degrees. Investigations into the UV/S+I system with these scavengers suggest that oxidizing species may contribute to further defluorination of PFAS. The efficacy of the UV/S+I

system was assessed using both legacy and modern AFFF formulations. Additionally, the system was further tested and improved by introducing a continuous drip-fed addition of sulfite to achieve the destruction of 600 mg/L PFBS. The continued exploration and refinement of the UV/S+I system hold promising potential for advancing the remediation of PFAS contaminants in diverse environmental matrices, offering a pathway towards more effective and sustainable treatment solutions in the future.

Résumé

Les substances per- et polyfluoroalkyles (PFAS) constituent une vaste catégorie de composés organofluorés aliphatiques synthétiques qui sont omniprésents, récalcitrants et liés à un nombre croissant d'effets toxicologiques. Caractérisés par leur forte proportion de liaisons carbone-fluor, ils ont tous en commun un groupement perfluoroalkyle $CnF¬2n$. Cette structure confère aux PFAS de nombreuses propriétés souhaitables, telles que l'hydrophobie, l'oléophobie, la tensioactivité et une grande stabilité. Fabriqués pour la première fois dans les années 1930, ils se sont largement répandus dans les applications commerciales et industrielles en raison de leurs propriétés avantageuses. Les produits commerciaux tels que le maquillage, les emballages de nourriture rapide et les textiles abandonnés dans les sites de décharge entraînent la lixiviation des PFAS dans l'environnement. De grandes quantités de PFAS sont directement répandues dans l'environnement par l'utilisation de mousse aqueuse formant un film (AFFF) pour éteindre les incendies. Étant donné que la contamination des sources d'eau par les PFAS suscite de plus en plus d'inquiétudes au niveau mondial, il est urgent de trouver des technologies capables de réaliser une minéralisation complète des composés PFAS, qui soit mesurée à la fois par la perte des PFAS initiaux et par la récupération quantitative des ions de fluorure qui en résultent.

Cette thèse avait pour objectif principal de développer une technologie de remédiation aqueuse capable de détruire complètement les PFAS, de manière efficace, économique et susceptible d'être mise à l'échelle pour des volumes de traitement plus importants. Dans le cadre de cette étude, l'efficacité du sulfite et de l'iodure dans un système alcalin tamponné au bicarbonate, activé par la lumière ultraviolette (UV), a été étudiée pour la destruction des PFAS. Le système UV/sulfite/iodure (UV/S+I) crée un environnement réducteur en générant des électrons aqueux qui favorisent la dégradation des PFAS. Le degré de dégradation et de défluoration a été examiné pour l'acide perfluorooctane sulfonique (PFOS), l'acide perfluorooctanoïque (PFOA), l'acide fluorotélomère sulfonique 6:2 (6:2 FTS) et l'acide perfluorobutane sulfonique (PFBS).

Lors des premières expériences utilisant le système UV/S+I, une dégradation de 100 % et une défluoration de plus de 90 % ont été obtenues pour le PFOS, le PFOA et le 6:2 FTS, tandis qu'une dégradation incomplète du PFBS a été observée. La caractérisation des produits de transformation a confirmé la rupture des liaisons carbone-carbone (C-C), carbone-soufre (C-S) et carbone-fluor (C-F) à la suite d'une attaque aqueuse par les électrons. Grâce à une meilleure compréhension du mécanisme, une série d'expériences d'optimisation a été menée dans le but d'obtenir une dégradation complète du PFBS. Le protocole optimisé comprenait une concentration initiale de sulfite plus élevée et l'ajout périodique de sulfite supplémentaire pendant l'activation UV, ce qui a permis d'obtenir une destruction à 99,9 % et une défluoration quantitative complète du PFBS.

Pour mieux comprendre la capacité du système UV/S+I à remédier les PFAS dans des matrices complexes, d'autres études ont été entreprises. Aux solutions de PFOS et de 6:2 FTS ont été ajoutées des quantités variables de capteurs de radicaux :

butylcarbitol, isopropanol, méthanol et nitrate. Ces agents ont été choisis en fonction de leur pertinence : le butylcarbitol est couramment présent dans les AFFF, le méthanol est le solvant standard pour l'extraction des PFAS des matrices et les nitrates sont souvent présents dans les sources d'eau. En augmentant les concentrations de ces agents de piégeage, la dégradation et la défluoration du PFOS et du 6:2 FTS ont été réduites, dans des proportions variables. Les recherches sur le système UV/S+I avec ces piégeurs suggèrent que les espèces oxydantes peuvent contribuer à une défluoration plus approfondie des PFAS. L'efficacité du système UV/S+I a été évaluée en utilisant des formulations AFFF anciennes et modernes. En outre, le système a été testé et amélioré en introduisant progressivement du sulfite afin d'obtenir la destruction de 600 mg/L de PFBS. Les explorations continues et le développement du système UV/S+I offrent la possibilité de faire progresser la remédiation des contaminants PFAS dans diverses matrices environnementales, offrant ainsi une voie vers des solutions de traitement plus efficaces et plus durables à l'avenir.

Co-authorship Statement

This thesis is written in manuscript (article-based) format. Natalia O'Connor is the sole author of Chapter 1, "Introduction", Chapter 2, "Literature Review", and Chapter 5, "Conclusions and Recommendations".

Chapter 3, "Forever no more: Complete mineralization of per- and polyfluoroalkyl substances (PFAS) using an optimized UV/sulfite/iodide system" was co-authored by Natalia O'Connor, David Patch, Diana Noble, Jennifer Scott, Iris Koch, Kevin Mumford, and Kela Weber. This work was published in Science of the Total Environment (STOTEN) in 2023. The results of this work were presented in ten main body figures, detailing the development of the work from initial development to the final system design. As the primary investigator, Natalia O'Connor was the main contributor towards experiment conceptualization, experimental design, method development, experimental investigation, formal analysis, writing, and visualization. Specifically, Natalia O'Connor developed the overall experimental concept and design for Figures 2-10, and directly performed the experiments for Figures 1, and 3-10, and provided direct supervision of Diana Noble, who performed the experiments for Figure 2 and assisted with Figures 6 and 7. David Patch contributed to the experimental conceptualization and design for Figure 1, with significant modifications by Natalia O'Connor. Instrumental analysis of the samples was performed by Natalia O'Connor, Diana Noble, and David Patch, with formal analysis of the generated data being performed by Natalia O'Connor. Data visualization was performed by Natalia O'Connor, David Patch, and Kevin Mumford, with additional input by Iris Koch and Kela Weber. Initial writing was performed by Natalia O'Connor, with literature review contributions by Diana Noble and David Patch. First rough draft edits and re-write was performed equally by Natalia O'Connor and David Patch. Second draft edits and writing were led by Natalia O'Connor, with input from David Patch, Iris Koch, Kevin Mumford, Jennifer Scott, and Kela Weber. Kela Weber also contributed towards project administration and funding acquisition.

Chapter 4, "Investigating the UV/Sulfite + Iodide System to Mineralize Per and Polyfluoroalkyl Substances (PFAS) in the Presence of Complex Matrices: Implications for Treatment of AFFF Concentrates" is unpublished work to be submitted for publication but is prepared in manuscript format for submission. The results of this work were presented in seven main body figures. As the primary investigator, Natalia O'Connor was the main contributor towards all aspects of the work except project administration and funding acquisition, which was led by Dr. Kela Weber, Dr. Iris Koch, and Dr. Kevin Mumford. Specifically, Natalia O'Connor developed the overall experimental concept and design for Figures 1-7, with input on Figure 3 from Michael Bentel, input from David Patch on Figure 4 and 6, and input from Dr. Kela Weber, Dr. Iris Koch, and Dr. Kevin Mumford. Natalia

O'Connor directly performed all the experiments for Figures 1-6, with the mechanistic data presented in Figure 7 developed equally by Natalia O'Connor, David Patch, Michael Bentel, and Jennifer Scott. Instrumental analysis of the samples was performed by Natalia O'Connor (fluoride) and David Patch (LC-HRMS), with formal analysis of the data being led by Natalia O'Connor, with assistance by David Patch and Michael Bentel. Data visualization was performed by Natalia O'Connor, with assistance from David Patch and templates developed by Kevin Mumford in Chapter 3. Initial writing, and first rough draft edits were performed by Natalia O'Connor. Second rough draft edits were led by Natalia O'Connor, with significant contributions from Michael Bentel and David Patch in the areas related to oxidative radical mechanisms. Additional rough drafts were circulated between Natalia O'Connor, David Patch, and Michael Bentel, with Natalia O'Connor finalizing the edits into a pre-thesis draft. Pre-thesis draft edits were performed by Kevin Mumford and Iris Koch, with contributions from Kela Weber. Incorporation of edits was performed by Natalia O'Connor, with formatting assistance from David Patch. While not listed as an author, Lauren Turner is acknowledged for templating/formatting assistance with conversion of Chapters 3 and 4 to the thesis format. Writing and formatting of the appendices were performed by Natalia O'Connor, with contributions from David Patch.

Table of Contents

List of Tables and Figures

List of Abbreviations

Acronym	Full name
AFFF	Aqueous film forming foam
ARA	Advanced reduction assay
CLPP	Community level physiological profiling
DGBE	Diethyl glycol monobutyl ether
ECF	Electrochemical fluorination
ECHA	European chemicals agency
FASAAs	N-Alkyl perfluoroalkane sulphonamido acetic acids
FASAs	Perfluoroalkane sulphonamides
FASEs	N-Alkyl perfluoroalkane sulphonamido ethanols
FFTA	Fire fighting training area
FtACs	Fluorotelomer acrylates
FtB	Fluorotelomer Betaines
FtCAs	Fluorotelomer carboxylic acids
FtIs	Fluorotelomer iodides
FtMACs	Fluorotelomer methacrylates
FtOHs	Fluorotelomer alcohols
FtOs	Fluorotelomer olefins
FTS	Fluorotelomer Sulfonates
FtSA	Fluorotelomer Sulfonic Acid
FtSAAM	Fluorotelomer Sulfonamido Amines
FtSaB	Fluorotelomer Sulfonamido Betaines
FtSOAOS	Fluorotelomer Sulfonyl Amido Sulfonate
FtTAOS	Fluorotelomer Thioamido Sulfonates
FtTHN	Fluorotelomer Thiohydroxy Ammonium
FtTP	Fluorotelomer thioether proprionate
FtUCAs	Fluorotelomer unsaturated carboxylic acids
GC/MS	Gas chromatography mass spectrometry
HRAM/MS	High resolution accurate mass mass spectrometry
MAC	Maximum acceptable concentration
MCL	Maximum contaminant limit
OECD	Organisation for Economic Co-operation
PAPs	Polyfluoroalkyl phosphates
PCTFE	Polychlorotrifluoroethylene
PFAA	Perfluoroalkyl acids
PFAAB	Perfluoroalkylamido Betaine
PFAIs	Perfluoroalkyl iodides
PFAS	Per and polyfluoroalkyl substances

PFBSs	Perfluoroalkyl sulphonic acids
PFCAs	Perfluoroalkyl carboxylic acids
PFECAs	Perfluoroether carboxylic acids
PFESAs	Perfluoroether sulphonic acids
PFOA	Perfluorooctanoic acid
PFOS	Perfluorooctane sulfonate
PFPAs	Perfluoroalkyl phosphonic acids
PFPIAs	Perfluoroalkyl phosphinic acids
PTFE	Polytertrafluoroethylene
qPCR	Quantitative polymerase chain reaction
RIS	Reactive iodine species
rRNA	Ribosomal RNA
SAMPAPs	Perfluorooctane sulphonamido ethanol-based phosphate esters
SDS	Sodium dodecyl sulfate
SPE	Solid phase extraction
TFE	Tetrafluoroethylene
TN	Total nitrate
TOC	Total organic carbon
TOP	Total oxidizable precursor
TROF	Total reducible organic precursor
USEPA	United States Environmental Protection Agency
WAX	Weak anion exchange
WWTP	Wastewater treatment plants

1. Introduction

1.1 Background

Per and polyfluoroalkyl substances (PFAS) are a large class of synthetic organofluorine compounds extensively employed in manufacturing since the 1950s due to their desirable properties. PFAS encompass a diverse group of fluorinated compounds with varying chemical structures, all sharing a common perfluoroalkyl moiety, represented as C_nF_{2n}.(Buck et al., 2011a). The carbon fluorine bond, characterized by the highest bond dissociation energy in organic chemistry, derives its strength from fluorine, as the most electronegative element, resulting in a highly polar carbon fluorine bond. The chemical structure of PFAS imparts high stability, tensioactivity, hydrophobicity, and oleophobicity (Naidu et al., 2020). These features, contributing to the robustness and versatility of PFAS, have led to their ubiquitous utilization in diverse industrial and commercial applications. However, the usage of PFAS in a variety of commercial and industrial products have also resulted in their widespread contamination of environmental and biological systems throughout the world (Wang et al., 2014a, 2014b). PFAS have been linked to several negative health effects including increased cancer risk, alterations to metabolism, and potential neurotoxicity and immunotoxicity (Barry et al., 2013; Boisvert et al., 2019; Rappazzo et al., 2017; Suja et al., 2009; Sunderland et al., 2019a). To address these concerns, governments have implemented restrictions on the safe levels of PFAS that can be present in drinking water, soil, and groundwater. Canada has recently proposed a draft drinking water guideline of 30 parts per trillion (ppt) for a sum of PFAS detected in drinking water (Southerland and Birnbaum, 2023) (Health Canada 2023).

To address these low PFAS guidelines in drinking water, significant effort is being made to develop effective treatment technologies capable of removing PFAS from aqueous matrices. These technologies, broadly, either remove PFAS from water by transferring it onto/into a new material (sorption), or by destroying the molecules themselves into innocuous byproducts, which is advantageous as it avoids the generation of secondary waste streams. There are several destructive treatment technologies that have been studied for treating PFAS-impacted waters, including hydrothermal, super/subcritical water oxidation, sonolysis, gamma irradiation, electron beam irradiation, and ultraviolet light irradiation. The use of ultraviolet light (typically 254 nm) is of particular interest because it can be tuned to destroy the contaminant of interest based on the selected photosensitizer and aqueous system conditions. The two most common methods of operation for UV-activated processes are UV-advanced oxidative processes (UV-AOP) and UV-advanced reductive processes (UV-ARP).

Research efforts in UV-ARP has investigated different photosensitizers for destroying PFAS, including sulfite, and/or iodide. Current efforts have achieved

near-complete destruction of long-chain PFAS, such as PFOS and PFOA, in under eight hours using a combined UV-activated sulfite/iodide system but can only achieve ~80% destruction of PFBS over a 24-hour period (Liu et al., 2022; O'Connor et al., 2023). Additional research is required to better understand the interactions between different photosensitizers and how they can be optimized to further improve destruction in simple (DI water) and increasingly complex (groundwater, aqueous film forming foam/AFFF) matrices.

1.2 Objectives

The goal of this research is to develop and optimize a UV-activated reduction system capable of achieving complete destruction of PFAS in aqueous matrices. Using a benchtop 36-watt, 254 nm UV lamp, the destruction of PFAS in aqueous matrices is evaluated in two phases. In the first phase, the destruction of PFAS amended in DI water is investigated with consideration of factors including photosensitizer types, concentrations, ratios, and additional timing/intervals. Several complementary analytical techniques are used to evaluate the efficacy of the UV-reduction technology, including liquid-chromatography tandem mass spectrometry (LC-MS/MS), LC-high resolution Orbitrap™ MS (LC-HRMS), and fluoride ion selective electrode (F-ISE). The second phase, the destruction of PFAS in complex matrices, i.e. AFFF, is investigated with consideration of organic matter content competition and scaling up the system. The overall research objectives were to:

1. Develop a UV light-activated reductive system capable of degrading and defluorinating a suite of PFAS from different classes.

2. Evaluate the effect of complex matrices, including the impact of various scavengers, higher concentrations of PFAS present, and larger volume scales on the effectiveness of the UV-ARP system at degrading and defluorinating a suite of PFAS.

1.3 Thesis Organization

This thesis is presented in a manuscript style, consisting of five chapters plus two appendices, as listed below.

Chapter 1 offers a brief background on the research topic, objectives, and structure of the thesis.

Chapter 2 provides a literature review of the background information of the thesis, including information on PFAS, UV-reductive technologies, and their applications in destroying PFAS.

Chapter 3 provides a detailed investigation of an optimized UV-sulfite/iodide system for the remediation of PFAS in DI water at multiple volume scales.

Chapter 4 provides a detailed investigation into the resilience of the UV-sulfite/iodide system in the presence of several aqueous electron scavengers and evaluating further optimization for the destruction of high concentrations of PFAS in DI water and AFFF.

Chapter 5 summarizes the overall outcomes of the thesis and provides recommendations for future work.

Appendix A contains supplemental information for Chapter 3.

Appendix B contains supplemental information for Chapter 4.

2. Literature Review

2.1 Per- and Polyfluoroalkyl Substances

First developed in the 1950's, per- and polyfluoroalkyl substances (PFAS) are a large and growing class of organofluorine compounds that are used heavily in industrial and commercial processes. The current definition of what constitutes the PFAS molecule is the presence of a single $-CF_3$ moetie or repeating $-CF_2$ moeties (Wang et al., 2021). Under this definition, PFAS can be grouped into two major categories: polymeric, and non-polymeric. Polymeric PFAS, like polytetrafluoroethylene (PTFE), are not typically of concern, but can have residual non-polymeric PFAS present, which are of concern. When PFAS are discussed in the environmental context, the focus is typically on non-polymeric PFAS, such as perfluorooctanoic acid (PFOA) or perfluorooctane sulfonic acid (PFOS). Non-polymeric PFAS are classically understood to be molecules with a high proportion of C-F bonds, and one (or more) functional chemical groups that bestow upon its different chemical properties. The carbon fluorine bond, well understood to be the strongest bond in organic chemistry, provides PFAS with a high degree of thermal and chemical resistance. When coupled with a non-fluorinated functional group, PFAS exhibit addition unique properties, such as a high degree of tensioactivity, hydrophobicity, and oleophobicity (Naidu et al., 2020). These features, contributing to the robustness and versatility of PFAS, have led to their ubiquitous utilization in diverse industrial and commercial applications.

The ability to confer oil, water, and stain resistance, coupled with the chemical and thermal stability of PFAS, makes them highly sought-after characteristics for commercial manufacturers and industrial processes. PFAS find widespread use across various industries, including food packaging, textiles, cosmetics, electronics, automotive, medical products, varnishes, and firefighting foams (Buck et al., 2021). However, the very properties that make PFAS desirable, pose environmental challenges when released during product disposal or spills (Cousins et al., 2020).

As consumer products reach the end of their lifecycle, they often end up in landfills, incinerators, and wastewater treatment plants, releasing PFAS over time (Stoiber et al., 2020). Industrial plants contribute to PFAS contamination by discharging waste into waterways and emitting PFAS into the air (Abunada et al., 2020). Consequently, PFAS contamination has become a global issue, with numerous PFAS compounds detected in groundwater, drinking water, soils, sediments, and sludge worldwide (Banzhaf et al., 2017; Kim and Kannan, 2007; Pickard et al., 2020; Vedagiri et al., 2018; Zacs and Bartkevics, 2016). Elevated levels of PFAS have been found in the bloodstream of people globally, including Americans, and in diverse ecosystems, from agricultural plants to aquatic wildlife, amphibians, birds, and mammals, even in remote arctic environments (Pickard et al., 2022).

This poses a huge environmental and health risk as PFAS have been found to be carcinogenic, immunotoxic, metabolism altering, and to possess potential neurotoxic effects (Barry et al., 2013; Boisvert et al., 2019; Rappazzo et al., 2017; Suja et al., 2009; Sunderland et al., 2019a). This is compounded by the fact that PFAS are very bioaccumulative and not biodegradable (Abercrombie et al., 2019; Coggan et al., 2019; Suja et al., 2009). These findings have prompted governments around the world to implement bans on certain PFAS to be manufacturing and guidelines for drinking water level concentrations (Abunada et al., 2020; Glüge et al., 2020; Longpré et al., 2020; Okazoe, 2009). In response to these bans and following a voluntary phase-out of C8 PFAS, a number of chemical manufacturing companies produced novel fluorinated compounds that have the same C-F bonds with different insertions and functional groups. However, these novel precursor congeners have been found to transform abiotically and biotically in the environment and *in-vivo* (Harding-Marjanovic et al., 2015a; Joudan and Mabury, 2022; Lee and Mabury, 2014; Li et al., 2019; Liu and Liu, 2016; Liu et al., 2010; Remde and Debus, 1996; Ruan et al., 2015). The terminal transformation products are retaining the same recalcitrant, bioaccumulative properties as the banned PFAS compounds, with some of the transformations resulting in the formation of banned compounds (Butt et al., 2014; D'Agostino and Mabury, 2014; Joudan and Mabury, 2022; Lee and Mabury, 2014; Yeung and Mabury, 2013). A few of the legacy PFAS which have been regulated such as, perfluoroalkyl octane sulfonate (PFOS) and perfluoroalkyl octanoic acid (PFOA) may end up as potential transformation end products (Dombrowski et al., 2018a; Suja et al., 2009). There is a large and growing lack of knowledge of how these compounds behave in the environment and their toxicity.

The investigation of PFAS fate, transport, remediation, and toxicity is a crucial subject, with far-reaching implications for the health of both wildlife and the human population (Rappazzo et al., 2017; Toms et al., 2019). One of the largest, direct sources of PFAS release into the environment is through the use of aqueous film forming foam (AFFF) to extinguish hydrocarbon fueled fires (Harding-Marjanovic et al., 2015a; Houtz et al., 2016, 2013; Milley et al., 2018; Nickerson et al., 2021; Yi et al., 2018). An important component of AFFF is PFAS due to their surfactant-type nature and heat resistance. Massive amounts of AFFF are used when extinguishing a fuel-based fire, resulting in significant concentrations of PFAS entering the environment.

The PFAS compounds present in AFFF often consist of long carbon chains and highly variable substitution chemistry, making them prone to adsorption to the soil. The remaining PFAS persist, and PFAS precursors transform into their terminal end products, many of which are legacy PFAS subject to existing bioaccumulation-based regulations. (D'Agostino and Mabury, 2014; Joudan and Mabury, 2022; Li et al., 2019). In instances where AFFF contains short-chain PFAS or long-chain PFAS transforms into shorter-chain counterparts, these compounds may migrate to lower

soil horizons and eventually reach the water table (Bolan et al., 2021; Brusseau et al., 2020; Liu and Liu, 2016; Liu et al., 2010; Shahsavari et al., 2021). The soil retentions of anionic, zwitterionic, and cationic PFAS compounds differ due to electrostatic and hydrophobic interactions (Backe et al., 2013; Martin et al., 2019; Nickerson et al., 2021). The remaining PFAS will persist, and PFAS precursors may transform into their terminal end products, many of which are legacy PFAS subject to existing bioaccumulation-based regulations. (Harding-Marjanovic et al., 2015a; Masoner et al., 2020; Yi et al., 2018).

2.2 History of PFAS

The initial synthesis of an organofluorine compound occurred in 1835 when Dumas et al. successfully produced methyl fluoride from dimethyl sulfate (Eq 1.) (Surya Prakash and Wang, 2012).

$$(CH_3O)_2SO_2 + 2KF \rightarrow 2CH_3F + K_2SO_4 \tag{1}$$

Organofluorine compounds were being prepared in the 19th century, even though elemental fluorine had not yet been isolated. Despite numerous attempts by various chemists, it was not until 1886 that Moissan successfully isolated fluorine. This achievement involved electrolyzing a melt mixture of potassium hydrogen difluoride and hydrogen fluoride to produce elemental fluorine. Following Moissan's breakthrough, there were minimal developments in organofluorine chemistry until the 1920s due to the unstable and hazardous nature of corrosive reagents. In 1928, spurred by the General Motors Corporation's quest for inert refrigerants for manufacturing refrigerators, a breakthrough occurred. $CCl2F2$, later known as Freon® -113, was synthesized using $CCl4$ and $SbF3$. Recognizing its potential, General Motors collaborated with E. I. du Pont de Nemours & Company (DuPont) to manufacture the compound. This collaboration led to the production of the first fluoropolymer, polychlorotrifluoroethylene (PCTFE), achieved through the dechlorination of Freon® -113 (Conte and Gambaretto, 2004; Okazoe, 2009).

Initially, early fluorinated polymers were prohibitively expensive for widespread manufacturing and market entry. The challenging nature of working with fluorine posed obstacles for chemists, and it wasn't until World War II that significant progress occurred in their development. The first notable application of fluoropolymers took place during the Manhattan Project for the production of the atomic bomb. Joseph Simons, a chemical engineer associated with the project, introduced a large-scale method for industrial fluorocarbon production known as electrochemical fluorination (ECF), or the Simons process. (Conte and Gambaretto, 2004).

In brief, the ECF process involves electrolyzing an organic substance (*e.g.*, octane sulfonyl fluoride, $C_8H_{17}SO_2F$) within anhydrous hydrogen fluoride at cell voltages

of 5-6 V. This results in the replacement of all hydrogen atoms with fluoride atoms. In 1948, Simons, along with two others from the Minnesota Mining & Manufacturing Company (3M), filed a patent for the ECF process to produce fluorocarbons. (Wang et al., 2014c). Another significant development, telomerization, was reported by Haszeldine in 1950. Telomerization involves reacting a perfluoroalkyl iodide with tetrafluoroethylene (TFE), with subsequent reaction with ethylene to produce building blocks for a range of fluorotelomer-based surfactants and polymers (Environmental Working Group (EWG), 2019).

In 1951, 3M established the first manufacturing plant for fluorocarbons, marking a milestone in the industry's growth. With continued advancements in ECF, the fluorocarbon product line expanded to include perfluoroethers, perfluoroacyl fluorides, perfluoroalkanesulfonyl fluorides, and perfluorinated amines.

2.3 Classifications of PFAS

PFAS represent a diverse class of chemicals comprising various families with numerous isomers and homologous congeners. The prefix 'per-' in perfluoroalkyl substances indicates the replacement of all hydrogen atoms on the carbon chain with fluorine, except for hydrogen atoms where substitution would fundamentally alter functional groups. On the other hand, 'poly-' signifies that only some of the hydrogen atoms have been replaced with fluorine. (Buck et al., 2021, 2011a; Wang et al., 2014c). Perfluoroalkyl moieties are commonly designated by the formula $C_nF_{2n+1}-$. Among PFAS compounds, per- and polyfluorocarboxylic acids (PFCAs) and per- and polyfluoroalkyl sulfonic acids (PFSAs) are extensively studied in literature. However, the vast array of congeners includes various groups, and novel compounds are continually being identified (Table 2.1). PFAS are commonly categorized as "short-chain" or "long-chain" based on their bioaccumulation/bioconcentration potential (Buck et al., 2021).

The Organisation for Economic Co-operation and Development (OECD) defines PFCAs with eight carbons or more and PFSAs with six carbons or more as "long-chain". The first paper attempting to harmonize and unify classifications was published by Buck *et al.* in 2011 (Buck et al., 2011a). Three general categories were established: nonpolymer perfluoroalkyl substances; nonpolymer polyfluoroalkyl substances; and fluoropolymers, perfluoropolyethers, and side-chain fluorinated polymers. In 2018 the OECD reported 4730 PFAS were assigned to eight different structure categories. Perfluoroalkyl carbonyl compounds (11% of PFAS listed), perfluoroalkane sulfonyl compounds (13%), perfluoroalkyl phosphate compounds (1%), fluorotelomer-related compounds (40%), per- and poly-fluoroalkyl ether-based compounds (8%), other PFAA precursors and related compounds – perfluoroalkyl ones (7%), other PFAA precursors or related compounds – semifluorinated (6%), and fluoropolymers (6%). Within each category, numerous

homologues exist, each differing by -CF2 moieties, and various isomers further complicate considerations related to applications, environmental transport, analysis, and toxicological concerns.

Table 2.1. A list of PFAS compounds. (Adapted from Nakayama et al., 2019)

Group Name	Acronym
Perfluoroalkyl sulphonic acids	PFBSs
Perfluoroalkyl carboxylic acids	PFCAs
Perfluoroalkyl phosphonic acids	PFPAs
Perfluoroalkyl phosphinic acids	PFPiAs
Perfluoroalkane sulphonamides	FASAs
N-Alkyl perfluoroalkane sulphonamido acetic acids	FASAAs
N-Alkyl perfluoroalkane sulphonamido ethanols	FASEs
Perfluoroalkyl iodides	PFAIs
Perfluoroether sulphonic acids	PFESAs
Perfluoroether carboxylic acids	PFECAs
Perfluorooctane sulphonamido ethanol-based phosphate esters	SAmPAPs
Cyclic perfluoroalkyl sulphonic acids	Cyclic PFSAs
Fluorotelomer sulphonic acids	FtSAs
Fluorotelomer carboxylic acids	FtCAs
Fluorotelomer unsaturated carboxylic acids	FtUCAs
Fluorotelomer olefins	FtOs
Fluorotelomer alcohols	FtOHs
Fluorotelomer iodides	FtIs
Fluorotelomer acrylates	FtACs
Fluorotelomer methacrylates	FtMACs
Polyfluoroalkyl phosphate monoesters	monoPAPs
Polyfluoroalkyl phosphates diesters	diPAPs

2.4 PFAS Used for Commercial and Industrial Applications

PFAS find widespread use in commercial and industrial applications, capitalizing on their unique properties (Glüge et al., 2020). Work by Wang *et al.* identified the global emissions of C4-C14 PFCAs from 1950 to 2015, identifying upwards of 21,000 tonnes emitted over the 65-year period (Wang et al., 2014c). Many authors have since published on the tonnage usage of PFAS across a variety of industrial sectors. Work by Gluuge *et al.* explored the utilization of polymeric and non-polymeric PFAS in Sweden, Finland, Norway, and Denmark from 2000 to 2017. Plastic and rubber production emerged as the predominant source of polymeric PFAS, primarily due to the synthesis of polytetrafluoroethylene (PTFE) (Glüge et al., 2020). Meanwhile, the electronics industry ranked highest in the consumption of non-polymeric PFAS. Additionally, close to 500 tonnes of non-polymeric PFAS were identified in the fire extinguishing and flame-retardant category, primarily used for firefighting applications, representing a major potential source of direct environmental release. Among various sources of incidental release, PFAS release from landfill leachate is of significant concern. (Lang et al., 2017; Masoner et al., 2020). Unlined landfills allow PFAS to leach directly through the soil into groundwater, where they can migrate through the water table. In contrast, lined landfills collect leachate and may either treat it on-site, send it to wastewater treatment plants (WWTP), or direct it to evaporation ponds. Lang *et. al.* investigated leachate from landfills and estimated the total volume of leachate produced in the United States to be 61.1 million m^3. The majority (79%) of this leachate originated from landfills in wet climates (with precipitation exceeding 75 cm/year). In 2013, an estimated 563 to 638 kg of PFAS generated from U.S. landfill leachate was sent to WWTPs. Notably, 5:3 fluorotelomer carboxylic acid (FtCA) exhibited the highest concentrations in most leachate samples (Lang et al., 2017).

2.5 PFAS in the Environment

The primary sources of PFAS release into the environment include industrial facilities engaged in the production, processing, or utilization of PFAS in manufacturing processes, waste management facilities like landfills, sites involved in the production of biosolids and their application, and locations where Class B fluorine-containing Aqueous Film Forming Foam (AFFF) is stored or released. (Houtz et al., 2016; Hutchinson et al., 2020; Masoner et al., 2020; Wang et al., 2018). The types and quantities of PFAS released can vary based on their source, ultimately depositing in various environmental systems (Brusseau et al., 2020). Numerous studies have identified PFAS in diverse matrices, including aqueous systems (groundwater, surface water, marine environments, etc.), solid systems (soil, sediment, plants, etc.), and atmospheric systems (Backe et al., 2013; Houtz et al., 2013; Lesmeister et al., 2021; Liu et al., 2020; Martin et al., 2019; Pickard et al., 2020; Zacs and Bartkevics, 2016).

Well water and tap water have been found to have relatively higher concentrations of PFAS compared to other water sources such as bottled water and raw water (Jian et al., 2017; Kleywegt et al., 2020). PFAS have even been detected in Arctic ice near Norway, with compounds released from melting ice cores reaching surface snow, river water, and the ocean. (Kwok et al., 2013). Work by Banzhaf *et al.* found average concentrations of PFAS in surface water (112 ng/L), groundwater (49 ng/L), and in the background screening lakes (3.4 ng/L) of Sweden. PFOS concentrations in groundwater varied significantly between samples taken from a FFTA at an airport (2700 - 2 910 000 ng/L) and samples taken from a suburb (42 200 ng/L) (Banzhaf et al., 2017).

A comprehensive review of PFAS detected in soils was conducted by Brusseau *et al.* across all continents in both urban and rural regions (Brusseau et al., 2020). Samples were taken from three types of sites: background, primary-source (manufacturing plants & FFTAs), and secondary-source (irrigation water use and biosolids application). PFAS were found in soil at almost every site. Concentrations of PFAS in soil are usually orders-of-magnitude higher than average concentrations found in groundwater. Highest concentrations found were of PFOS in FFTAs in Australia at a maximum of 460 000 µg/kg. PFAS have also been detected in the atmosphere. Atmospheric deposition plays a critical role in reincorporating PFAS into the water system, causing PFAS contamination to be identified in locations far removed from PFAS point sources. Persaud *et al.* observed a general trend of decreasing PFAS deposition with increasing latitude. (Pickard et al., 2020). Liu *et al*. identified unknown precursors in background soil sites due to atmospheric deposition during the study of AFFF impacted sites. While PFAS migration in AFFF-impacted soils was limited horizontally, vertical transfer through the soil occurred. Airports, where AFFF is used and stored, have been investigated as potential sources of PFAS (M. Liu et al., 2022). Milley *et al.* found 152 to 420 airport sites which may be impacting nearby surface waters in Canada (Milley et al., 2018). PFAS can undergo transport, eventually entering human or animal systems where they can bioaccumulate and potentially cause toxicological effects. (Trudel et al., 2008).

2.6 Aqueous Film Forming Foam (AFFF) Formulations

D'Agostino *et al*. investigated the presence of PFAS in AFFF formulations. Research was focused on Canadian AFFFs, collecting samples from Toronto, Cobourg, Maxville, and Eastern Ontario. These AFFFs were made by numerous manufacturers in the early 2000s including Hazard Control Tech, Angus Fire, 3M, Ansul, and Mason Chemical. Mabury identified a number of complex PFAS molecules, often functionalized with a variety of groups including, amines, amides, betaines, esters, ethers, thiols, sulfonates (D'Agostino and Mabury, 2014).

Backe *et al.* identified twenty-six zwitterionic, cationic, and anionic PFAS through the characterization of groundwater taken from US military bases. Similar to those identified by D'Agostino, many of the PFAS were highly functionalized with a number of different chemical groups. The high degree of chemical functionalization results in complex fluorinated compounds (i.e. 6:2 fluorotelomer sulfonamido betaine) which can potentially transform in the environment (Backe et al., 2013).

PFAA precursors present in AFFF impacted groundwater and soil was investigated by Houtz *et al.* The PFAS in the stock concentrate of 3M (1988-2001), Chemguard (2008, 2010), Ansul (1986-2010), Buckeye (2009), and National Foam (2005-2008) were quantified. PFSAs, PFCAs and perfluoroalkyl amido amides & amines were the main components found in 3M. FtTAoS congeners were detected in Chemguard and Ansul. Congeners of FtBs were found in Buckeye. 6:2 FtSaB was found to be the principal component of National Foam (Houtz and Sedlak, 2012a).

Table 2.2. A selection of novel compound classes identified in various AFFFs in literature.

Group Name	Acronym
Fluorotelomer Sulfonic Acid	FtSA
Fluorotelomer Betaines	FtB
Fluorotelomer Sulfonamido Betaines	FtSaB
Perfluoroalkylamido Betaine	PFAaB
Fluorotelomer Sulfonamido Amines	FtSAAm
Fluorotelomer Thioamido Sulfonates	FtTAoS
Fluorotelomer Sulfonyl Amido Sulfonate	FtSoAoS
Fluorotelomer Thiohydroxy Ammonium	FtTHN

The PFAS compounds found in these AFFFs have been found to enter the environment following AFFF application. Once in the environment, these PFAS undergo complex transport phenomena based on their physicochemical properties and their interactions with co-contaminants, water saturation, and trapped gas[51].
Depending on the hydrogeological properties of the area, these PFAS will typically sorb to soil, especially to clay and organic-rich soil types (Barzen-Hanson et al., 2017a). They can also enter into the groundwater and eventually end up in fresh or marine water systems, where they will accumulate in organisms including fish, birds, and mammals. Regardless of their fate, these PFAS can undergo transformation, adding further complexity to evaluating their fate, transport, and toxicity (Li et al., 2019).

2.7 Biological Transformation of PFAS

PFAS have been documented to transform into terminal PFAS products biotically and to a lesser extent abiotically in the environment. Abiotic transformations of PFAS typically involve reactions with oxygen (oxidation) or water (hydrolysis), with X:2 FTCAs being most susceptible to this reaction due to the single -CH_2 moiety, which can partake in an -HF elimination reaction (Wu et al. 2024).

A review by Butt *et al.* (2014) summarizes the transformation of fluorotelomers, including FtOH, FtCA, and diPaP, in a variety of environmental systems including soils, bacteria microcosms, rats, and fish. These fluorotelomers were found to have half lives in the ranges of minutes to weeks depending on the system. Fluorotelomers were also found to undergo a number of different types of transformations depending on the fluorotelomer chemistry and the system (Butt et al., 2014).

Work by Nabb *et al.* (2007) identified the half life and biotransformation of 8:2 FtOH across four different species, looking at mouse, rat, trout, and human hepatocytes, as well as mouse, rat, and human liver cells. The half life of 8:2 FtOH was found to range between 5 minutes and 7 days. 8:2 FtOH was found to be cleared from the rat system first, followed by the mouse system, then equally cleared by human and trout. Many transformation products were identified, including FtCAs, FtUCAs, and secondary fluorotelomer alcohols. Terminal PFCAs were identified as transformation products in rat and mouse systems, but not in human or trout, suggesting that FtOH transformation poses a higher risk to rodents than to humans (Nabb et al., 2007).

Work by Weiner *et al.* (2013) identified the biodegradation of fluorotelomermercaptoalkylamido sulfonate in aerobic sludge. A variety of PFAS intermediate products were identified, including FtSH, FtSAS-SO, and FtOH (Weiner et al., 2013). These intermediate products eventually underwent further transformation, resulting in the formation of PFCA terminal products.

Yi *et al.* (2018) investigated the biotransformation of 6:2 fluorotelomer thioether amido sulfonate (6:2 FtTAoS) in anaerobic sulfate-reducing microcosms. 6:2 FtTAoS was found to undergo significant transformation into a number of intermediate products before finally degrading into 6:2 fluorotelomer thioether propionate (6:2 FtTp). It is possible that 6:2 FtTp would undergo continued transformation into PFCAs in an aerobic system. The formation of terminal PFCA products is typically found in aerobic systems, as this is a result of oxidative degradation (Yi et al., 2018).

Lee *et al.* (2010) simulated a WWTP system using sludge to investigate PAPs in an aerobic microbial system. Previous work has shown that PAPs degrade to PFCAs in a rat model. This study demonstrated that 6:2 mono and diPAPs have the potential

to transform into 6:2 FtOH through microbial hydrolysis of 6:2 monoPAP. 6:2 FtOH is the most commonly studied precursor. Pathways in the literature suggest 6:2 FtOH transforms into 6:2 FtCA through oxidation. 6:2 FtCA is postulated to transform into PFHpA through oxidation of α-carbon to form odd chain PFCAs. Literature has suggested 6:2 FtUCA may undergo hydroxylation, oxidation, and decarboxylation to form 5:2 ketone. Lee *et al.* proposed fluorotelomer precursors transform predominantly through β-oxidation-like mechanisms. β-oxidation is known for hydrocarbon fatty acid metabolism. However, they also detected odd-chain PFCAs which suggest other pathways may be possible (Lee et al., 2010).
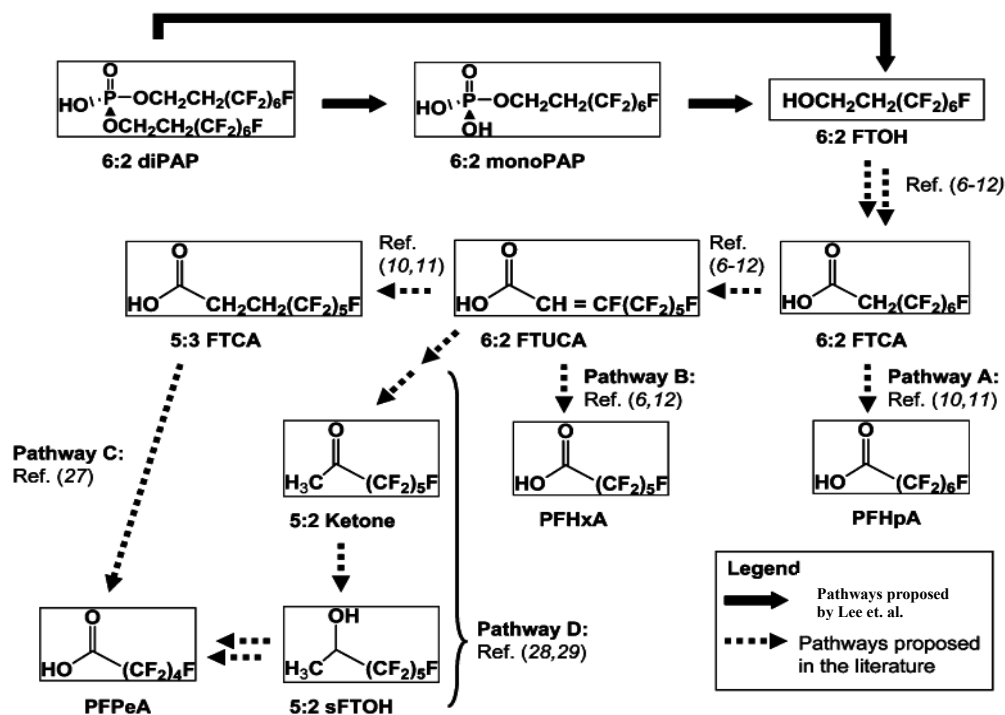
Figure 2.1 Proposed biotransformation pathway of 6:2 diPAP by Lee *et al.* represented with solid lines. Dashed lines represent transformation pathways proposed in the literature (Lee et al., 2010).

The biotransformation of PFAS in sludge and soil systems is caused by the presence of soil microbes, as numerous biotransformation studies have found limited transformation in sterilized microcosm systems. Identification of soil microbes and their role in biotransformation is therefore critical to understand the extent of potential PFAS degradation.

2.8 UV-Activated Reductive Remediation of PFAS-Impacted Aqueous Matrices

Several technologies have been developed to destroy PFAS, including bioremediation, sonochemical destruction, incineration, smoldering, mechanochemical degradation, gamma/electron beam radiolysis, and UV-activated oxidation or reduction technologies (Bentel et al., 2019; Hori et al., 2008, 2005; Houtz and Sedlak, 2012b; Lassalle et al., 2021; Merino et al., 2016; Patch et al., 2022; Trojanowicz et al., 2020, 2019a, 2018; Tseng, 2012; Zhang et al., 2014). When applied to the treatment of PFAS-impacted water, the most successful techniques are ones that can achieve complete defluorination of PFAS rapidly, with the most effective use of resources. Technologies that fit this criterion are ones that often enable a reductive aqueous environment, like UV-activated advanced reduction systems (UV-ARP) (Bruton and Sedlak, 2017; Yang et al., 2020). These systems utilize UV-light to activate reducing agent photosensitizers, which generate signicant amounts of aqueous electrons and other reactive radical species. However, one of the challenges of UV-ARP systems is the susceptibility of the aqueous electrons to being quenched by radical scavengers like dissolved oxygen and protons (Bentel et al., 2020, 2019b Patch et al., 2022). To avoid this, UV-ARP systems are typically operated at alkaline pHs (pH >9) and are purged of dissolved oxygen, either manually (e.g. N_2 purging) or chemically (e.g. addition of dissolved oxygen scavengers). One of the most important variables in UV-ARP studies is the specific selection of photosensitizer, as this directly influences the radical chemistry that is possible within the aqueous system.

Several different photosensitizers have been investigated in UV-ARP systems, including iodide (Park et al., 2011, 2009; Vecitis et al., 2009), sulfite (Abusallout et al., 2021; Bentel et al., 2020a; Tenorio et al., 2020), indoles (Kugler et al., 2021; Wang et al., 2023), and phenol (Gu et al., 2017; Jortner et al., 1963). The UV/iodide system has been found to achieve moderate destruction of PFAS, with significant formation of several fluorinated transformation products, including iodine-substiuted fluorocarbons (Park et al., 2009). Despite the effective degradation of PFAS in the UV/iodide system, the need to manually remove oxygen from the system, and the formation of reactive iodine species that diminish the effectiveness of the system (Burgess and Davidson, 2012; Park et al., 2011) are two limiting factors.

To avoid these limitations, many authors have investigated PFAS destruction using the UV/sulfite system, which can remove dissolved oxygen directly from the system because of side reactions with generated sulfite radicals, and the byproducts of the reaction (e.g. sulfate) do not interfere with the system chemistry. UV/sulfite has been used to degrade a broad range of PFAS, including PFCAs, PFSAs, flurootelomers, and GenX (Abusallout et al., 2021; Bao et al., 2018; Bentel et al., 2020a, 2019b; Liu et al., 2021; Tenorio et al., 2020). The UV/sulfite system has achieved high levels (>90%) of PFAS destruction in moderate time spans (<24 hours) but struggles with

degrading highly recalcitrant PFAS like short-chain PFSAs (e.g. PFBS) or degrading PFAS in concentrated AFFF formulations (Tenorio et al., 2020). While being highly effective, the UV/sulfite system may not result in complete defluorination of PFAS compounds, instead resulting in several fluorinated transformation products, with the most common being the -nF/+nH exchanged PFAS product. To overcome this, authors have investigated modifications to the UV/sulfite system, such as the addition of UV-activated oxidation technologies before and/or after the UV/sulfite system to allow for the complete destruction of PFAS (Liu et al., 2021). While this has resulted in further improvements to PFAS destruction, it adds a significant level of complexity to the overall remediation process.

It is possible that, instead of adding additional stages to the UV-ARP process (e.g. oxidation), the UV-ARP process could be further optimized to achieve complete PFAS destruction of all PFAS, even the highly recalcitrant short-chain PFSAs, in simple or complex aqueous matrices. For example, work by Fennell et al. (2021) hypothesized that the presence of other reactive radical species, such as the sulfite radical, may act as a mild oxidizing agent capable of breaking down recalcitrant PFAS transformation products (Fennell et al. 2021).

To this end, this thesis seeks first and foremost to build upon existing literature to design a UV-ARP system capable of achieving complete destruction of PFAS rapidly, using PFBS as a model PFAS to evaluate overall system performance. This UV-ARP system will investigate multiple photosensitizers, independently and together, to identify the best starting point from which to optimize the resultant system. Subsequent system optimization will then focus on varying the concentrations of different reagents, using limits established in the literature (e.g. upper limit of 50 mM SO_3^{2-} identified by Fennell et al. (2023)). Lastly, the effectiveness of the developed system will be evaluated in the presence of several well-known (e.g. nitrate) and lesser known (e.g. butyl carbitol) radical scavengers to evaluate the system robustness (Fennell et al., 2023, 2022, 2021). The PFAS transformation products formed during degradation and interactions between the developed UV-ARP system and the different scavengers will be used to elucidate insights into the different radicals present in the UV-ARP system.

2.9 References - Chapter 1 & 2

Abercrombie, S.A., de Perre, C., Choi, Y.J., Tornabene, B.J., Sepúlveda, M.S., Lee, L.S., Hoverman, J.T., 2019. Larval amphibians rapidly bioaccumulate poly- and perfluoroalkyl substances. Ecotoxicol Environ Saf 178, 137–145. https://doi.org/10.1016/j.ecoenv.2019.04.022

Abunada, Z., Alazaiza, M.Y.D., Bashir, M.J.K., 2020. An overview of per-and polyfluoroalkyl substances (Pfas) in the environment: Source, fate, risk and regulations. Water (Switzerland) 12, 1–28. https://doi.org/10.3390/w12123590

Abusallout, I., Wang, J., Hanigan, D., 2021. Emerging investigator series: Rapid defluorination of 22 per- And polyfluoroalkyl substances in water using sulfite irradiated by medium-pressure UV. Environ Sci (Camb) 7, 1552–1562. https://doi.org/10.1039/d1ew00221j

Backe, W.J., Day, T.C., Field, J.A., 2013. Zwitterionic, cationic, and anionic fluorinated chemicals in aqueous film forming foam formulations and groundwater from U.S. military bases by nonaqueous large-volume injection HPLC-MS/MS. Environ Sci Technol 47, 5226–5234. https://doi.org/10.1021/es3034999

Banzhaf, S., Filipovic, M., Lewis, J., Sparrenbom, C.J., Barthel, R., 2017. A review of contamination of surface-, ground-, and drinking water in Sweden by perfluoroalkyl and polyfluoroalkyl substances (PFASs). Ambio 46, 335–346. https://doi.org/10.1007/s13280-016-0848-8

Bao, Y., Huang, J., Cagnetta, G., Yu, G., 2019. Removal of F–53B as PFOS alternative in chrome plating wastewater by UV/Sulfite reduction. Water Res 163, 114907. https://doi.org/10.1016/j.watres.2019.114907

Barry, V., Winquist, A., Steenland, K., 2013. Perfluorooctanoic acid (PFOA) exposures and incident cancers among adults living near a chemical plant. Environ Health Perspect 121, 1313–1318. https://doi.org/10.1289/ehp.1306615

Barzen-Hanson, K.A., Davis, S.E., Kleber, M., Field, J.A., 2017. Sorption of Fluorotelomer Sulfonates, Fluorotelomer Sulfonamido Betaines, and a Fluorotelomer Sulfonamido Amine in National Foam Aqueous Film-Forming Foam to Soil. Environ Sci Technol 51, 12394–12404. https://doi.org/10.1021/acs.est.7b03452

Bentel, M.J., Liu, Z., Yu, Y., Gao, J., Men, Y., Liu, J., 2020a. Enhanced Degradation of Perfluorocarboxylic Acids (PFCAs) by UV/Sulfite Treatment: Reaction Mechanisms and System Efficiencies at pH 12. Environ Sci Technol Lett 7, 351–357. https://doi.org/10.1021/acs.estlett.0c00236

Bentel, M.J., Liu, Z., Yu, Y., Gao, J., Men, Y., Liu, J., 2020b. Enhanced Degradation of Perfluorocarboxylic Acids (PFCAs) by UV/Sulfite Treatment: Reaction Mechanisms and System Efficiencies at pH 12. Environ Sci Technol Lett 7, 351–357. https://doi.org/10.1021/acs.estlett.0c00236

Bentel, M.J., Yu, Y., Xu, L., Li, Z., Wong, B.M., Men, Y., Liu, J., 2019a. Defluorination of Per- and Polyfluoroalkyl Substances (PFASs) with Hydrated

Electrons: Structural Dependence and Implications to PFAS Remediation and Management. Environ Sci Technol 53, 3718–3728. https://doi.org/10.1021/acs.est.8b06648

Bentel, M.J., Yu, Y., Xu, L., Li, Z., Wong, B.M., Men, Y., Liu, J., 2019b. Defluorination of Per- and Polyfluoroalkyl Substances (PFASs) with Hydrated Electrons: Structural Dependence and Implications to PFAS Remediation and Management. Environ Sci Technol 53, 3718–3728. https://doi.org/10.1021/acs.est.8b06648

Boisvert, G., Sonne, C., Rigét, F.F., Dietz, R., Letcher, R.J., 2019. Bioaccumulation and biomagnification of perfluoroalkyl acids and precursors in East Greenland polar bears and their ringed seal prey. Environmental Pollution 252, 1335–1343. https://doi.org/10.1016/j.envpol.2019.06.035

Bolan, N., Sarkar, B., Yan, Y., Li, Q., Wijesekara, H., Kannan, K., Tsang, D.C.W., Schauerte, M., Bosch, J., Noll, H., Ok, Y.S., Scheckel, K., Kumpiene, J., Gobindlal, K., Kah, M., Sperry, J., Kirkham, M.B., Wang, H., Tsang, Y.F., Hou, D., Rinklebe, J., 2021. Remediation of poly- and perfluoroalkyl substances (PFAS) contaminated soils – To mobilize or to immobilize or to degrade? J Hazard Mater 401. https://doi.org/10.1016/j.jhazmat.2020.123892

Brusseau, M.L., Anderson, R.H., Guo, B., 2020. PFAS concentrations in soils: Background levels versus contaminated sites. Science of the Total Environment 740, 140017. https://doi.org/10.1016/j.scitotenv.2020.140017

Bruton, T.A., Sedlak, D.L., 2017. Treatment of Aqueous Film-Forming Foam by Heat-Activated Persulfate under Conditions Representative of in Situ Chemical Oxidation. Environ Sci Technol 51, 13878–13885. https://doi.org/10.1021/acs.est.7b03969

Buck, R.C., Franklin, J., Berger, U., Conder, J.M., Cousins, I.T., Voogt, P. De, Jensen, A.A., Kannan, K., Mabury, S.A., van Leeuwen, S.P.J., 2011. Perfluoroalkyl and polyfluoroalkyl substances in the environment: Terminology, classification, and origins. Integr Environ Assess Manag 7, 513–541. https://doi.org/10.1002/ieam.258

Buck, R.C., Korzeniowski, S.H., Laganis, E., Adamsky, F., 2021. Identification and classification of commercially relevant per- and poly-fluoroalkyl substances (PFAS). Integr Environ Assess Manag 17, 1045–1055. https://doi.org/10.1002/ieam.4450

Butt, C.M., Muir, D.C.G., Mabury, S.A., 2014. Biotransformation pathways of fluorotelomer-based polyfluoroalkyl substances: A review. Environ Toxicol Chem 33, 243–267. https://doi.org/10.1002/etc.2407

Coggan, T.L., Anumol, T., Pyke, J., Shimeta, J., Clarke, B.O., 2019. A single analytical method for the determination of 53 legacy and emerging per- and polyfluoroalkyl substances (PFAS) in aqueous matrices. Anal Bioanal Chem 411, 3507–3520. https://doi.org/10.1007/s00216-019-01829-8

Conte, L., Gambaretto, G.P., 2004. Electrochemical fluorination: State of the art and future tendences. J Fluor Chem 125, 139–144. https://doi.org/10.1016/j.jfluchem.2003.07.002

Cousins, I.T., Dewitt, J.C., Glüge, J., Goldenman, G., Herzke, D., Lohmann, R., Ng, C.A., Scheringer, M., Wang, Z., 2020. The high persistence of PFAS is sufficient for their management as a chemical class. Environ Sci Process Impacts 22, 2307–2312. https://doi.org/10.1039/d0em00355g

D'Agostino, L.A., Mabury, S.A., 2014. Identification of novel fluorinated surfactants in aqueous film forming foams and commercial surfactant concentrates. Environ Sci Technol 48, 121–129. https://doi.org/10.1021/es403729e

Dombrowski, P.M., Kakarla, P., Caldicott, W., Chin, Y., Sadeghi, V., Bogdan, D., Barajas-Rodriguez, F., Chiang, S.Y.D., 2018. Technology review and evaluation of different chemical oxidation conditions on treatability of PFAS. Remediation 28, 135–150. https://doi.org/10.1002/rem.21555

Environmental Working Group (EWG), 2019. For 50 years, polluters knew pfas chemicals were dangerous but hid risks from public 1–26.

Fennell, B.D., Mezyk, S.P., McKay, G., 2021. Critical Review of UV-Advanced Reduction Processes for the Treatment of Chemical Contaminants in Water. ACS Environmental Au. https://doi.org/10.1021/acsenvironau.1c00042

Glüge, J., Scheringer, M., Cousins, I.T., Dewitt, J.C., Goldenman, G., Herzke, D., Lohmann, R., Ng, C.A., Trier, X., Wang, Z., 2020. An overview of the uses of per-And polyfluoroalkyl substances (PFAS). Environ Sci Process Impacts 22, 2345–2373. https://doi.org/10.1039/d0em00291g

Harding-Marjanovic, K.C., Houtz, E.F., Yi, S., Field, J.A., Sedlak, D.L., Alvarez-Cohen, L., 2015. Aerobic Biotransformation of Fluorotelomer Thioether Amido Sulfonate (Lodyne) in AFFF-Amended Microcosms. Environ Sci Technol 49, 7666–7674. https://doi.org/10.1021/acs.est.5b01219

Health Canada, Environment and Climate Change Canada. 2023. DRAFT State of Per- and Polyfluoroalkyl Substances (PFAS) Report. Government of Canada.

Hori, H., Nagaoka, Y., Sano, T., Kutsuna, S., 2008. Iron-induced decomposition of perfluorohexanesulfonate in sub- and supercritical water. Chemosphere 70, 800–806. https://doi.org/10.1016/j.chemosphere.2007.07.015

Hori, H., Yamamoto, A., Hayakawa, E., Taniyasu, S., Yamashita, N., Kutsuna, S., Kiatagawa, H., Arakawa, R., 2005. Efficient decomposition of environmentally persistent perfluorocarboxylic acids by use of persulfate as a photochemical oxidant. Environ Sci Technol 39, 2383–2388. https://doi.org/10.1021/es0484754

Houtz, E.F., Higgins, C.P., Field, J.A., Sedlak, D.L., 2013. Persistence of Per fl uoroalkyl Acid Precursors in AFFF-Impacted Groundwater and Soil.

Houtz, E.F., Sedlak, D.L., 2012a. Oxidative conversion as a means of detecting precursors to perfluoroalkyl acids in urban runoff. Environ Sci Technol 46, 9342–9349. https://doi.org/10.1021/es302274g

Houtz, E.F., Sedlak, D.L., 2012b. Oxidative conversion as a means of detecting precursors to perfluoroalkyl acids in urban runoff. Environ Sci Technol 46, 9342–9349. https://doi.org/10.1021/es302274g

Houtz, E.F., Sutton, R., Park, J.S., Sedlak, M., 2016. Poly- and perfluoroalkyl substances in wastewater: Significance of unknown precursors, manufacturing shifts, and likely AFFF impacts. Water Res 95, 142–149. https://doi.org/10.1016/j.watres.2016.02.055

Hutchinson, S., Rieck, T., Wu, X.L., 2020. Advanced PFAS precursor digestion methods for biosolids. Environmental Chemistry 17, 558–567. https://doi.org/10.1071/EN20008

Jian, J.M., Chen, D., Han, F.J., Guo, Y., Zeng, L., Lu, X., Wang, F., 2018. A short review on human exposure to and tissue distribution of per- and polyfluoroalkyl substances (PFASs). Science of the Total Environment 636, 1058–1069. https://doi.org/10.1016/j.scitotenv.2018.04.380

Jian, J.M., Guo, Y., Zeng, L., Liang-Ying, L., Lu, X., Wang, F., Zeng, E.Y., 2017. Global distribution of perfluorochemicals (PFCs) in potential human exposure source–A review. Environ Int 108, 51–62. https://doi.org/10.1016/j.envint.2017.07.024

Joudan, S., Mabury, S.A., 2022. Aerobic biotransformation of a novel highly functionalized polyfluoroether-based surfactant using activated sludge from a wastewater treatment plant. Environ Sci Process Impacts 24, 62–71. https://doi.org/10.1039/d1em00358e

Kim, S.K., Kannan, K., 2007. Perfluorinated acids in air, rain, snow, surface runoff, and lakes: Relative importance of pathways to contamination of urban lakes. Environ Sci Technol 41, 8328–8334. https://doi.org/10.1021/es072107t

Kleywegt, S., Raby, M., McGill, S., Helm, P., 2020. The impact of risk management measures on the concentrations of per- and polyfluoroalkyl substances in source and treated drinking waters in Ontario, Canada. Science of the Total Environment 748, 141195. https://doi.org/10.1016/j.scitotenv.2020.141195

Kwok, K.Y., Yamazaki, E., Yamashita, N., Taniyasu, S., Murphy, M.B., Horii, Y., Petrick, G., Kallerborn, R., Kannan, K., Murano, K., Lam, P.K.S., 2013. Transport of Perfluoroalkyl substances (PFAS) from an arctic glacier to downstream locations: Implications for sources. Science of the Total Environment 447, 46–55. https://doi.org/10.1016/j.scitotenv.2012.10.091

Lang, J.R., Allred, B.M.K., Field, J.A., Levis, J.W., Barlaz, M.A., 2017. National Estimate of Per- and Polyfluoroalkyl Substance (PFAS) Release to U.S. Municipal Landfill Leachate, Environmental Science and Technology. https://doi.org/10.1021/acs.est.6b05005

Lassalle, J., Gao, R., Rodi, R., Kowald, C., Feng, M., Sharma, V.K., Hoelen, T., Bireta, P., Houtz, E.F., Staack, D., Pillai, S.D., 2021. Degradation of PFOS and PFOA in soil and groundwater samples by high dose Electron Beam Technology. Radiation Physics and Chemistry 189, 109705. https://doi.org/10.1016/j.radphyschem.2021.109705

Lee, H., Deon, J., Mabury, S.A., 2010. Biodegradation of polyfluoroalkyl phosphates as a source of perfluorinated acids to the environment. Environ Sci Technol 44, 3305–3310. https://doi.org/10.1021/es9028183

Lee, H., Mabury, S.A., 2014. Global Distribution of Polyfluoroalkyl and Perfluoroalkyl Substances and their Transformation Products in Environmental Solids. Transformation Products of Emerging Contaminants in the Environment: Analysis, Processes, Occurrence, Effects and Risks 797–826. https://doi.org/10.1002/9781118339558.ch27

Lesmeister, L., Lange, F.T., Breuer, J., Biegel-Engler, A., Giese, E., Scheurer, M., 2021. Extending the knowledge about PFAS bioaccumulation factors for agricultural plants – A review. Science of the Total Environment 766, 142640. https://doi.org/10.1016/j.scitotenv.2020.142640

Li, R., Munoz, G., Liu, Y., Sauvé, S., Ghoshal, S., Liu, J., 2019. Transformation of novel polyfluoroalkyl substances (PFASs) as co-contaminants during biopile remediation of petroleum hydrocarbons. J Hazard Mater 362, 140–147. https://doi.org/10.1016/j.jhazmat.2018.09.021

Liu, C., Liu, J., 2016. Aerobic biotransformation of polyfluoroalkyl phosphate esters (PAPs) in soil. Environmental Pollution 212, 230–237. https://doi.org/10.1016/j.envpol.2016.01.069

Liu, J., Wang, N., Szostek, B., Buck, R.C., Panciroli, P.K., Folsom, P.W., Sulecki, L.M., Bellin, C.A., 2010. 6-2 Fluorotelomer alcohol aerobic biodegradation in soil and mixed bacterial culture. Chemosphere 78, 437–444. https://doi.org/10.1016/j.chemosphere.2009.10.044

Liu, M., Munoz, G., Vo Duy, S., Sauvé, S., Liu, J., 2022. Per- and Polyfluoroalkyl Substances in Contaminated Soil and Groundwater at Airports: A Canadian Case Study. Environ Sci Technol 56, 885–895. https://doi.org/10.1021/acs.est.1c04798

Liu, S., Junaid, M., Zhong, W., Zhu, Y., Xu, N., 2020. A sensitive method for simultaneous determination of 12 classes of per- and polyfluoroalkyl substances (PFASs) in groundwater by ultrahigh performance liquid chromatography coupled with quadrupole orbitrap high resolution mass spectrometry. Chemosphere 251, 126327. https://doi.org/10.1016/j.chemosphere.2020.126327

Liu, Z., Bentel, M.J., Yu, Y., Ren, C., Gao, J., Pulikkal, V.F., Sun, M., Men, Y., Liu, J., 2021. Near-Quantitative Defluorination of Perfluorinated and Fluorotelomer Carboxylates and Sulfonates with Integrated Oxidation and Reduction. Environ Sci Technol 55, 7052–7062. https://doi.org/10.1021/acs.est.1c00353

Longpré, D., Lorusso, L., Levicki, C., Carrier, R., Cureton, P., 2020. PFOS, PFOA, LC-PFCAS, and certain other PFAS: A focus on Canadian guidelines and guidance for contaminated sites management. Environ Technol Innov 18, 100752. https://doi.org/10.1016/j.eti.2020.100752

Martin, D., Munoz, G., Mejia-Avendaño, S., Duy, S.V., Yao, Y., Volchek, K., Brown, C.E., Liu, J., Sauvé, S., 2019. Zwitterionic, cationic, and anionic perfluoroalkyl and polyfluoroalkyl substances integrated into total oxidizable precursor assay of contaminated groundwater. Talanta 195, 533–542. https://doi.org/10.1016/j.talanta.2018.11.093

Masoner, J.R., Kolpin, D.W., Cozzarelli, I.M., Smalling, K.L., Bolyard, S.C., Field, J.A., Furlong, E.T., Gray, J.L., Lozinski, D., Reinhart, D., Rodowa, A., Bradley, P.M., 2020. Landfill leachate contributes per-/poly-fluoroalkyl substances (PFAS) and pharmaceuticals to municipal wastewater. Environ Sci (Camb) 6, 1300–1311. https://doi.org/10.1039/d0ew00045k

Merino, N., Qu, Y., Deeb, R.A., Hawley, E.L., Hoffmann, M.R., Mahendra, S., 2016. Degradation and Removal Methods for Perfluoroalkyl and Polyfluoroalkyl Substances in Water. Environ Eng Sci 33, 615–649. https://doi.org/10.1089/ees.2016.0233

Milley, S.A., Koch, I., Fortin, P., Archer, J., Reynolds, D., Weber, K.P., 2018. Estimating the number of airports potentially contaminated with perfluoroalkyl and polyfluoroalkyl substances from aqueous film forming foam: A Canadian example. J Environ Manage 222, 122–131. https://doi.org/10.1016/j.jenvman.2018.05.028

Nabb, D.L., Szostek, B., Himmelstein, M.W., Mawn, M.P., Gargas, M.I., Sweeney, L.M., Stadler, J.C., Buck, R.C., Fasano, W.J., 2007. In vitro metabolism of 8-2 fluorotelomer alcohol: Interspecies comparisons and metabolic pathway refinement. Toxicological Sciences 100, 333–344. https://doi.org/10.1093/toxsci/kfm230

Naidu, R., Nadebaum, P., Fang, C., Cousins, I., Pennell, K., Conder, J., Newell, C.J., Longpré, D., Warner, S., Crosbie, N.D., Surapaneni, A., Bekele, D., Spiese, R., Bradshaw, T., Slee, D., Liu, Y., Qi, F., Mallavarapu, M., Duan, L., McLeod, L., Bowman, M., Richmond, B., Srivastava, P., Chadalavada, S., Umeh, A., Biswas, B., Barclay, A., Simon, J., Nathanail, P., 2020. Per- and poly-fluoroalkyl substances (PFAS): Current status and research needs. Environ Technol Innov 19. https://doi.org/10.1016/j.eti.2020.100915

Nakayama, S.F., Yoshikane, M., Onoda, Y., Nishihama, Y., Iwai-Shimada, M., Takagi, M., Kobayashi, Y., Isobe, T., 2019. Worldwide trends in tracing poly- and perfluoroalkyl substances (PFAS) in the environment. TrAC - Trends in Analytical Chemistry 121, 115410. https://doi.org/10.1016/j.trac.2019.02.011

Nickerson, A., Rodowa, A.E., Adamson, D.T., Field, J.A., Kulkarni, P.R., Kornuc, J.J., Higgins, C.P., 2021. Spatial Trends of Anionic, Zwitterionic, and Cationic PFASs at an AFFF-Impacted Site. Environ Sci Technol 55, 313–323. https://doi.org/10.1021/acs.est.0c04473

Okazoe, T., 2009. Overview on the history of organofluorine chemistry from the viewpoint of material industry. Proc Jpn Acad Ser B Phys Biol Sci 85, 276–289. https://doi.org/10.2183/pjab.85.276

Olsen, G.W., Ellefson, M.E., Mair, D.C., Church, T.R., Goldberg, C.L., Herron, R.M., Medhdizadehkashi, Z., Nobiletti, J.B., Rios, J.A., Reagen, W.K., Zobel, L.R., 2011. Analysis of a homologous series of perfluorocarboxylates from American Red Cross adult blood donors, 2000-2001 and 2006. Environ Sci Technol 45, 8022–8029. https://doi.org/10.1021/es1043535

Olsen, G.W., Mair, D.C., Church, T.R., Ellefson, M.E., Reagen, W.K., Boyd, T.M., Herron, R.M., Medhdizadehkashi, Z., Nobiletti, J.B., Rios, J.A., Butenhoff, J.L., Zobel, L.R., 2008. Decline in perfluorooctanesulfonate and other polyfluoroalkyl chemicals in American red cross adult blood donors, 2000-2006. Environ Sci Technol 42, 4989–4995. https://doi.org/10.1021/es800071x

Olsen, G.W., Mair, D.C., Lange, C.C., Harrington, L.M., Church, T.R., Goldberg, C.L., Herron, R.M., Hanna, H., Nobiletti, J.B., Rios, J.A., Reagen, W.K., Ley, C.A., 2017. Per- and polyfluoroalkyl substances (PFAS) in American Red Cross adult blood donors, 2000–2015. Environ Res 157, 87–95. https://doi.org/10.1016/j.envres.2017.05.013

Park, H., Vecitis, C.D., Cheng, J., Choi, W., Mader, B.T., Hoffmann, M.R., 2009. Reductive defluorination of aqueous perfluorinated alkyl surfactants: Effects of ionic headgroup and chain length. Journal of Physical Chemistry A 113, 690–696. https://doi.org/10.1021/jp807116q

Patch, D., O'Connor, N., Koch, I., Cresswell, T., Hughes, C., Davies, J.B., Scott, J., O'Carroll, D., Weber, K., 2022. Elucidating degradation mechanisms for a range of per- and polyfluoroalkyl substances (PFAS) via controlled irradiation studies. Science of the Total Environment 832, 154941. https://doi.org/10.1016/j.scitotenv.2022.154941

Pickard, H.M., Criscitiello, A.S., Persaud, D., Spencer, C., Muir, D.C.G., Lehnherr, I., Sharp, M.J., de Silva, A.O., Young, C.J., 2020. Ice Core Record of Persistent Short-Chain Fluorinated Alkyl Acids: Evidence of the Impact from Global Environmental Regulations. Geophys Res Lett 47. https://doi.org/10.1029/2020GL087535

Rappazzo, K.M., Coffman, E., Hines, E.P., 2017. Exposure to perfluorinated alkyl substances and health outcomes in children: A systematic review of the epidemiologic literature. Int J Environ Res Public Health 14, 1–22. https://doi.org/10.3390/ijerph14070691

Remde, A., Debus, R., 1996. Biodegradability of fluorinated surfactants under aerobic and anaerobic conditions. Chemosphere 32, 1563–1574. https://doi.org/10.1016/0045-6535 (96)00066-5

Ruan, T., Lin, Y., Wang, T., Jiang, G., Wang, N., 2015. Methodology for studying biotransformation of polyfluoroalkyl precursors in the environment. TrAC - Trends in Analytical Chemistry 67, 167–178. https://doi.org/10.1016/j.trac.2014.11.017

Shahsavari, E., Rouch, D., Khudur, L.S., Thomas, D., Aburto-Medina, A., Ball, A.S., 2021. Challenges and Current Status of the Biological Treatment of PFAS-Contaminated Soils. Front Bioeng Biotechnol 8, 1–15. https://doi.org/10.3389/fbioe.2020.602040

Stoiber, T., Evans, S., Naidenko, O. V., 2020. Disposal of products and materials containing per- and polyfluoroalkyl substances (PFAS): A cyclical problem. Chemosphere 260, 127659. https://doi.org/10.1016/j.chemosphere.2020.127659

Suja, F., Pramanik, B.K., Zain, S.M., 2009. Contamination, bioaccumulation and toxic effects of perfluorinated chemicals (PFCs) in the water environment: A review paper. Water Science and Technology 60, 1533–1554. https://doi.org/10.2166/wst.2009.504

Sunderland, E.M., Hu, X.C., Dassuncao, C., Tokranov, A.K., Wagner, C.C., Allen, J.G., 2019. A review of the pathways of human exposure to poly- and perfluoroalkyl substances (PFASs) and present understanding of health effects. J Expo Sci Environ Epidemiol 29, 131–147. https://doi.org/10.1038/s41370-018-0094-1

Surya Prakash, G.K., Wang, F., 2012. Fluorine: The new kingpin of drug discovery. Chimica Oggi/Chemistry Today 30, 30–36.

Tenorio, R., Liu, J., Xiao, X., Maizel, A., Higgins, C.P., Schaefer, C.E., Strathmann, T.J., 2020. Destruction of Per-and Polyfluoroalkyl Substances (PFASs) in Aqueous Film-Forming Foam (AFFF) with UV-Sulfite Photoreductive Treatment. Environ Sci Technol 54, 6957–6967. https://doi.org/10.1021/acs.est.0c00961

Toms, L.M.L., Bräunig, J., Vijayasarathy, S., Phillips, S., Hobson, P., Aylward, L.L., Kirk, M.D., Mueller, J.F., 2019. Per- and polyfluoroalkyl substances (PFAS) in Australia: Current levels and estimated population reference values for selected compounds. Int J Hyg Environ Health 222, 387–394. https://doi.org/10.1016/j.ijheh.2019.03.004

Trojanowicz, M., Bartosiewicz, I., Bojanowska-Czajka, A., Kulisa, K., Szreder, T., Bobrowski, K., Nichipor, H., Garcia-Reyes, J.F., Nałęcz-Jawecki, G., Męczyńska-Wielgosz, S., Kisała, J., 2019. Application of ionizing radiation in decomposition of perfluorooctanoate (PFOA) in waters. Chemical Engineering Journal 357, 698–714. https://doi.org/10.1016/j.cej.2018.09.065

Trojanowicz, M., Bartosiewicz, I., Bojanowska-Czajka, A., Szreder, T., Bobrowski, K., Nałęcz-Jawecki, G., Męczyńska-Wielgosz, S., Nichipor, H., 2020. Application of ionizing radiation in decomposition of perfluorooctane sulfonate (PFOS) in aqueous solutions. Chemical Engineering Journal 379, 122303. https://doi.org/10.1016/j.cej.2019.122303

Trojanowicz, M., Bojanowska-Czajka, A., Bartosiewicz, I., Kulisa, K., 2018. Advanced Oxidation/Reduction Processes treatment for aqueous perfluorooctanoate (PFOA) and perfluorooctanesulfonate (PFOS) – A review of

recent advances. Chemical Engineering Journal 336, 170–199. https://doi.org/10.1016/j.cej.2017.10.153

Trudel, D., Horowitz, L., Wormuth, M., Scheringer, M., Cousins, I.T., Hungerbühler, K., 2008. Estimating consumer exposure to PFOS and PFOA. Risk Analysis 28, 251–269. https://doi.org/10.1111/j.1539-6924.2008.01017.x

Tseng, N.S., 2012. Feasibility of Biodegradation of Polyfluoroalkyl and Perfluoroalkyl Substances. eScholarship 23, 401–516.

Vedagiri, U.K., Anderson, R.H., Loso, H.M., Schwach, C.M., 2018. Ambient levels of PFOS and PFOA in multiple environmental media. Remediation 28, 9–51. https://doi.org/10.1002/rem.21548

Vendl, C., Taylor, M.D., Bräunig, J., Gibson, M.J., Hesselson, D., Gregory Neely, G., Lagisz, M., Nakagawa, S., 2022. PFAS exposure of humans, animals and the environment: Protocol of an evidence review map and bibliometric analysis. Environ Int 158. https://doi.org/10.1016/j.envint.2021.106973

Wang, J., Pan, Y., Cui, Q., Yao, B., Wang, Jianshe, Dai, J., 2018. Penetration of PFASs Across the Blood Cerebrospinal Fluid Barrier and Its Determinants in Humans. Environ Sci Technol 52, 13553–13561. https://doi.org/10.1021/acs.est.8b04550

Wang, Y., Yu, N., Zhu, X., Guo, H., Jiang, J., Wang, X., Shi, W., Wu, J., Yu, H., Wei, S., 2018. Suspect and Nontarget Screening of Per- and Polyfluoroalkyl Substances in Wastewater from a Fluorochemical Manufacturing Park. Environ Sci Technol 52, 11007–11016. https://doi.org/10.1021/acs.est.8b03030

Wang, Z., Cousins, I.T., Scheringer, M., Buck, R.C., Hungerbühler, K., 2014. Global emission inventories for C4-C14 perfluoroalkyl carboxylic acid (PFCA) homologues from 1951 to 2030, Part I: Production and emissions from quantifiable sources. Environ Int 70, 62–75. https://doi.org/10.1016/j.envint.2014.04.013

Weiner, B., Yeung, L.W.Y., Marchington, E.B., D'Agostino, L.A., Mabury, S.A., 2013. Organic fluorine content in aqueous film forming foams (AFFFs) and biodegradation of the foam component 6:2 fluorotelomermercaptoalkylamido sulfonate (6:2 FTSAS). Environmental Chemistry 10, 486–493. https://doi.org/10.1071/EN13128

Yang, L., He, L., Xue, J., Ma, Y., Xie, Z., Wu, L., Huang, M., Zhang, Z., 2020. Persulfate-based degradation of perfluorooctanoic acid (PFOA) and perfluorooctane sulfonate (PFOS) in aqueous solution: Review on influences, mechanisms and prospective. J Hazard Mater. https://doi.org/10.1016/j.jhazmat.2020.122405

Yeung, L.W.Y., Mabury, S.A., 2013. Bioconcentration of aqueous film-forming foam (AFFF) in juvenile rainbow trout (oncorhyncus mykiss). Environ Sci Technol 47, 12505–12513. https://doi.org/10.1021/es403170f

Yi, S., Harding-Marjanovic, K.C., Houtz, E.F., Gao, Y., Lawrence, J.E., Nichiporuk, R. v., Iavarone, A.T., Zhuang, W.Q., Hansen, M., Field, J.A., Sedlak,

D.L., Alvarez-Cohen, L., 2018. Biotransformation of AFFF Component 6:2 Fluorotelomer Thioether Amido Sulfonate Generates 6:2 Fluorotelomer Thioether Carboxylate under Sulfate-Reducing Conditions. Environ Sci Technol Lett 5, 283–288. https://doi.org/10.1021/acs.estlett.8b00148

Yi, S., Zhu, L., Mabury, S.A., 2019. First Report on in Vivo Pharmacokinetics and Biotransformation of Chlorinated Polyfluoroalkyl Ether Sulfonates in Rainbow Trout. Environ Sci Technol. https://doi.org/10.1021/acs.est.9b05258

Wu, Goodrow, Chen, Li, 2024. Distinctive biotransformation and biodefluorination of 6 :2 vs 5 :3 fluorotelomer carboxylic acids by municpal activated sludge. Water Research Volume 254, 121431. https://doi.org/10.1016/j.watres.2024.121431

Zacs, D., Bartkevics, V., 2016. Trace determination of perfluorooctane sulfonate and perfluorooctanoic acid in environmental samples (surface water, wastewater, biota, sediments, and sewage sludge) using liquid chromatography – Orbitrap mass spectrometry. J Chromatogr A 1473, 109–121. https://doi.org/10.1016/j.chroma.2016.10.060

Zhang, Z., Chen, J.J., Lyu, X.J., Yin, H., Sheng, G.P., 2014. Complete mineralization of perfluorooctanoic acid (PFOA) by γ-irradiation in aqueous solution. Sci Rep 4, 1–6. https://doi.org/10.1038/srep07418

3. Forever No More: Complete mineralization of per- and polyfluoroalkyl substances (PFAS) using an optimized UV/sulfite/iodide system.

Natalia O'Connor†, David Patch†, Diana Noble†, Jennifer Scott†, Iris Koch†, Kevin G. Mumford ††, Kela Weber†*

† Department of Chemistry and Chemical Engineering, Royal Military College of Canada, Kingston, ON, Canada K7K 7B4.

††Department of Civil Engineering, Queen's University, Kingston, ON, Canada.

* Corresponding Author: Kela.Weber@rmc.ca

3.1 Abstract

As the global issue of PFAS contamination in water continues to grow there exists a need for technologies capable of fully mineralizing PFAS in water, with destruction being measured as both a loss of the initial PFAS and a quantitative recovery of the resultant fluoride ions. This study investigates the use of sulfite and iodide in a bicarbonate-buffered alkaline system activated with ultraviolet (UV) light to destroy PFAS. The UV/sulfite/iodide system creates a reductive environment through the generation of aqueous electrons, which can degrade PFAS. The extent of degradation and defluorination was explored for perfluorooctane sulfonic acid (PFOS), perfluorooctanoic acid (PFOA), 6:2 fluorotelomer sulfonic acid (6:2 FTS), and perfluorobutane sulfonic acid (PFBS). An initial UV/sulfite/iodide system achieved 100% degradation and >90% defluorination for PFOS, PFOA, and 6:2 FTS, but was not capable of completely degrading PFBS. Transformation product elucidation experiments were performed for PFOS under different UV systems, and 6:2 FtSaB using the initial UV/sulfite/iodide system. Several transformation products were identified including -nF/+nH PFOS (n=1-13), -F/+H shorter-chain PFSAs, 6:2 fluorotelomer sulfonamidoamine (6:2 FtSaAm), 6:2 fluorotelomer sulfonamide, and 6:2 fluorotelomer unsaturated sulfonamide. Novel identification of -F/+H perfluoropropane sulfonic acid (PFPS) and -F/+H perfluoroethane sulfonic acid (PFES) following degradation of PFOS confirms C-C bond cleavage, and different isomers of -F/+H PFOS confirms the potential for C-F bond cleavage to occur throughout the perfluoroalkyl chain. Additional optimization experiments were performed aiming to fully degrade PFBS. The optimal protocol found in this study involved an elevated initial sulfite concentration and adding additional sulfite at regular intervals during UV-activation, achieving >99.9% destruction and complete quantitative defluorination of PFBS.

3.2 Introduction

Per- and polyfluoroalkyl substances (PFAS) are a growing group of recalcitrant anthropogenic chemicals that are made up of polymeric and nonpolymeric substances (Buck et al., 2011b). These compounds, first developed by 3M in the early 1950's, are characterized by containing one or more carbon-fluorine moieties ($-CF_2$) and are used in a variety of applications exploiting their unique physicochemical properties.

To address the growing issue of PFAS contamination in the world, significant research has focused on PFAS remediation. Research into the destruction of PFAS-contaminated materials has investigated bioremediation, sonochemical destruction, incineration, smoldering, mechanochemical degradation, electron beam irradiation, gamma irradiation, chemical reduction, and chemical oxidation (Battye et al., 2022; Bentel et al., 2019; Chen et al., 2022; Duchesne et al., 2020; Hori et al., 2008, 2005; Houtz and Sedlak, 2012b; Lassalle et al., 2021; Merino et al., 2016; Patch et al., 2022; Trojanowicz et al., 2020, 2019a, 2018; Tseng, 2012; Turner et al., 2021; Zhang et al., 2014). However, the same chemical properties that make PFAS so attractive to manufacturers also make them exceptionally recalcitrant. The high bond dissociation energy of the C-F bond, electron-dense fluorine shell, helical structure, increasingly variable functional groups, and variable fluorocarbon chain lengths make remediation efforts difficult (Bentel et al., 2020b, 2019a; Dombrowski et al., 2018b; Liu et al., 2021b; Mahinroosta and Senevirathna, 2020; Mifkovic et al., 2022; Trojanowicz et al., 2018; Wang et al., 2017).

Attempts to destroy PFAS using chemical oxidation techniques found success when applied to perfluorocarboxylic acids (PFCAs) and fluorotelomers, but little success when applied to the more recalcitrant perfluorosulfonic acid (PFSA) class of PFAS (Bruton and Sedlak, 2017; Yang et al., 2020). On the other hand, techniques facilitating a reductive aqueous environment have been found to be more successful at degrading a wider range of PFAS compounds. Ultraviolet-activated advanced reductive processes (UV-ARP) technology has proven to be effective in remediating PFAS through the utilization of reagents like sulfite, iodide, and phenol to generate aqueous electrons (Table A1). These reagents, also referred to as sensitizers, have unique quantum yields (rate of aqueous electron formation) (Φ), molar absorptivities (ε) (how strongly a chemical attenuates photons at a given wavelength) and photoinitiated reactions (eq 1-3) (Fennell et al., 2021; Gu et al., 2017; Sauer et al., 2004).

$$SO_3{}^{2-} \xrightarrow{h\nu} SO_3{}^{\cdot-} + e_{aq}^- \qquad \Phi = 0.116 \qquad \varepsilon = 18\text{-}20 \text{ M}^{-1}\text{ cm}^{-1} \qquad (1)$$

$$I^- + H_2O \xrightarrow{h\nu} I^\cdot + H_2O + e_{aq}^- \qquad \Phi = 0.170 - 0.286 \; \varepsilon = 162\text{-}220 \text{ M}^{-1}\text{ cm}^{-1} \quad (2)$$

$$C_6H_5OH \xrightarrow{h\nu} C_6H_5O^\cdot + H^+ + e_{aq}^- \qquad \Phi = 0.23\text{-}0.25 \; \varepsilon = 942 \text{ M}^{-1}\text{ cm}^{-1} \qquad (3)$$
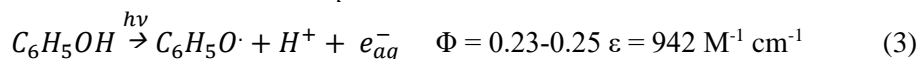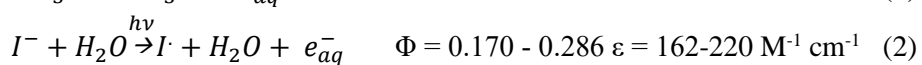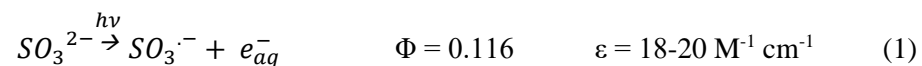
With a reduction potential of -3.1V, aqueous electrons have shown to be capable of breaking C-C, C-F, and C-S bonds in PFAS, resulting in several transformation products (Bachman et al., 2022; Banayan Esfahani and Mohseni, 2022; Bentel et al., 2019; Buxton et al., 1988; Liu et al., 2021b; Park et al., 2011, 2009; Patch et al., 2022; Qu et al., 2010). Subsequent reaction of the transformation products with additional aqueous electrons or other species present in the system can result in the formation of smaller organic compounds (*e.g.* acetate, formate), as well as lead to complete mineralization, yielding fluoride and carbon dioxide, (Fennell et al., 2021; Trojanowicz et al., 2020, 2019, 2018). The reaction between PFOS and PFOA with aqueous electrons is described below, alongside its associated bimolecular rate constant (eq 4-6).

$$PFOA + e_{aq}^- \rightarrow PFOA^{\cdot} \qquad k = 1.7 \text{ x } 10^7 - 7.1 \text{ x } 10^8 \text{ M}^{-1}\text{s}^{-1} \qquad (4)$$

$$PFOS + e_{aq}^- \rightarrow PFOS^{\cdot} \qquad k = 2.4 \text{ x } 10^9 \text{ M}^{-1}\text{s}^{-1} \qquad (5)$$

$$PFOX^{\cdot} + Additional\ reactions \rightarrow F^- + CO_2/\ C_2H_3O_2^-/HCOO^- \qquad (6)$$
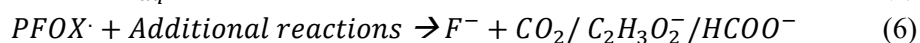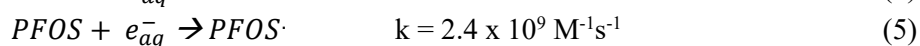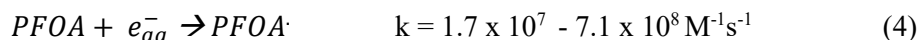
The degradation of contaminants with UV systems is often performed in anaerobic, alkaline environments to avoid unwanted scavenging reactions that reduce the presence of aqueous electrons. Two of the most prevalent aqueous electron quenching reactions involves the reaction with dissolved oxygen in solution and protons under acidic conditions (eq 7,8) (Park et al., 2011).

$$e_{aq}^- + O_2 \rightarrow O_2^{\cdot -} \qquad k = 1.9 \text{ x } 10^{10} \text{ M}^{-1}\text{s}^{-1} \qquad (7)$$

$$e_{aq}^- + H^+ \rightarrow H^{\cdot} \qquad k = 2.3 \text{ x } 10^{10} \text{ M}^{-1}\text{s}^{-1} \qquad (8)$$
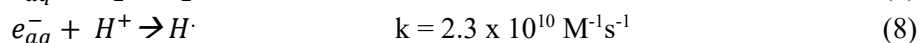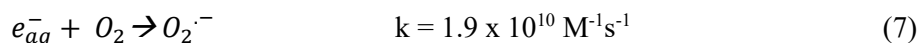
Depending on the sensitizers used in the UV system, anaerobic conditions can be created and maintained as a result of the reaction itself. This is the case with the UV/sulfite system, which can deplete oxygen rapidly through the photoinitiated chain autooxidation of sulfur (IV) (eq 9) (Li et al., 2014).

$$(1), \text{then: } SO_3^{\cdot -} + O_2 \rightarrow SO_5^{\cdot -} \qquad k = 1.5 \text{ x } 10^9 \text{ M}^{-1}\text{s}^{-1} \qquad (9)$$

Many of these UV systems require careful optimization to find the ideal concentrations of reagents to add. This is particularly true with UV/iodide systems. With a higher quantum yield and molar absorptivity than sulfite, the UV/iodide system is expected to be more effective at remediating halogenated contaminants than the UV/sulfite system. However, the UV/sulfite system has been identified as the more efficient stand-alone UV sensitizer when degrading halogenated contaminants like PFAS or monochloroacetic acid and is able to function at higher reagent concentrations (Z. Liu et al., 2022; Yu et al., 2018). This is due to the

formation of reactive iodine species (RIS) in the UV/iodide system, which scavenge iodide and aqueous electrons, reducing the overall effectiveness of the system (eq 10-12) (Park et al., 2011).

$$I^. + I^- \rightarrow I_2^{.-} \qquad k = 1.2 \times 10^4 \text{ M}^{-1}\text{s}^{-1} \qquad (10)$$
$$I^. + I^. \rightarrow I_2 \qquad k = 1.0 \times 10^{10} \text{ M}^{-1}\text{s}^{-1} \qquad (11)$$
$$I_2 + e_{aq}^- \rightarrow I_2^{.-} \qquad k = 5.3 \times 10^{10} \text{ M}^{-1}\text{s}^{-1} \qquad (12)$$
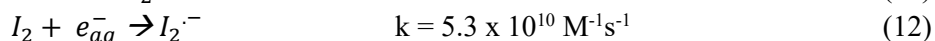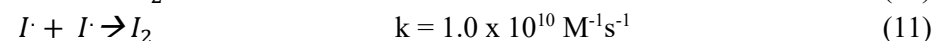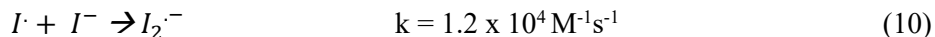
Other authors (Z. Liu et al., 2022; Yu et al., 2018) have identified the enhanced effectiveness in the combined UV/sulfite/iodide systems. Liu *et al.* (2022) demonstrated that the presence of I^- and SO_3^{2-} together could destroy PFBS after 24 hours, achieving ~78% defluorination. No difference was seen between 2 mM and 5 mM I^-, with a minimal difference observed between 10 mM and 20 mM SO_3^{2-}, and the highest degradation occurring at pH 12.

The accelerated degradation of PFAS in the combined UV/sulfite/iodide systems is due to the higher quantum yield and molar absorptivity of the iodide, and the use of sulfite to scavenge oxygen and react with the RIS that form over time, regenerating the iodide (Z. Liu et al., 2022; Yu et al., 2018) (eq 13).

$$I^. + SO_3^{2-} \rightarrow I^- + SO_3^{.-} \qquad k = 1.4 \times 10^9 \text{ M}^{-1}\text{s}^{-1} \qquad (13)$$
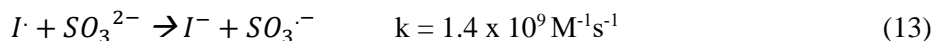
However, many authors see diminishing returns when using sulfite concentrations higher than 10 mM (Abusallout et al., 2021; Bentel et al., 2020b). This is due to sulfite's ability to scavenge electrons, which becomes significant at 10 mM and higher (Buxton et al., 1988; Fennell et al., 2021) (eq 14).

$$SO_3^{2-} + e_{aq}^- \rightarrow product \qquad k = <1.5 \times 10^6 \quad \text{M}^{-1}\text{s}^{-1} \qquad (14)$$
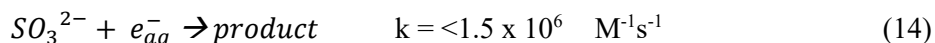
It is well understood that of the various PFAS studied, PFCAs are most readily degraded, followed by PFSAs then fluorotelomers. This is due to the protective nature of the sulfonate headgroup (comparing PFOA to PFOS), and the additional recalcitrance created when the functional group is separated from the fluoroalkyl chain by intermediate $-CH_2$ linkers (comparing PFOS to fluorotelomers) (Liu et al., 2021b). PFAS recalcitrance is also influenced by chain length, with short- and ultra-short chain PFSAs noted as being particularly resistant to degradation (Z. Liu et al., 2022; Patch et al., 2022). Increasingly stringent drinking water requirements require high removals of PFAS, including short-chain PFSAs, from aqueous matrices. The use of sulfite and iodide as UV-activated aqueous electron generators is a promising technology that demands further investigation to identify its place in the growing list of effective PFAS remediation options. One of the key parameters required to better understand the technology is identifying the optimal concentrations and ratios of

sulfite and iodide when combined. For example, authors have observed diminishing PFAS destruction when using iodide concentrations above 0.3 mM in the UV/iodide system (Qu et al., 2010). However, when combined with sulfite, iodide concentrations of up to 2 mM were found to be effective (Z. Liu et al., 2022). Given the synergistic reactions between sulfite and iodide, it is hypothesized that higher concentrations of iodide will allow for the use of higher concentrations of sulfite, either added all right away or sequentially over the course of the reaction. If successful, these further optimizations will help in overcoming the three main barriers precluding UV-ARP from widescale implementation: large UV doses, undesirable aqueous electron sensitizer byproducts, and scavenging of aqueous electrons by oxygen (Fennell et al., 2021).

The present study is focused on further development of the UV-activated sulfite/iodide system to achieve complete degradation of PFAS, including short chain PFSAs. This objective was addressed using a series of experiments conducted in four phases: 1) identification of successful aqueous electron generators; 2) identification of their effectiveness on degrading PFOS, PFOA, 6:2 FTS, 6:2 FtSaB, and PFBS; 3) investigation of different concentrations of reagents to improve the degradation of PFBS; and 4) development of a dynamic UV/sulfite/iodide system capable of achieving complete degradation of PFBS.

3.3 Materials and Methods

3.3.1 Reagents
PFOS, PFOA, 6:2 FTS, and PFBS were purchased as powders from Synquest Labs (>97% purity) and used to prepare 100 mg/L stock solutions by dissolving the powder in deionized water. Stock solutions were mixed for at least one week before use and stored at 4°C when not in use. Solutions were inversion mixed before taking any subsamples to ensure homogeneous distribution of PFAS. PFOS was technical grade purity, containing 25% branched and 75% linear isomers. PFAS standards used for analytical calibration were purchased from Wellington Labs (PFAC-24PAR) and made up in different concentrations in 1:1 water/methanol. Perfluoropropanoic acid was purchased from Sigma Aldrich. Potassium iodide was purchased from Fluka (98% purity) and sodium sulfite from VWR (98% purity). Sodium bicarbonate (99.9%), sodium hydroxide (97%), acetic acid (99.5%), phenol (98%), calcium sulfate (98%), aluminum sulfate (98%), and methanol (99.9%) were purchased from Sigma-Aldrich. AFFF (Ansul) was sourced from internal inventories and contained 6:2 FtSaB as its predominant PFAS compound.

3.3.2   UV Irradiation Set-Up

All irradiation experiments were performed using a Coospider CTUV (36 W) 254 nm UV lamp. Initial reducing agent investigation and subsequent PFBS optimization experiments were performed in 1 mL UV-transmissible cuvettes (Brandtech ®, VWR) distanced 3.5 cm away from the lamp. The cuvettes were housed in a 3D printed holder and the irradiation was performed in a fume hood with adequate air flow to keep the cuvettes from warming (Figure A3). The volume-normalized photon irradiance for the cuvette set-up was calculated at 3.01 J s^{-1} L^{-1} using chemical actinometry (described in appendix A). Subsequent experiments involving irradiation of PFOS, PFOA, 6:2 FTS, 6:2 FtSaB, and PFBS (individually) were performed in 250 mL beakers with the lamp immersed in each beaker (Figure A3). The volume-normalized photon irradiance for the beaker set-up was calculated at 7.26 J s^{-1} L^{-1} using chemical actinometry. PFBS degradation experiments were also performed using a 1 L beaker to determine the energy efficiency (E_{EO}) of a scaled-up system. In both beaker set-ups the beakers were wrapped in aluminum foil and gentle stirring of the solutions during irradiation was provided by a stir bar. The 250 mL beakers were irradiated in a water basin that was kept at room temperature using ice packs. The 1 L beaker was irradiated without temperature control. Temperature measurements were taken at each sampling point, with the temperature average being 26 ± 2°C.

The initial investigation to identify the best combination of reducing agents was performed with 10 mM of each reagent (sulfite, iodide, or phenol), 10 mM of NaHCO$_3$, 150 mM NaOH (pH 13.2±0.1), and a mixture of PFOS and PFOA (~1 mg/L each), which was activated with UV light for 6 hours. Degradation of PFOS, PFOA, 6:2 FTS, 6:2 FtSaB, and PFBS were investigated individually using 10 mM sulfite, 10 mM iodide, 10 mM NaHCO$_3$, and 150 mM NaOH. The degradation of each PFAS was explored over different time periods based on their recalcitrance, with the sampling periods varied for each PFAS. Controls were run with each experiment, specifically, UV-controls (exposure of PFAS to UV without active reagents) and reagent controls (exposure of PFAS to the active reagents with no UV activation). Experiments in the immersion system were performed in duplicate. Experiments in the cuvette system were performed in triplicate. A complete list of reagent concentrations used in this study can be found in appendix A (Table A2).

3.3.3   PFAS and Fluoride Analysis

Detailed approach to target, non-target, and fluoride analysis is described in appendix A. In brief, target PFAS analysis was performed on a ThermoFisher Exploris 120 Orbitrap coupled to a Vanquish ultra-high-performance liquid chromatography system using a 100 mm x 2.1 mm x 3 µm ACME C18 analytical column. Mobile phases consisted of 5 mM ammonium acetate in deionized (DI)

water (A) and acetonitrile (B). The elution profile started at 90% A/10% B, transitioning to 100% B over 10 minutes, holding for 2 minutes, then equilibrating at starting conditions for 3 minutes, using a flow rate of 0.3 mL/min. Non-target PFAS analysis was performed as described in previous work with an expanded transformation product identification workflow (appendix A) (Patch et al., 2022). Fluoride analysis was performed with a fluoride ion-selective electrode (Fisher Scientific) after diluting samples 1:1 with total ionic strength adjustment buffer.

3.4   Results and Discussion

3.4.1 Phase One – Initial Reagent Selection

Several different UV-activated systems have been explored for the degradation of PFOS (Bentel et al., 2020b; Fennell et al., 2021; Z. Liu et al., 2022; Park et al., 2011). To identify the effectiveness of reagent combination, 20 mg/L of PFOS was subjected to 6 hours of UV irradiation in the presence of 10 mM $NaHCO_3$, 150 mM NaOH (pH 13.2), and 10 mM of sulfite, iodide, or phenol, either independently or combined in different permutations (Figure 3.1).
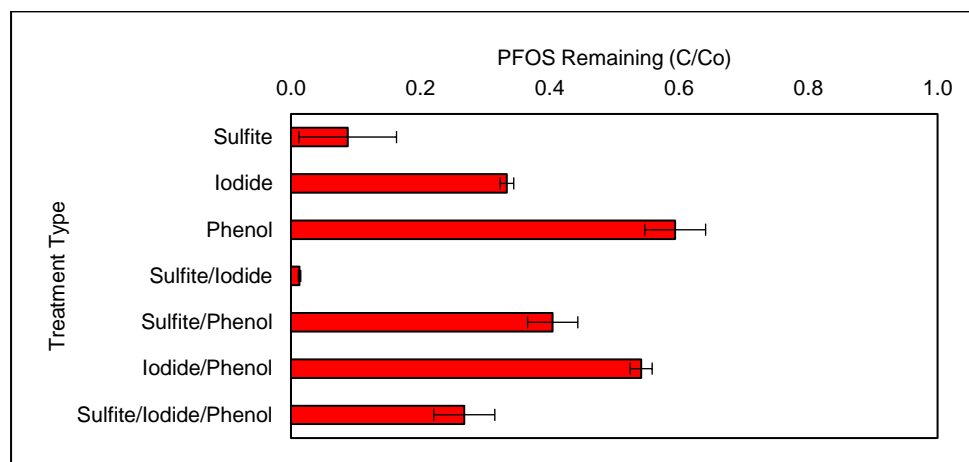
Figure 3.1 Phase 1 reagent investigation exploring the degradation of PFOS in seven different UV-activated systems performed in the cuvette set-up (PFOS C_o = 20 mg/L). Error bars represent the standard deviation of system triplicates. The concentration remaining of PFOS of the different treatment systems were relativized initial PFOS concentration of 20 mg/L. Control samples were amended with $NaHCO_3$ and NaOH only, and not exposed to UV.

3.4.2   Single Reagent Investigation

PFOS underwent 91±8%, 67±1%, and 41±5% degradation in the UV/sulfite, UV/iodide, and UV/phenol systems respectively. The different levels of degradation are due to the quantum yield, molar absorptivity, and aqueous electron quenching reactions occurring in each of the UV activated systems (Table 3.1).

Table 3.1 Quantum yield (Φ) and molar absorptivity (ε, M^{-1} cm^{-1}) (Boschloo and Hagfeldt, 2009; Buxton et al., 1988; Das et al., 1999; Fennell et al., 2021; Li and Hoffman, 1999) for the three individual systems.

Eq	Elementary Reaction	Φ	ε (M^{-1} cm^{-1})
15	$SO_3^{2-} + UV \rightarrow SO_3^{\bullet-} + e^-_{aq}$	0.116	18-20
16	$I^- + H_2O + UV \rightarrow I^\bullet + H_2O + e^-_{aq}$	0.170-0.286	162-220
17	$C_6H_5OH + UV \rightarrow C_6H_5O^\bullet + H^+ + e^-_{aq}$	0.230-0.240	942

Based on the quantum yield and molar absorptivity of the three different reagents, it would be expected that PFOS would be most effectively degraded by phenol, followed by iodide and then sulfite. However, the opposite trend is observed in Figure 3.1 and in work by other researchers (Yu et al., 2018). The reason for this unexpected trend lies in the quenching reactions that can occur in each of the systems.

Each UV system degradation was performed at high pH (150 mM NaOH, pH 13.2), which effectively minimized any aqueous electron quenching by protons (eq 8). However, none of the systems were sparged with nitrogen or another inert gas prior to commencing the reaction. This allowed for dissolved oxygen present in the solution to scavenge electrons in the UV/iodide and UV/phenol systems (k = 1.9 x 10^{10} M^{-1} s^{-1}, eq 7). Conversely, minimal aqueous electron scavenging by oxygen is expected in the UV/sulfite system due to the ability of the anionic radical sulfite to react with oxygen (eq 9) (Li et al., 2014). This results in a higher concentration of aqueous electrons able to react with and degrade PFOS.

Of the three systems, sulfite also has the lowest quenching reaction rate (reaction with an aqueous electron, eq 14) (k <1.5 x 10^6 M^{-1} s^{-1}), although it has been found to become significant at concentrations higher than 10 mM sulfite (Fennell et al., 2021). This allows for higher concentrations of sulfite to be employed for degradation compared to iodide and phenol.

The higher degradation of PFOS in the UV/iodide system compared to the UV/phenol system is due to the complexity of the associated quenching reactions. While the reactive iodide species generated in the UV/iodide system have a higher rate of quenching than phenol (Table 3.2), these systems are complex and dominated by several competing rate constants (eq 19-26, Table 3.2), therefore the aqueous electron quenching reactions are not immediately dominant in the UV/iodide system. Additionally, the iodide radical itself has been hypothesized as capable of reacting

with and degrading PFOS, allowing for more varied degradation pathways to occur (Park et al., 2011, 2009).

Table 3.2 – Rate constants for reactions involved with the quenching of iodide and aqueous electrons, and generation of reactive iodine species (Park et al., 2011; Yu et al., 2018).

Eq	Quenching Reaction	Rate Constant k ($M^{-1}s^{-1}$)
UV/Iodide		
18	$I^{\cdot} + I^{-} \rightarrow I_2^{\cdot-}$	1.2×10^4
19	$I^{\cdot} + I^{\cdot} \rightarrow I_2$	1×10^{10}
20	$I^{\cdot} + I_2^{\cdot-} \rightarrow I_3^{-}$	$>6.4 \times 10^9$
21	$I_2^{\cdot-} + I_2^{\cdot-} \leftrightarrow I_3^{-} + I^{-}$	3.2×10^9
22	$I^{-} + I_2 \rightarrow I_3^{-}$	7.2×10^2
23	$e^{-}_{aq} + I_2 \rightarrow I_2^{\cdot-}$	5.3×10^{10}
24	$e^{-}_{aq} + I_2^{\cdot-} \rightarrow 2I^{-}$	9.0×10^{10}
25	$e^{-}_{aq} + I_3^{-} \rightarrow I^{-} + I_2^{\cdot-}$	3.5×10^{10}

In contrast to the UV/iodide system, phenol will quench aqueous electrons directly ($k = 2.0 \times 10^7$ M^{-1} s^{-1}) and generated phenol radicals will consume the initial phenol through a dimerization reaction ($k = 2.6 \times 10^9$ M^{-1} s^{-1}), reducing the amount of phenol available for aqueous electron generation (Li and Hoffman, 1999). The formation of 2-phenoxyphenol and other phenol dimers were identified in the UV/phenol system after irradiation, providing further evidence to this dimerization reaction. It is possible that these generated phenol dimers are capable of further scavenging aqueous electrons.

3.4.3   *Multiple Component Investigation*

PFOS underwent 98.7±0.2%, 60±4%, 46±2%, and 73±5% degradation in the UV/sulfite/iodide, UV/sulfite/phenol, UV/iodide/phenol, and UV/sulfite/iodide/phenol systems respectively (Figure 3.1). Synergistic reactions present in the UV/sulfite/iodide system are hypothesized to be responsible for the enhanced PFOS degradation, with sulfite capable of scavenging oxygen and converting generated reactive iodine species back to iodide due to the spontaneous redox reaction that can occur (eq 26-28, eq 29-33 in Table 3.3).

$$I^{\cdot} + e^{-} \rightarrow I^{-} \qquad\qquad E° = 1.33 \text{ V} \qquad\qquad\qquad (26)$$

$$SO_3{}^{2-} \rightarrow SO_3{}^{\cdot-} + e^-$$ \qquad E° = -0.73 V \qquad (27)

$$I^\cdot + SO_3{}^{2-} \rightarrow I^- + SO_3{}^{\cdot-}$$ \qquad ΔE° = +0.66 V , ΔG° = -63.7 kJ \qquad (28)
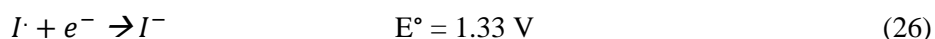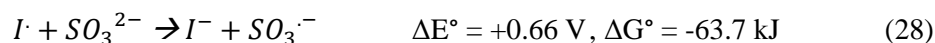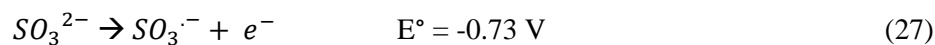
Table 3.3 – Rate constants for reactions between RIS and sulfite, resulting in the regeneration of iodide (Park et al., 2011; Yu et al., 2018).

Eq	Elementary Reactions	Rate Constant k ($M^{-1}s^{-1}$)
UV/Sulfite/Iodide		
29	$I^\cdot + SO_3{}^{2-} \rightarrow I^- + SO_3{}^{\cdot-}$	1.4×10^9
30	$I_2{}^{\cdot-} + SO_3{}^{2-} \rightarrow 2I^- + SO_3{}^{\cdot-}$	1.9×10^8
31	$I_3{}^- + SO_3{}^{2-} \rightarrow 2I^- + ISO_3{}^-$	2.9×10^8
32	$I_2 + SO_3{}^{2-} \rightarrow ISO_3{}^- + I^-$	3.1×10^9
33	$ISO_3{}^- + H_2O \rightarrow SO_4{}^{2-} + I^- + 2H^+$	8.5×10^6 (s^{-1})

The reduced effectiveness of the UV/sulfite/phenol and UV/iodide/phenol systems when compared to the individual UV/sulfite and UV/iodide systems is likely due to the aqueous electron scavenging capacity of phenol. It is possible that in smaller quantities phenol could benefit the UV/iodide system through the regeneration of reactive iodine species back into iodide, but it would not be more effective than sulfite.

3.4.4   *Phase Two – UV Activated Sulfite/Iodide System*

Following its identification as an effective combination of reagents, the UV/sulfite/iodide system (10 mM sulfite, 10 mM iodide, 10 mM bicarbonate, 150 mM hydroxide) was used to degrade PFOS and PFOA, as well as 6:2 FTS, and PFBS. Targeted PFAS analysis and fluoride analysis were performed at different time points for PFOS, PFOA, 6:2 FTS, and PFBS to identify both total degradation and total defluorination (Figure 3.2). Time points were selected to attempt to capture both the initial PFAS degradation and the resultant fluoride generation.
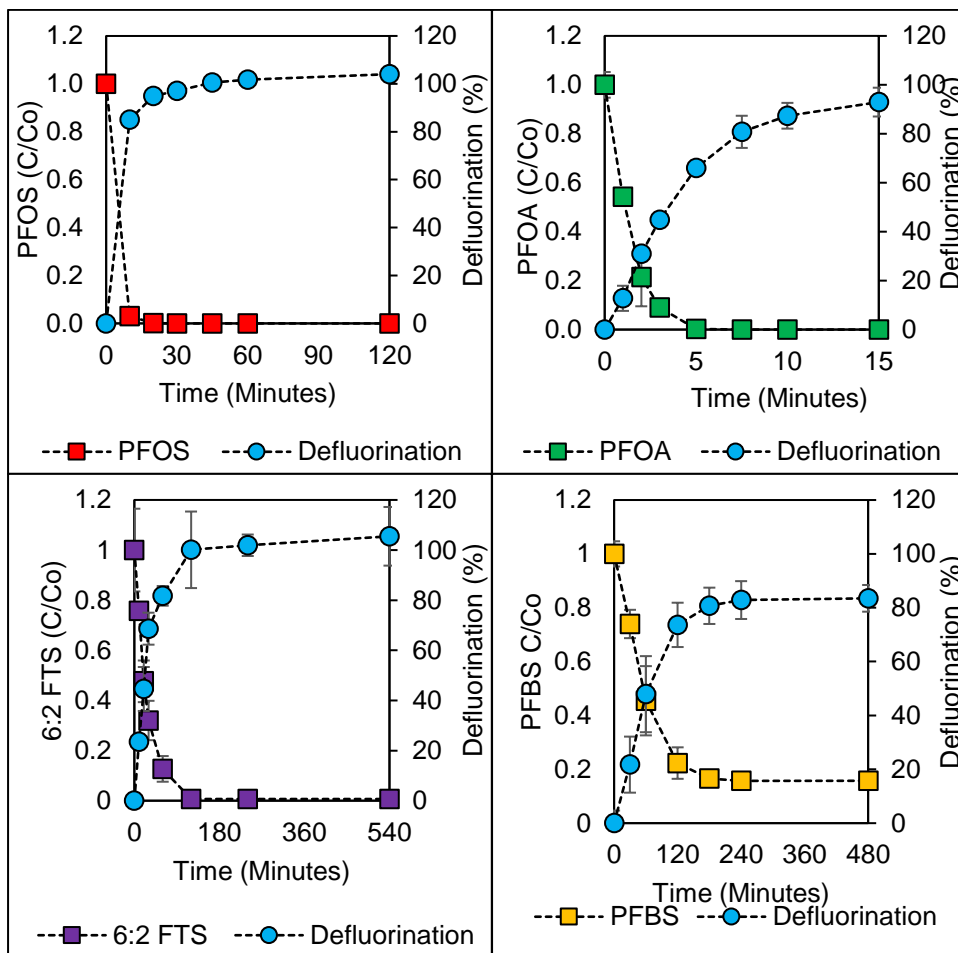
Figure 3.2 – Investigation of PFOS (1 mg/L), PFOA (1 mg/L), 6:2 FTS (1 mg/L), and PFBS (30 mg/L) following UV-activated sulfite/iodide (10 mM SO_3^{2-}, 10 mM I^-, 10 mM HCO_3^-, 150 mM OH^-) degradation reactions in beakers. Error bars are the standard deviation of the experimental duplicates. Some error bars are too small to be seen.

PFOS reached >99.99% degradation (non-detectable in triplicate) by 30 minutes, with >100% defluorination being measured at 45 minutes. The higher PFOS degradation seen in the present study compared to previously reported degradation using a similar system (92 % after 24 hours, Liu *et al*. 2022) is thought to be a result of the increased lamp strength (36 W in the present study vs 18 W in the Liu *et al*. 2022 study), or the higher concentrations of iodide and bicarbonate used in the present study. The lag between PFOS degradation and defluorination was expected (97% destruction at 20 minutes, but only 85% defluorination) as previous authors have found the formation of -F/+H PFSA transformation products. These hydrodefluorinated transformation products are understood to be more recalcitrant than their perfluorinated counterparts (Bentel et al., 2019; Z. Liu et al., 2022). However, these compounds could not be found likely due to the low concentration at which they were formed.

PFOA reached >99.9% degradation by 5 minutes (non-detectable in triplicate), with defluorination reaching 93±6% at 15 minutes. As identified by other authors, PFCAs like PFOA are more susceptible to degradation than PFSAs like PFOS, with PFOA being completely removed more rapidly than PFOS (Bentel et al., 2019; Patch et al., 2022). Based on the rate of defluorination it is believed that complete defluorination would be achieved with a longer irradiation time. The lag between PFOA degradation and fluoride recovery was unexpected, suggesting intermediate transformation products that were more difficult to degrade than PFOA. Subsequent high-resolution analysis revealed the generation of -F/+H PFOA as a function of time (Figure A12), with the highest concentration (~13% of the initial PFOA concentration) at 2 minutes of UV-activation and reaching its lowest concentration of <0.5% by 15 minutes (Figure A5).

6:2 FTS reached >99.9% degradation (non-detectable in triplicate) and >100% defluorination by 120 minutes. The longer degradation time for 6:2 FTS compared to PFOS aligns well with previous observations made in the literature, suggesting that the presence of the central $-CH_2$ moieties results in more resistance to reductive-based degradation strategies (but complete susceptibility to oxidative degradation strategies). These results are similar to the results obtained by Liu *et al*. (2022) (98.9% degradation of 6:2 FTS following 24 hours of irradiation using 10 mM sulfite, 2 mM iodide and 5 mM carbonate, at pH 12). It is important to note that in the Liu *et al*. (2022) study, this irradiation was performed in a 3% NaCl brine, which is different than the deionized water system in the present study.

PFBS was found to undergo 81±1% degradation and reached 83±2% defluorination, plateauing after four hours of irradiation. This is very similar to observations made by Liu *et al*. (2022), where PFBS defluorination reached 78 ± 1% after 24 hours of irradiation. High resolution analysis revealed the trace presence of -nF/+nH (n = 1-4) and -2F, +H, +OH PFBS. The lack of complete PFBS degradation in the present study suggests either a depletion of aqueous electrons, or the formation of highly recalcitrant transformation products that require more aqueous electrons to degrade. However, the short-chain nature of PFBS makes identifying any shorter-chain transformation products difficult. Therefore, identifying the transformation products following the degradation of PFOS and identifying their degradation trends over time may indicate how to better degrade PFBS.

3.4.5   Transformation of PFOS in the UV/Sulfite, UV/Iodide, and UV/Sulfite/Iodide Systems

The identification of a lag period between PFAS degradation and defluorination was expected and hypothesized to be due to the formation of -F/+H exchanged PFAS. However, these transformation products could only be initially identified in appreciable quantities in the degradation of PFOA (starting concentration 1 mg/L).

To confirm these transformation products, PFOS at a higher initial concentration (10 mg/L) was degraded under the UV/sulfite, UV/iodide, and two different UV/sulfite/iodide systems (using reagent concentrations published by Liu *et al.* (2022), and this study) for two hours and the transformation products identified (Figure 3.3).
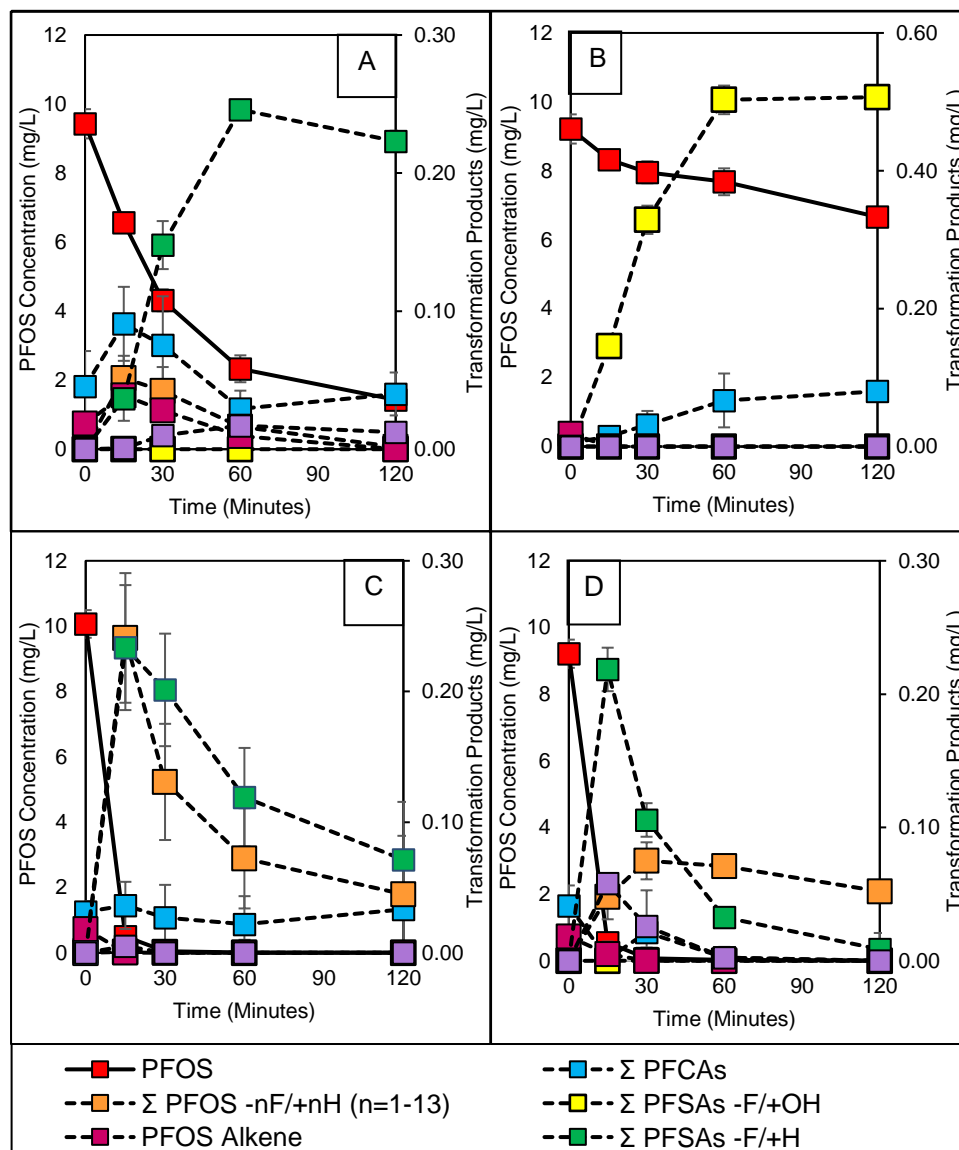
Figure 3.3 – Investigation of PFOS transformation products following degradation in the following systems: A - UV/sulfite, B - UV/iodide, C - UV/sulfite/iodide using conditions by Liu *et al.* (10 mM SO_3^{2-}, 2 mM I^-, 5 mM HCO_3^-, pH 12), and D - UV/sulfite/iodide using conditions in this study (10 mM SO_3^{2-}, 10 mM I^-, 10 mM HCO_3^-, pH 13.2). Dashed line compounds are represented on the second Y-axis, which are semi-quantified.

Several transformation products were found, including PFCAs, $-_nF/+_nH$ PFOS (n=1–13), -F/+OH PFOS/PFHpS, an unsaturated PFOS alkene, -F/+H shorter-chain PFSAs, and -2F/+H, +OH PFOS. In the UV/sulfite (A) and UV/iodide (B) systems, the sum of these semi-quantified transformation products reaches a maximum of ~3% and ~8% of the initial PFOS concentration respectively. In the UV/sulfite/iodide systems (C, D), the sum of these products reaches ~5% and ~4% of the initial PFOS concentration in the first 15 minutes, before degrading to <1% by two hours. It is important to note the added level of uncertainty associated with comparing the semi-quantified concentrations of PFAS transformation products with the standard quantified concentrations of the initial PFOS concentration. For example, quantifying -4F/+4H PFOS using the more accurate 6:2 FTS instrument response yields a concentration 4.5x higher than quantifying it with its original PFOS instrument response.

In the UV/sulfite (A) and UV/sulfite/iodide (C, D) systems the most abundant transformation products are the shorter chain PFSAs with a single -F/+H exchange, PFOS undergoing multiple -F/+H exchanges, and PFCAs. These products have been found by numerous other authors, although the -F/+H shorter-chain PFSAs have previously been attributed to shorter-chain PFSA impurities undergoing an -F/+H exchange through C-F bond cleavage (Bentel et al., 2019). However, evidence in this study suggests that these -F/+H PFSAs are formed mainly from the C-C bond cleavage of PFOS. For example, the identification of -F/+H perfluoropropane sulfonic acid (PFPS) and -F/+H perfluoroethane sulfonic acid (PFES) could only occur through C-C cleavage as PFPS and PFES are not found as impurities in the untreated control or stock solutions. Additionally, the chromatograms of the aforementioned -F/+H PFSAs all suggest a single isomer, which would occur following C-C cleavage, whereas the chromatograms for -F/+H PFOS and -F/+H PFHpS (PFHpS is present as an impurity in the stock solution) suggest multiple isomers, which would occur from C-F bond breakage at various locations and subsequent reaction with water (Figure A7). The presence of C2-C6 single isomer -F/+H PFSAs supports the cleavage of C-C bonds 2-6 in PFOS (Figure A6, A8). This is also supported by PFOS modelling work in the literature, identifying the central C-C bonds as being easier to break than the C1-C2 and C7-C8 carbon bonds (Banayan Esfahani and Mohseni, 2022; Bentel et al., 2019).
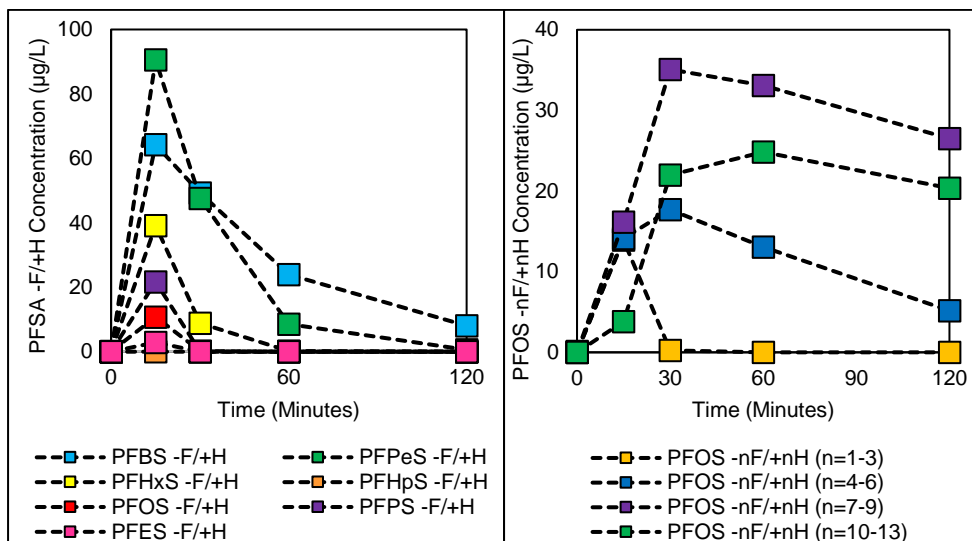
Figure 3.4 – Semi-quantified concentrations of -F/+H shorter-chain PFSAs and -nF/+nH PFOS in the UV/sulfite/iodide system (10 mg/L PFOS, 10 mM SO_3^{2-}, 10 mM I^-, 10 mM HCO_3^-, pH 13.2).

Interestingly, the concentrations of -nF/+nH exchanged PFOS and PFCAs in the UV/sulfite/iodide system with Liu's reagent concentrations are higher than those found using the reagent concentrations in this study. This suggests that the higher concentration of iodide in the UV/sulfite/iodide system allows for more rapid destruction of the recalcitrant PFAS transformation products.

The identification of PFOA in the UV/sulfite and UV/sulfite/iodide systems following the degradation of PFOS provides evidence of C-S bond cleavage. Evidence for C-F, C-C, and C-S bond cleavage indicates that aqueous electrons can attack PFAS at multiple locations, thereby creating multiple degradation pathways (Figure 3.5).

UV System	Σ PFCAs	Σ PFSAs -F/+H	Σ PFOS -nF/+nH (n=1-13)	PFOS Alkene	Σ PFASs -F/+OH	PFOS -2F/ +H, +OH
Sulfite Only	Detected	Detected	Trace Detected	Detected	Not Detected	Detected
Iodide Only	Detected	Detected	Not Detected	Not Detected	Detected	Not Detected
Sulfite/Iodide	Trace Detected	Detected	Detected	Not Detected	Trace Detected	Detected

†Not detected, hypothesized transformation or intermediate product

Figure 3.5 – Proposed transformation pathways for PFOS following C-C, C-F, and C-S bond cleavage based on identified transformation products.

Following C-C bond cleavage (Pathway 1), the resulting carbon radical can react with water, forming either a -F/+H or -F/+OH shorter chain PFSA. Following C-F bond cleavage (Pathway 2), the resulting carbon radical can react with water, forming either a -F/+H or -F/+OH PFOS. The -F/+H PFOS can then undergo a base-catalyzed elimination reaction, resulting in the loss of HF and formation of a PFOS alkene. The alkene can then react with water, forming a -2F/+H, +OH PFOS molecule. It is also possible that this forms directly from a second aqueous electron attack of the -F/+H or -F/+OH PFOS and subsequent reaction with water. Given the fact that up to thirteen -F/+H exchanges on PFOS have been observed, it is possible that a second exchange could involve an OH substitution. Following C-S bond cleavage (Pathway 3), the PFAS radical can react with water to either form a -SO₃/+H fluorinated alkane (not detectable by LC-MS), or a -SO₃/+OH perfluorooctanol (not detected). The perfluorooctanol can undergo subsequent

57

reaction to form perfluorooctanoic acid. The identified transformation products will likely undergo subsequent C-C, C-F, and (if possible), C-S bond cleavage, resulting in eventual full defluorination.

3.4.6   *Degradation and Transformation of 6:2 FtSaB in AFFF*

Following initial degradation trials of PFOS, PFOA, 6:2 FTS, PFBS, and the identification of PFOS transformation products, the transformation of 6:2 fluorotelomer sulfonamidobetaine (6:2 FtSaB) was explored (Figure 3.6). As new PFAS precursors enter the market, it is important to identify if they can be destroyed, and what potential transformation products may occur in the environment. This is of particular concern when dealing with modern AFFF formulations, which can contain numerous isomers and chain lengths of these PFAS precursors, such as 6:2 FtSaB.
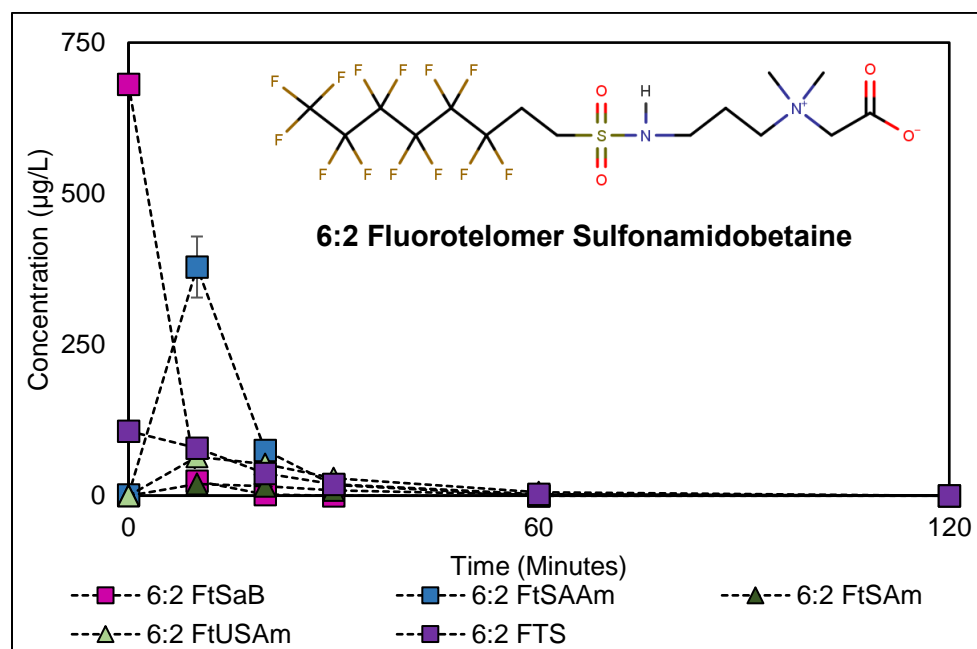
Figure 3.6 – Degradation of 6:2 FtSaB (diluted Ansul) in the UV/SO$_3^{2-}$/I$^-$ system (concentrations here). Error bars are the standard deviation of the beaker duplicates. Some error bars are too small to be seen. Structure of 6:2 FtSaB shown in figure. Concentrations are semi-quantified using PFOSA instrument response.

An initial analysis of the diluted Ansul AFFF identified the presence of two major components: 6:2 FtSaB and 6:2 FTS (Figures A13, A14). Additional PFAS compounds were also identified, including 8:2, 10:2, and 12:2 FtSaB, but in substantially lower quantities relative to the 6:2 FtSaB. Trace amounts of 6:2 fluorotelomer sulfonamidoamine (FtSaAm) were also found in the samples before irradiation.

6:2 FtSaB underwent >99.99% degradation by 20 minutes of irradiation, compared to 120 minutes required to completely degrade 6:2 FTS. Within the first 10 minutes of irradiation, several FtSaB transformation products were identified, or increased in concentration, including 6:2 FtSaAm, 6:2 fluorotelomer sulfonamide (FtSam), and 6:2 fluorotelomer unsaturated sulfonamide (6:2 FTuSam) (Figures 3.6, A15-A17). It is likely that 6:2 FTS is also a transformation product of 6:2 FtSaB, but it is difficult to confirm with 6:2 FTS being present in the sample at the outset. The transformation products themselves are subsequently degraded over time, and no transformation products can be identified by 120 minutes of irradiation. Fluoride analysis was not performed as the initial concentration of 6:2 FtSaB is semi-quantified, and therefore may not provide an accurate initial concentration required for defluorination calculations.

It is hypothesized that the degradation of 6:2 FtSaB follows a series of aqueous electron attacks focused on the nitrogen group in the betaine or sulfonamido moiety (Figure 3.7).
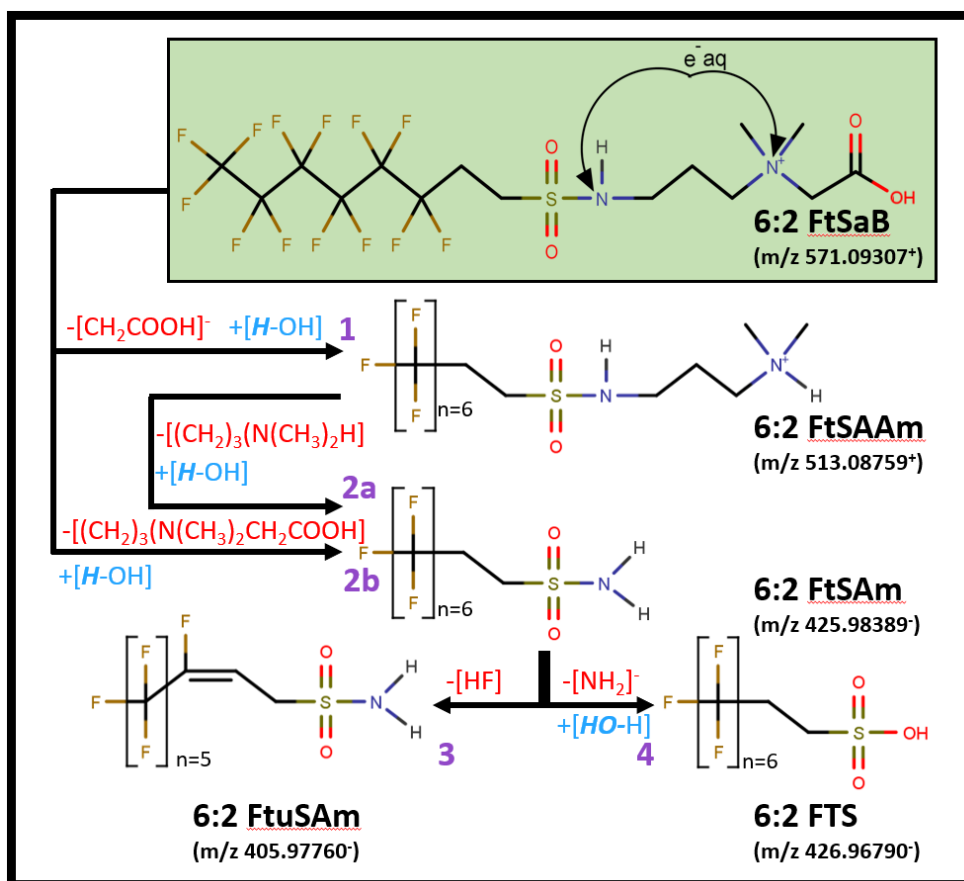
Figure 3.7 – Reductive degradation mechanism of 6:2 FtSaB and subsequent transformation products.

If the reaction proceeds through step 1 in Figure 3.7, an aqueous electron attacks the nitrogen in the betaine functional group, resulting in ejection of an acetic acid moiety. The resulting amine radical will react with water, resulting in a tertiary ammonium salt, the 6:2 FtSaAm molecule. Consecutive aqueous electron attacks of the N in 6:2 FtSaAm may result in a single and then double -CH_3/+H exchange of the methyl moieties on the tertiary ammonium salt, resulting in the generation of the secondary ammonium salt 6:2 FtSaAm (m/z 499.07194$^+$) (detected, not shown in Figure 3.7) and the primary ammonium salt (possible but not detected in this study, likely due to low intensity of the product).

If the reaction proceeds through step 2b initially or proceeds from 6:2 FtSaAm following 2a, aqueous electron attack will occur on the sulfonamido nitrogen, resulting in the ejection of the betaine or ammonium moiety, respectively, both of which will most likely attract a proton from water or intramolecular proton transfer. The newly generated amine radical can then react with water to form 6:2 FtSam. Following reaction 3, aqueous electron attack of the fluorotelomer alkyl chain can result in the formation of an unsaturated 6:2 FtuSam. Lastly, aqueous electron attack of the sulfonamide sulfur atom (reaction 4) will result in the ejection of an -NH_2 anion (quickly converted into NH_3 upon reaction with water) and subsequent reaction of the functional group with water to form 6:2 FtS.

The lack of PFCA transformation products following degradation of 6:2 FtSaB indicates that subsequent degradation likely continues after the formation of 6:2 FTS or 6:2 FtUSAm resulting in complete defluorination, a process identified by this study and others (Bentel et al., 2019; Patch et al., 2022).

3.4.7   *Phase Three - Sulfite/Iodide Optimization Investigation*

Based on previous difficulties degrading PFBS identified in the literature of (Bentel et al., 2019; Z. Liu et al., 2022; Patch et al., 2022), it was hypothesized that PFBS would be difficult to degrade using the initial unoptimized UV/sulfite/iodide system. Following the inability to achieve complete degradation of PFBS, a series of optimization experiments were performed. Initially, the degradation of PFBS was re-run using the standard conditions (10 mM of each sulfite, iodide, bicarbonate, 150 mM hydroxide). The degradation of PFBS under the standard conditions in the cuvette set-up was compared to the findings from the immersion system. PFBS underwent 83±6% degradation in the cuvette system, compared to 81±1% in the immersion system. These results indicate good agreement between the two systems.

The degradation of PFBS was then explored under five new conditions (shown in Table A2), including an initial iodide concentration of 20 mM, an initial sulfite concentration of 20 mM and 50 mM, adding 10 mM sulfite at 2 and 4 hours, and

having a system with both an initial sulfite concentration of 20 mM and sequential additions of 10 mM sulfite after two and four hours of irradiation (Figure 3.8).
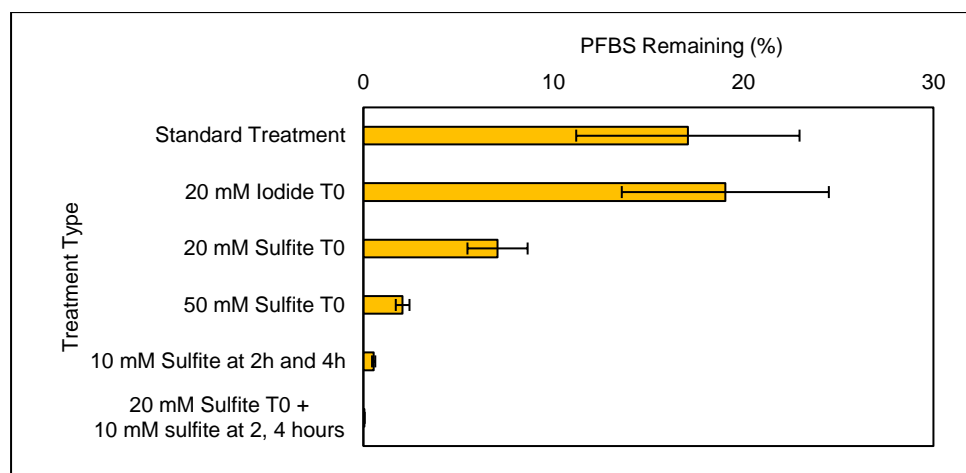
Figure 3.8 – Investigation of PFBS (C_o = 24.2±0.3 mg/L PFBS) degradation under six different treatments. *Standard treatment* (10 mM SO_3^{2-}, 10 mM I^-, 10 mM HCO_3^-, 150 mM OH^-). *20 mM Iodide T0* (10 mM SO_3^{2-}, 20 mM I^-, 10 mM HCO_3^-, 150 mM OH^-). *20 mM Sulfite T0* (20 mM SO_3^{2-}, 10 mM I^-, 10 mM HCO_3^-, 150 mM OH^-). *50 mM Sulfite T0* (50 mM SO_3^{2-}, 10 mM I^-, 10 mM HCO_3^-, 150 mM OH^-). *10 mM Sulfite at 2h and 4h* (10 mM SO_3^{2-}, 10 mM I^-, 10 mM HCO_3^-, 150 mM OH^- with 10 mM SO_3^{2-} added at 2 hours and 4 hours). *20 mM Sulfite T0 + 10 mM Sulfite at 2, 4 hours* (20 mM SO_3^{2-}, 10 mM I^-, 10 mM HCO_3^-, 150 mM OH^-, with 10 mM SO_3^{2-} added at 2 hours and 4 hours).

Doubling the initial sulfite concentration from 10 mM to 20 mM resulted in an increased degradation of PFBS, from 81±6% to 93±2%. This contrasts with previous work (Liu *et al*. 2022), where almost no increase in degradation was observed when going from 10 mM to 20 mM sulfite. However, the present experiments used a different sulfite/iodide ratio (2:1) from the ratio used for the optimal PFBS degradation (5:1) ratio in Liu *et al*. (2022). The increased degradation in the present study suggests that an increase in sulfite concentration can assist in degradation if starting with higher concentrations of iodide.

Increasing the initial concentration of iodide from 10 mM to 20 mM had no effect on PFBS degradation, due to the aqueous electron scavenging effect that occurs with iodide, especially at higher concentrations.

Increasing the initial concentration of sulfite to 50 mM did improve degradation, increasing it to 97.9±0.4%. However, this does demonstrate substantial diminishing returns in degradation, most likely due to the fact that sulfite scavenges aqueous electrons at higher concentrations, as discussed previously.

Degradation of PFBS following two additions of 10 mM sulfite at two hours and four hours resulted in an increase in degradation from 80±7% to 99.5±0.1%. This

results in a total added sulfite concentration of 30 mM (3:1 sulfite/iodide). Adding the sulfite at regular intervals allows the iodide reaction to be regenerated and last for a longer duration as it is consumed through both UV-activation and reaction with reactive iodide species. It also minimizes the scavenging of aqueous electrons by sulfite at higher concentrations.

The final system tested was the combination of 20 mM sulfite initially, followed by 10 mM sulfite spikes at two and four hours. This resulted in 99.95±0.02% of PFBS within six hours, at a final reagent concentration of 40 mM of sulfite and 10 mM of iodide. This combination appeared to provide the best combination of reagents required to reach virtually complete degradation of PFBS in 6 hours.

To better understand the role of sulfite on PFBS degradation a kinetics experiment was performed with 10:10 sulfite: iodide, 50 mM sulfite:iodide and (20+10+10+10):10 sulfite:iodide (Figure 3.9, where sulfite:iodide are represented by S:I).
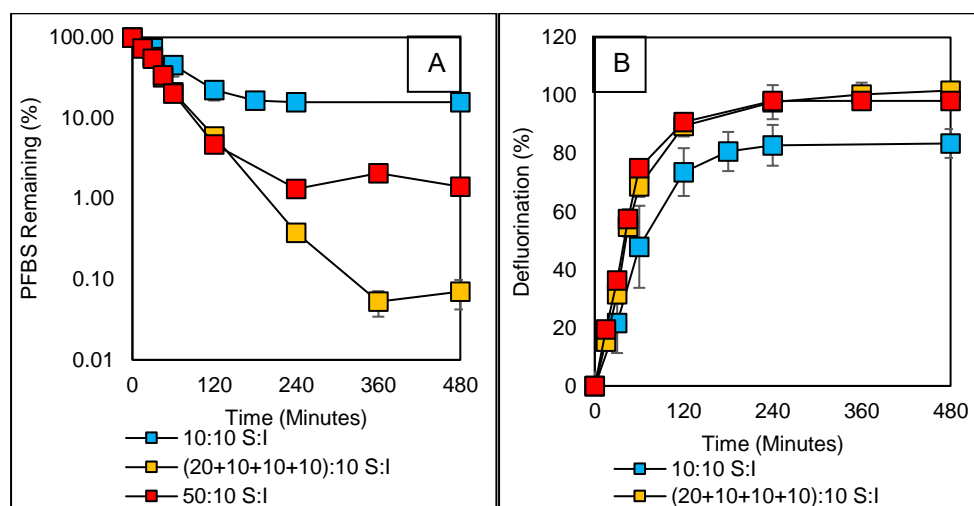
Figure 3.9 – Investigation of PFBS degradation (A) and defluorination (B) under three different sulfite concentrations in the UV/sulfite/iodide system. Error bars are the standard deviation of cuvette triplicates. 10 mM of sulfite added every two hours for the (20+10+10+10):10 sulfite/iodide system.

The rate constants for the degradation of PFBS was found to be 0.76 h^{-1}, 1.57 h^{-1}, and 1.46 h^{-1} for the first two hours of the 10:10, 50:10, and (20+10+10+10):10 sulfite: iodide systems, respectively ($R^2 > 0.99$). However, the (20+10+10+10):10 sulfite:iodide system continues to follow first order decay kinetics for up to six hours, albeit with a slightly decreased rate (1.29 h^{-1}, $R^2 > 0.99$), whereas the 10:10 and 50:10 sulfite:iodide systems appear to plateau after two and four hours, respectively. This provides evidence of the importance of subsequent sulfite additions, as it

maintains the reaction conditions and allows the destruction of PFBS to follow a first order decay rate.

3.4.8   *Phase Four - Degradation of PFBS Using Optimized Sulfite/Iodide System*

The system changes identified as most influential on PFBS degradation in the optimization investigation were (1) an increase to the initial sulfite concentration (10 mM to 20 mM) and (2) adding 10 mM of sulfite at regular intervals during the reaction (every two hours). These two changes were combined to investigate the degradation of PFBS (~30 mg/L) over an 11-hour irradiation period in the cuvette system (Figure 3.10).
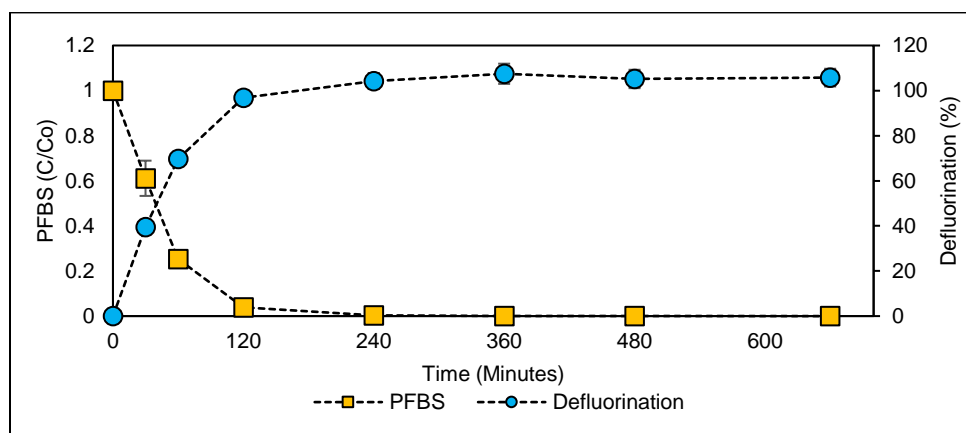
Figure 3.10 – Degradation of 30 mg/L PFBS in cuvettes using an optimized UV/sulfite/iodide system (20 mM SO_3^{2-}, 10 mM I^-, 10 mM HCO_3^-, 150 mM OH^-, 11 hours total irradiation) and 10 mM sulfite added at 2, 4, 6, and 8 hours (60 mM sulfite total). Error bars are the standard deviation of the cuvette triplicates. Some error bars are too small to be seen.

The optimized system results in the addition of 60 mM sulfite and 10 mM iodide (6:1), with 40 of the 60 mM being added in 10 mM increments every two hours over the course of the degradation. The optimized system resulted in >99.9% degradation of PFBS (30.4 mg/L to 0.7 μg/L, below the quantitation limit but above the detection limit, with one of the three triplicates being non-detect). Total defluorination (as measured) of PFBS was also achieved, with the resultant measured fluoride equating to 106 ± 4% defluorination. The rate of degradation of PFBS followed a first order decay, with a rate constant of 1.08 h^{-1} over the 11-hour period (R^2 = 0.98) (1.31 h^{-1} over the first 6 hours, R^2 = 0.99), confirming that regular additions of sulfite allows for a first order decay rate for PFBS (Figure A9).

To identify the EE/O of the system (defined as the electrical energy consumed to lower the pollutant concentration by one order-of-magnitude), the optimized

UV/sulfite/iodide system was employed in a one-liter beaker set-up, irradiating 800 mL of PFBS-impacted DI water (11 mg PFBS/L) (Figure A10). The EE/O can be determined from the following equation:

$$E_{EO} = -\ln\left(\frac{C}{C_0}\right) * \frac{P}{kV}$$

Where P is the power of the lamp (kW), k is the first order rate constant (h^{-1}), and V is the volume of water (m^3). With a lamp power of 0.036 kW, first order rate constant of ~0.89 h^{-1}, and water volume of 0.0008 m^3, the E$_{EO}$ was calculated as 116 kW h m^{-3} (Figure A11). The first order rate constant for the degradation of PFBS using the optimized UV/sulfite/iodide system in the beaker is 4.7x faster than that found in work by Liu *et al*., resulting in the E$_{EO}$ value calculated in this study being half the E$_{EO}$ value found by Liu *et al*. using their energy-saving setting (116 kW h m^{-3} compared to 230 kW h m^{-3}) (Z. Liu et al., 2022). This is likely due to optimized reagent concentrations and a higher lamp strength. The higher lamp strength also resulted in an increased temperature in the beaker, with the solution reaching 64°C due to gradual heating with no cooling water bath.

With PFBS reported as the most recalcitrant PFAS to date, the demonstrated complete degradation and defluorination achieved with this optimized UV/sulfite/iodide system represents a promising method to destroy PFAS present in aqueous matrices.

3.5 Conclusions

This study examined the use of a UV-activated sulfite/iodide system for the degradation of PFOS, PFOA, 6:2 FTS, 6:2 FtSaB, and PFBS. Complete or near-complete defluorination was achieved for PFOS, PFOA, and 6:2 FTS using the initially investigated reagent concentrations. Several transformation products were identified following the degradation of PFOS and 6:2 FtSaB, providing a mechanistic understanding into these compounds' degradation upon being subjected to an aqueous-electron rich environment. Detailed understanding of the underlying sulfite/iodide chemistry and transformation products allowed for a mechanistic understanding to be presented. Initial failure to reach complete PFBS degradation resulted in the development of an optimized UV/sulfite/iodide system, consisting of a higher initial sulfite concentration and sulfite additions at intervals over the course of the reaction. These optimized conditions achieved the study goal of complete defluorination of PFBS, currently understood to be the most recalcitrant individual PFAS. The complete destruction of all investigated PFAS suggests that this system could be applied to aqueous matrices impacted with a wide and novel range of PFAS compounds, including PFSAs, PFCAs, and fluorotelomers. Future work will benefit from investigating the impact of co-contaminants, aqueous matrices containing high

organic matter, and the effectiveness of the UV/sulfite/iodide system on a wider range of relevant PFAS, such as GenX.

3.6 Acknowledgements

3.7 References

Abusallout, I., Wang, J., Hanigan, D., 2021. Emerging investigator series: Rapid defluorination of 22 per- And polyfluoroalkyl substances in water using sulfite irradiated by medium-pressure UV. En-viron Sci (Camb) 7, 1552–1562. https://doi.org/10.1039/d1ew00221j

Bachman, B.F., Zhu, D., Bandy, J., Zhang, L., Hamers, R.J., 2022. Detection of Aqueous Solvated Electrons Produced by Photoemission from Solids Using Transient Absorption Measurements. ACS Measurement Science Au 2, 46–56. https://doi.org/10.1021/acsmeasuresciau.1c00025

Banayan Esfahani, E., Mohseni, M., 2022. Fluence-based photo-reductive decomposition of PFAS us-ing vacuum UV (VUV) irradiation: Effects of key parameters and decomposition mechanism. J Environ Chem Eng 10, 107050. https://doi.org/10.1016/j.jece.2021.107050

Battye, N.J., Patch, D.J., Roberts, D.M.D., O'Connor, N.M., Turner, L.P., Kueper, B.H., Hulley, M.E., Weber, K.P., 2022. Use of a horizontal ball mill to remediate per- and polyfluoroalkyl substances in soil. Science of The Total Environment 835, 155506. https://doi.org/https://doi.org/10.1016/j.scitotenv.2022.155506

Bentel, M.J., Liu, Z., Yu, Y., Gao, J., Men, Y., Liu, J., 2020. Enhanced Degradation of Perfluorocar-boxylic Acids (PFCAs) by UV/Sulfite Treatment: Reaction Mechanisms and System Efficiencies at pH 12. Environ Sci Technol Lett 7, 351–357. https://doi.org/10.1021/acs.estlett.0c00236

Bentel, M.J., Yu, Y., Xu, L., Li, Z., Wong, B.M., Men, Y., Liu, J., 2019. Defluorination of Per- and Polyfluoroalkyl Substances (PFASs) with Hydrated Electrons: Structural Dependence and Impli-cations to PFAS Remediation and Management. Environ Sci Technol 53, 3718–3728. https://doi.org/10.1021/acs.est.8b06648

Boschloo, G., Hagfeldt, A., 2009. Characteristics of the iodide/triiodide redox mediator in dye-sensitized solar cells. Acc Chem Res 42, 1819–1826. https://doi.org/10.1021/ar900138m

Bruton, T.A., Sedlak, D.L., 2017. Treatment of Aqueous Film-Forming Foam by Heat-Activated Persulfate under Conditions Representative of in Situ Chemical Oxidation. Environ Sci Technol 51, 13878–13885. https://doi.org/10.1021/acs.est.7b03969

Buck, R.C., Franklin, J., Berger, U., Conder, J.M., Cousins, I.T., Voogt, P. de, Jensen, A.A., Kannan, K., Mabury, S.A., van Leeuwen, S.P.J., 2011. Perfluoroalkyl and polyfluoroalkyl substances in the environment: Terminology, classification, and origins. Integr Environ Assess Manag 7, 513–541. https://doi.org/10.1002/ieam.258

Buxton, G. V., Greenstock, C.L., Helman, W.P., Ross, A.B., 1988. Critical Review of rate constants for reactions of hydrated electrons, hydrogen atoms and hydroxyl radicals (·OH/·O− in Aqueous Solution. J Phys Chem Ref Data 17, 513–886. https://doi.org/10.1063/1.555805

Chen, G., Liu, S., Shi, Q., Gan, J., Jin, B., Men, Y., Liu, H., 2022. Hydrogen-polarized vacuum ultravi-olet photolysis system for enhanced destruction of perfluoroalkyl substances. Journal of Hazard-ous Materials Letters 3, 100072. https://doi.org/10.1016/j.hazl.2022.100072

Das, T.N., Huie, R.E., Neta, P., 1999. Reduction potentials of SO3 center dot-, SO5 center dot-, and S4O6 center dot 3- radicals in aqueous solution. Journal of Physical Chemistry A 103, 3581–3588.

Dombrowski, P.M., Kakarla, P., Caldicott, W., Chin, Y., Sadeghi, V., Bogdan, D., Barajas-Rodriguez, F., Chiang, S.Y.D., 2018. Technology review and evaluation of different chemical oxidation con-ditions on treatability of PFAS. Remediation 28, 135–150. https://doi.org/10.1002/rem.21555

Duchesne, A.L., Brown, J.K., Patch, D.J., Major, D., Weber, K.P., Gerhard, J.I., 2020. Remediation of PFAS-Contaminated Soil and Granular Activated Carbon by Smoldering Combustion. Environ Sci Technol 54, 12631–12640. https://doi.org/10.1021/acs.est.0c03058

Fennell, B.D., Mezyk, S.P., McKay, G., 2021. Critical Review of UV-Advanced Reduction Processes for the Treatment of Chemical Contaminants in Water. ACS Environmental Au. https://doi.org/10.1021/acsenvironau.1c00042

Gu, J., Ma, J., Jiang, J., Yang, L., Yang, J., Zhang, J., Chi, H., Song, Y., Sun, S., Tian, W.Q., 2017. Hydrated electron (eaq−) generation from phenol/UV: Efficiency, influencing factors, and mecha-nism. Appl Catal B 200, 585–593. https://doi.org/10.1016/j.apcatb.2016.07.034

Hori, H., Nagaoka, Y., Sano, T., Kutsuna, S., 2008. Iron-induced decomposition of perfluorohex-anesulfonate in sub- and supercritical water. Chemosphere 70, 800–806. https://doi.org/10.1016/j.chemosphere.2007.07.015

Hori, H., Yamamoto, A., Hayakawa, E., Taniyasu, S., Yamashita, N., Kutsuna, S., Kiatagawa, H., Ara-kawa, R., 2005. Efficient decomposition of environmentally persistent perfluorocarboxylic acids by use of persulfate as a photochemical oxidant. Environ Sci Technol 39, 2383–2388. https://doi.org/10.1021/es0484754

Houtz, E.F., Sedlak, D.L., 2012. Oxidative conversion as a means of detecting precursors to perfluoro-alkyl acids in urban runoff. Environ Sci Technol 46, 9342–9349. https://doi.org/10.1021/es302274g

Lassalle, J., Gao, R., Rodi, R., Kowald, C., Feng, M., Sharma, V.K., Hoelen, T., Bireta, P., Houtz, E.F., Staack, D., Pillai, S.D., 2021. Degradation of PFOS and PFOA in soil and groundwater samples by high dose Electron Beam Technology. Radiation Physics and Chemistry 189, 109705. https://doi.org/10.1016/j.radphyschem.2021.109705

Li, C., Hoffman, M.Z., 1999. One-Electron Redox Potentials of Phenols in Aqueous Solution. Journal of Physical Chemistry B 103, 6653–6656. https://doi.org/10.1021/jp983819w

Li, X., Fang, J., Liu, G., Zhang, S., Pan, B., Ma, J., 2014. Kinetics and efficiency of the hydrated elec-tron-induced dehalogenation by the sulfite/UV process. Water Res 62, 220–228. https://doi.org/10.1016/j.watres.2014.05.051

Liu, Z., Bentel, M.J., Yu, Y., Ren, C., Gao, J., Pulikkal, V.F., Sun, M., Men, Y., Liu, J., 2021. Near-Quantitative Defluorination of Perfluorinated and Fluorotelomer Carboxylates and Sulfonates with Integrated Oxidation and Reduction. Environ Sci Technol 55, 7052–7062. https://doi.org/10.1021/acs.est.1c00353

Liu, Z., Chen, Z., Gao, J., Yu, Y., Men, Y., Gu, C., Liu, J., 2022. Accelerated Degradation of Per-fluorosulfonates and Perfluorocarboxylates by UV/Sulfite + Iodide: Reaction Mechanisms and System Efficiencies. Environ Sci Technol 56, 3699–3709. https://doi.org/10.1021/acs.est.1c07608

Mahinroosta, R., Senevirathna, L., 2020. A review of the emerging treatment technologies for PFAS contaminated soils. J Environ Manage 255, 109896. https://doi.org/10.1016/j.jenvman.2019.109896

Merino, N., Qu, Y., Deeb, R.A., Hawley, E.L., Hoffmann, M.R., Mahendra, S., 2016. Degradation and Removal Methods for Perfluoroalkyl and Polyfluoroalkyl Substances in Water. Environ Eng Sci 33, 615–649. https://doi.org/10.1089/ees.2016.0233

Mifkovic, M., van Hoomissen, D.J., Vyas, S., 2022. Conformational distributions of helical perfluoroal-kyl substances and impacts on stability. J Comput Chem 43, 1656–1661. https://doi.org/10.1002/jcc.26967

Park, H., Vecitis, C.D., Cheng, J., Choi, W., Mader, B.T., Hoffmann, M.R., 2009. Reductive defluori-nation of aqueous perfluorinated alkyl surfactants: Effects of ionic headgroup and chain length. Journal of Physical Chemistry A 113, 690–696. https://doi.org/10.1021/jp807116q

Park, H., Vecitis, C.D., Cheng, J., Dalleska, N.F., Mader, B.T., Hoffmann, M.R., 2011. Reductive deg-radation of perfluoroalkyl compounds with aquated electrons generated from iodide photolysis at 254 nm. Photochemical and Photobiological Sciences 10, 1945–1953. https://doi.org/10.1039/c1pp05270e

Patch, D., O'Connor, N., Koch, I., Cresswell, T., Hughes, C., Davies, J.B., Scott, J., O'Carroll, D., We-ber, K., 2022. Elucidating degradation mechanisms for a range of per- and polyfluoroalkyl sub-stances (PFAS) via controlled irradiation studies. Science of the Total Environment 832, 154941. https://doi.org/10.1016/j.scitotenv.2022.154941

Qu, Y., Zhang, C., Li, F., Chen, J., Zhou, Q., 2010. Photo-reductive defluorination of perfluorooctano-ic acid in water. Water Res 44, 2939–2947. https://doi.org/10.1016/j.watres.2010.02.019

Sauer, M.C., Crowell, R.A., Shkrob, I.A., 2004. Electron photodetachment from aqueous anions. 1. Quantum yields for generation of hydrated electron by 193 and 248 nm laser photoexcitation of miscellaneous inorganic anions. Journal of Physical Chemistry A 108, 5490–5502. https://doi.org/10.1021/jp049722t

Trojanowicz, M., Bartosiewicz, I., Bojanowska-Czajka, A., Kulisa, K., Szreder, T., Bobrowski, K., Nichipor, H., Garcia-Reyes, J.F., Nałęcz-Jawecki, G., Męczyńska-Wielgosz, S., Kisała, J., 2019. Application of ionizing radiation in decomposition of perfluorooctanoate (PFOA) in waters. Chemical Engineering Journal 357, 698–714. https://doi.org/10.1016/j.cej.2018.09.065

Trojanowicz, M., Bartosiewicz, I., Bojanowska-Czajka, A., Szreder, T., Bobrowski, K., Nałęcz-Jawecki, G., Męczyńska-Wielgosz, S., Nichipor, H., 2020. Application of ionizing radiation in de-composition of perfluorooctane sulfonate (PFOS) in aqueous solutions. Chemical Engineering Journal 379, 122303. https://doi.org/10.1016/j.cej.2019.122303

Trojanowicz, M., Bojanowska-Czajka, A., Bartosiewicz, I., Kulisa, K., 2018. Advanced Oxida-tion/Reduction Processes treatment for aqueous perfluorooctanoate (PFOA) and perfluorooc-tanesulfonate (PFOS) – A review of recent advances. Chemical Engineering Journal 336, 170–199. https://doi.org/10.1016/j.cej.2017.10.153

Tseng, N.S., 2012. Feasibility of Biodegradation of Polyfluoroalkyl and Perfluoroalkyl Substances. eScholarship 23, 401–516.

Turner, L.P., Kueper, B.H., Jaansalu, K.M., Patch, D.J., Battye, N., El-Sharnouby, O., Mumford, K.G., Weber, K.P., 2021. Mechanochemical remediation of perfluorooctanesulfonic acid (PFOS) and perfluorooctanoic acid (PFOA) amended sand and aqueous film-forming foam (AFFF) impacted soil by planetary ball milling. Science of the Total Environment 765, 142722. https://doi.org/10.1016/j.scitotenv.2020.142722

Wang, S., Yang, Q., Chen, F., Sun, J., Luo, K., Yao, F., Wang, X., Wang, D., Li, X., Zeng, G., 2017. Photocatalytic degradation of perfluorooctanoic acid and perfluorooctane sulfonate in water: A critical review. Chemical Engineering Journal 328, 927–942. https://doi.org/10.1016/j.cej.2017.07.076

Yang, L., He, L., Xue, J., Ma, Y., Xie, Z., Wu, L., Huang, M., Zhang, Z., 2020. Persulfate-based deg-radation of perfluorooctanoic acid (PFOA) and perfluorooctane sulfonate (PFOS) in aqueous solu-tion: Review on influences, mechanisms and prospective. J Hazard Mater. https://doi.org/10.1016/j.jhazmat.2020.122405

Yu, K., Li, X., Chen, L., Fang, J., Chen, H., Li, Q., Chi, N., Ma, J., 2018. Mechanism and efficiency of contaminant reduction by hydrated electron in the sulfite/iodide/UV process. Water Res 129, 357–364. https://doi.org/10.1016/j.watres.2017.11.030

Zhang, Z., Chen, J.J., Lyu, X.J., Yin, H., Sheng, G.P., 2014. Complete mineralization of perfluorooc-tanoic acid (PFOA) by γ-irradiation in aqueous solution. Sci Rep 4, 1–6. https://doi.org/10.1038/srep07418

4. Investigating the UV/Sulfite + Iodide System to Mineralize Per and Polyfluoroalkyl Substances (PFAS) in the Presence of Complex Matrices: Implications for Treatment of AFFF Concentrates

Natalia O'Connor†, David Patch†, Michael Bentel†††, Iris Koch†, Kevin G. Mumford ††, Kela Weber†*

† Department of Chemistry and Chemical Engineering, Royal Military College of Canada, Kingston, ON, Canada

††Department of Civil Engineering, Queen's University, Kingston, ON, Canada.

†††Department of Chemical and Environmental Engineering, Cincinnati, Ohio

* Corresponding Author: Kela.Weber@rmc.ca

4.1 Introduction

PFAS are a growing class of ubiquitous, anthropogenic, fluorinated recalcitrant chemicals with links to several negative health effects (Buck et al., 2011b; Olsen et al., 2017; Sunderland et al., 2019b; Wang et al., 2021). Their presence in aqueous matrices is of particular concern, representing a main exposure pathway for uptake into biological receptors. Significant research has focused on the development of technologies to destroy PFAS present in aqueous systems, with ultraviolet-light activated advanced reductive processes (UV-ARPs) showing promise for their abilities to effectively generate highly reducing (-2.87 V) aqueous electrons (Fennel et al., 2021). The reduction potential of these aqueous electrons has the capability to break the recalcitrant bonds present in PFAS (Fennel et al., 2021).

The use of UV-ARP systems to destroy PFAS has been investigated by several researchers, examining the type and concentrations of photosensitizers used (e.g. sulfite, iodide, phenol), presence of dissolved oxygen, system pH, effects of electron scavengers (e.g. nitrate, nitrite), system volume, photon fluence rate, and the effect of molecule structure (e.g. chain length, functional group, fluorine saturation) on PFAS recalcitrance (Abusallout et al., 2021; Bentel et al., 2020a, 2019a; Liu et al., 2021b; O'Connor et al., 2023; Tenorio et al., 2020). These investigations have resulted in iterative improvements to the effectiveness of the studied UV-ARP systems by maximizing the generation and utilization of aqueous electrons, which have been identified in studies as responsible for initiating the degradation of a wide range of PFAS species (Bentel et. al., 2019, O'Connor et. al., 2023).

The use of sulfite and iodide as photosensitizers in the UV-ARP system (hereafter referred to as the UV/S+I system) has been found to achieve a high degree of defluorination of various PFAS, including PFOS, PFOA, 6:2 FTS, and PFBS (Cao et al., 2021; Z. Liu et al., 2022; O'Connor et al., 2023). The complete defluorination of PFBS is particularly noteworthy as it has not been accomplished in previously studied single component UV-ARP systems (e.g. UV/S, UV/I). In the UV/S+I system, the use of UV light activates iodide and sulfite anions, resulting in the generation of aqueous electrons, sulfite radical anions, and iodide radicals:

$$SO_3^{2-} + h\nu \rightarrow SO_3^{-\cdot} + e_{aq}^- \qquad (1)$$
$$I^- + h\nu \rightarrow I^\cdot + e_{aq}^- \qquad (2)$$
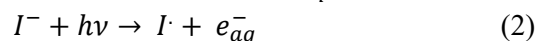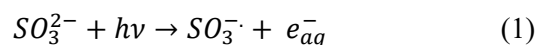
Subsequent reduction of the iodide radical by sulfite regenerates the iodide anion ($K=1.4 \times 10^9$ M^{-1} s^{-1}), while generating additional sulfite radical anions:

$$I^\cdot + SO_3^{2-} \rightarrow I^- + SO_3^{-\cdot} \qquad (3)$$
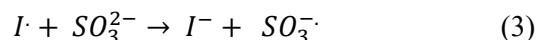
Following equations 1–3, the activation of one sulfite and one iodide anion with UV light will generate two aqueous electrons, and two sulfite radicals. When considering the higher molar absorptivity and quantum yield of iodide, it is more accurate to

consider iodide the primary photosensitizer in this study, with the generation of sulfite radicals occurring mainly from the regeneration of iodide and a smaller contribution from direct UV activation. In addition to sulfite regenerating iodide, the subsequent generation of sulfite radicals enables the removal of dissolved oxygen from solution:

$$SO_3^- \cdot + O_2 \rightarrow SO_5^- \cdot \qquad (4)$$

The removal of dissolved oxygen from solution in the UV/S+I system is important to avoid the scavenging of aqueous electrons by dissolved oxygen. Work by Cao et al. (2021) has identified that the UV/S system can act as a reducing system (anaerobic) or oxidizing system (aerobic) depending on the presence and replenishment of dissolved oxygen. As dissolved oxygen is consumed and peroxymonosulfate radicals are generated, they will subsequently undergo reaction with sulfite, or other peroxymonosulfate (PMS) radicals, to form sulfate and sulfate radicals:

$$SO_5^- \cdot + SO_3^{2-} \rightarrow SO_4^- \cdot + SO_4^{2-} \qquad (5)$$
$$2SO_5^- \cdot \rightarrow 2SO_4^- \cdot + O_2 \qquad (6)$$
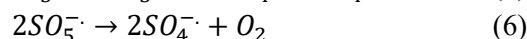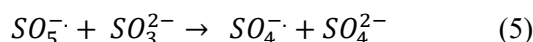
While the peroxymonosulfate and sulfate radicals are both strongly oxidizing species (2.5-3.1 V), they can also react with other dissolved species, like hydroxide and carbonate, to generate the respective radicals (Das, 2001; Deister and Warneck, 1990; Guan et al., 2011; Liu et al., 2018; Medinas et al., 2007; Ross and Neta, 1982):

$$SO_4^- \cdot + OH^- \rightarrow SO_4^{2-} + OH \cdot \qquad (7)$$
$$SO_4^- \cdot + CO_3^{2-} \rightarrow SO_4^{2-} + CO_3^- \cdot \qquad (8)$$
$$OH \cdot + CO_3^{2-} \rightarrow OH^- + CO_3^- \cdot \qquad (9)$$
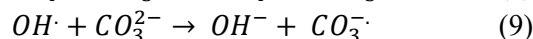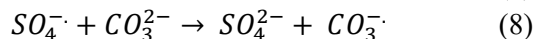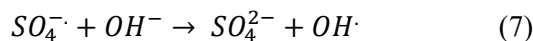
With equations 1–9 in mind, several authors have identified the oxidation of different substrates, including perchlorate, isopropanol, nitrate, and various pharmaceuticals, by the oxidizing species generated in the UV/sulfite system (Amador et al., 2023; Fennell et al., 2021; Guan et al., 2011; Liu et al., 2018). However, the potential for these oxidizing radicals to support the defluorination of PFAS, in particular -F/+H PFAS transformation products, has not been previously discussed or postulated for the UV/S+I system, despite the presence of these radicals being identified in other aqueous remediation technologies (e.g. gamma irradiation, electron beam) (Patch et al., 2022; Trojanowicz et al., 2018; Zhang et al., 2014). Furthermore, the oxidizing radicals generated may enable the UV/S+I system to maintain effective PFAS destruction in the presence of different aqueous electron scavengers, such as nitrate, dissolved organic matter, or high concentrations of PFAS itself (Fennel et al., 2021, 2022, 2023). Liu identified OH⋅ species as conducive for promoting defluorination within the UV/S+I mechanism. However, research into other oxidative species has not been explored.

To this end, the specific objectives of this study are to: 1) evaluate parent PFAS degradation and defluorination in the presence of several reductive and oxidative scavengers; 2) optimize the system parameters to promote destruction of high concentrations of PFAS, 3) apply the optimized conditions to evaluate the treatment effectiveness of legacy and modern AFFF formulations, and 4) use the data derived from objectives 1–3 to postulate a mechanism of PFAS degradation and defluorination initiated by aqueous electrons, but subsequently driven by a mix of oxidative and reductive species. The outcome of this work will further improve understanding of the underlying mechanism (s) responsible for the effective degradation and defluorination of PFAS in the UV/S+I system.

4.2 Materials and Methods

4.2.1 Reagents

All PFAS stock solutions (PFOS, 6:2 FTS, PFBS) were prepared by dissolution of powders purchased from Synquest Labs (>97% purity) in MilliQ ® deionized water. Stock solutions were mixed for at least one week prior to use and stored at 4°C when not in use. PFAS calibration standards were purchased from Wellington Labs®. Potassium iodide was purchased from Fluka (98% purity) and sodium sulfite from VWR (98% purity). Sodium bicarbonate (99.9%), sodium hydroxide (97%), acetic acid (99.5%), butyl carbitol (99%), isopropanol (99.9%) and methanol (99.9%) were purchased from Sigma-Aldrich. Four AFFF formulations (3M, National Foam 1982, National Foam 1990, Ansul) were selected from internal inventories and were previously identified as being PFSA-, PFCA-, 6:2 FTSaB-, and FtB-dominant respectively (Patch et al. 2024).

4.2.2 Experimental Design

The experimental trials in this study were performed in two phases, with the first phase focusing on the effect of different concentrations of scavengers on PFAS destruction using the UV/S+I system, and the second phase investigating the effectiveness of the UV/S+I system for the destruction of two dilute AFFF formulations and a concentrated PFBS solution (600 mg/L).

In the first phase, different concentrations of butyl carbitol, methanol, isopropanol, nitrate, and carbonate were investigated as scavengers using PFOS, 6:2 FTS, and/or PFBS as model PFAS compounds. Butyl carbitol was selected at an upper concentration of 1000 mM due to its presence and similar concentration in AFFF formulations (Harding-Marjanovic et al., 2015b). Methanol was selected as a simple oxidizing agent scavenger, with its resultant oxidized form (formaldehyde) being relatively non-reactive (Wilkinson & Hamer, 2007). Isopropanol was selected as an oxidizing agent scavenger, but with a resultant oxidized form (acetone) functioning an aqueous electron scavenger (Hunt and Chase, 1977; Fennel et. al., 2023). The concentrations of methanol and isopropanol were selected according to

concentrations having an impact on PFAS degradation in preliminary investigations. Nitrate was selected as another (well-studied) aqueous electron scavenger, of interest because it has a high bimolecular rate constant, and can be present in natural, industrial, and wastewater systems. Different concentrations of bicarbonate were investigated as the exact role of bicarbonate in various aqueous remediation technologies (e.g. UV-ARP, UV-AOP, gamma irradiation, electron beam) is unknown, with different studies identifying either an enhancement or inhibition of PFAS destruction (references).

For the investigations of butyl carbitol, methanol, isopropanol, and nitrate, PFOS and 6:2 FTS were selected as the PFAS chemicals to be studied due to their prevalence in legacy and modern AFFF formulations, as well as their sensitivity to different reductive and oxidative radicals (Barzen-Hanson et al., 2017b; Houtz and Sedlak, 2012b; Javed et al., 2020; Patch et al., 2022). It was hypothesized that different reductive or oxidative radical scavengers would have different impacts on the degradation of PFOS and 6:2 FTS. PFBS was selected as the PFAS of study for the bicarbonate trials due to its slower rate of degradation compared to PFOS and 6:2 FTS allowing for easier determination as to the impacts of different bicarbonate concentrations (Liu et al., 2022; Bentel et al., 2020). For example, preliminary bicarbonate trials using PFOS and 6:2 FTS were inconclusive due to their faster rate of degradation compared to PFBS. A summarized list of the experiments and their variable of interest can be seen in Table 4.1. For a complete description of the experimental protocol for each trial, please see Appendix B.

Table 4.1- Experimental trials performed in this study, evaluating the degradation and defluorination of PFOS, 6:2 FTS, PFBS, and AFFF under different scenarios. O.F.= organic fluorine. P.A.= pipette addition. S.P. = syringe pump.

	Interferent		PFAS		UV System			
	Compound	**Concentration**	**Compound**	**Concentration**	**Reactor Type**	**Reagent Concentration SO_3^{2-}, I^-, HCO_3^-, OH^- (mM)**	**Time (Hours)**	**Figure**
Scavenger Investigation	Butyl carbitol	0-1000 mM	PFOS	5 μM	Cuvette	50, 10, 10, 150	4	4.1
		0-100 mM	6:2 FTS	5 μM				4.1
	Methanol	0-6200 mM (0-25% v:v)	PFOS	4 μM	Cuvette	50, 10, 10, 150	4	4.2
	Isopropanol	0-3300 mM (0-25% v:v)	PFOS	4 μM				4.2
	Nitrate	0-50 mM NaNO₃	PFOS	5 μM	Cuvette	50, 10, 10, 150	4	4.3
			6:2 FTS	5 μM				4.3
	Bicarbonate	0-100 mM NaHCO₃	PFBS	50 μM	Cuvette	50, 10, X, 150	6	4.4
	Tap Water	~1 mM CaCO₃						
	Hydroxide/pH	0-500 mM NaOH	PFBS	10 μM	Cuvette	50, 10, 10, X	6	B3
System Evaluation	N/A	N/A	3M AFFF	~50 μM OF	1L Beaker w/ P.A.	(20+10+10+10+10), 10, 10, 150	10	4.5
	N/A	N/A	Ansul AFFF	~40 μM OF	1L Beaker w/ P.A.	(20+10+10+10+10), 10, 10, 150	10	4.5
	N/A	N/A	PFBS	2000 μM	1L Beaker w/ S.P.	20 + 10 mM SO_3^{2-}/hour (dropwise) (140, 10, 10, 150)	12	4.6

4.2.3 PFAS and Fluoride Analysis

Analysis of fluoride and PFAS concentrations were performed as described in previous work (O'Connor et al., 2023). In brief, target PFAS analysis and analysis of PFAS transformation products were performed using a ThermoFisher Exploris 120 Orbitrap coupled to a Vanquish ultra-high-performance liquid chromatography system using a 100 mm x 2.1 mm x 3 μm ACME C18 analytical column. Mobile phases consisted of 0.1% acetic acid in deionized (DI) water (A) and acetonitrile (B). The elution profile started at 90% A:10% B, transitioning to 100% B over 6 min, holding for 2 min, then equilibrating at starting conditions for 4 min, using a flow rate of 0.3 mL/min. For details on PFAS analysis, including the detection and semi-quantitation of PFAS transformation products, please see previous work (O'Connor et al., 2023). Initial fluoride analysis identified significant matrix effects in the

presence of high concentrations of alcohols. For details on this matrix effect and the applied correction factor, please see Appendix B.

4.3 Results and Discussion

4.3.1 Effect of Butyl Carbitol on PFAS Degradation and Defluorination

The impacts of different BC concentrations are shown in Figure 4.1. Aqueous electron-initiated degradation of both 6:2 FTS and PFOS were inhibited by the presence of BC, albeit to different extents. The degradation of PFOS was unaffected by 100 mM of BC, whereas only 60% of 6:2 FTS was degraded at the same concentration. At 1000 mM of BC, PFOS underwent ~40% degradation, with ~20% defluorination.
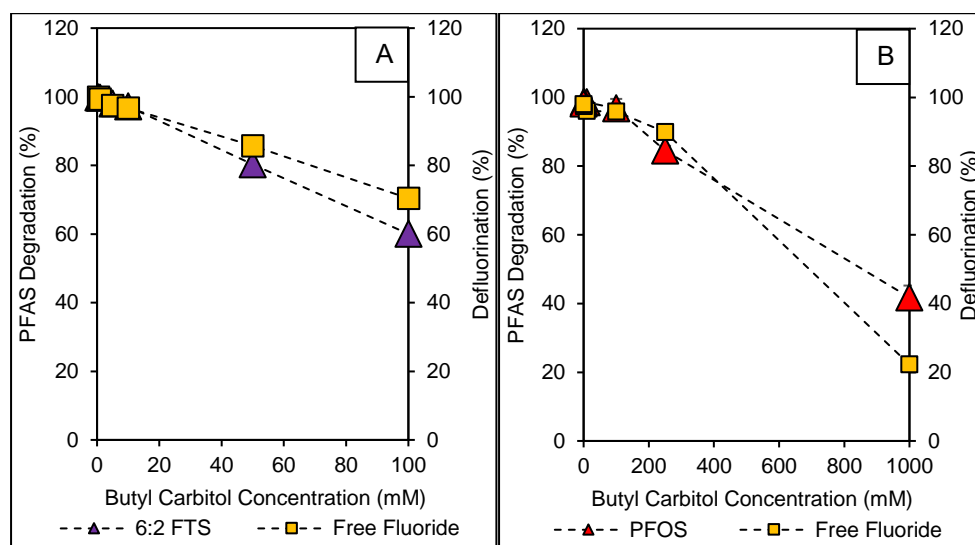
Figure 4.1 PFAS degradation and defluorination of (A) 6:2 FTS and (B) PFOS, following application of the UV/S+I system (50 mM Na2SO3, 10 mM KI, 10 mM NaHCO3, 150 mM NaOH) in the presence of butyl carbitol. Data points are the average of triplicates. Error bars are the standard deviation of the triplicates. Some error bars are too small to be seen.

The difference in 6:2 FTS and PFOS degradation in the presence of BC provides insight into the radical (s) responsible for their initial degradation. It is well understood that PFOS is immune to degradation using oxidative radicals but that 6:2 FTS is particularly susceptible, resulting in the generation of PFCAs (Houtz and Sedlak, 2012b; Javed et al., 2020; Patch et al., 2022; Yang et al., 2020). At the same time, the presence of -CH2 moieties in the fluoroalkyl chain of 6:2 FTS increases the recalcitrance of the molecule to reduction-driven degradation (Bentel et al., 2019; Liu et al., 2021b). Therefore, the inhibition of 6:2 FTS degradation in the presence of smaller amounts of BC (relative to the concentration that inhibited PFOS

76

degradation) suggests that 6:2 FTS is degraded at least in part by oxidative radical mechanisms, with which the BC is interfering. It is likely that, at higher concentrations, BC is able to exert enough of an aqueous electron scavenging effect to also inhibit the degradation of PFOS.

The ability for low concentrations of BC to inhibit the degradation of fluorotelomers suggests that an oxidative pre-treatment may be required to remove DOM before subjecting it to degradation in the UV/S+I system. This would have the added benefit of converting fluorotelomers into PFCAs, which are degraded substantially faster than fluorotelomers and PFSAs in the UV/S+I system (Liu et al., 2021b; O'Connor et al., 2023).

4.3.2 Effect of Methanol, and Isopropanol on PFAS Degradation and Defluorination

The use of BC as a model DOM substrate is relevant to AFFF treatment scenarios but may be too complex of a molecule to best elucidate mechanistic impacts, especially considering that different DOM species can have a wide range of aqueous electron scavenging rates (Fennell et al., 2023). To this end, methanol and isopropanol were selected to investigate their impact on the degradation and defluorination of PFOS. The impacts of methanol and isopropanol on PFOS degradation and defluorination are shown in Figure 4.2.
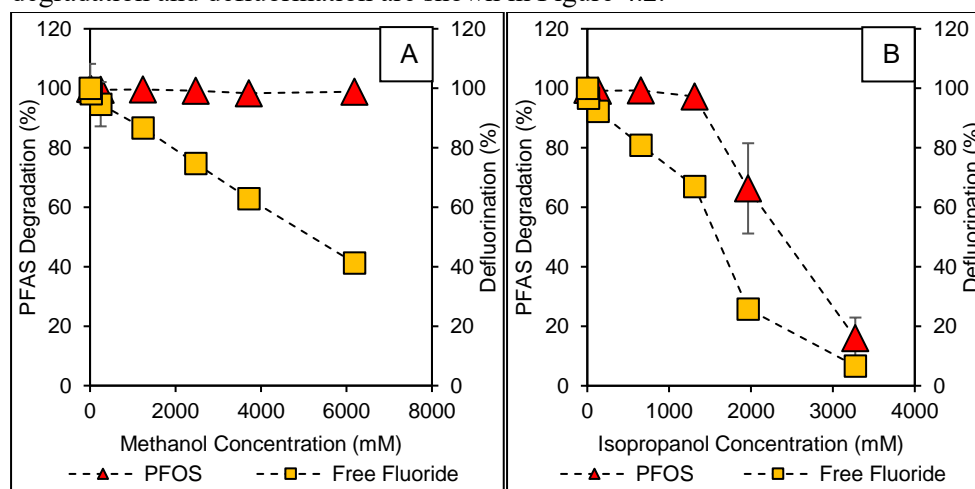
Figure 4.2 PFAS degradation and defluorination of PFOS following application of the UV/S+I system (50 mM Na_2SO_3, 10 mM KI, 10 mM $NaHCO_3$, 150 mM NaOH) (A) in the presence of methanol, and (B) isopropanol. Data points are the average of triplicates. Error bars are the standard deviation of the triplicates. Some error bars are too small to be seen.

Degradation of PFOS was found to be unaffected at all concentrations of methanol evaluated, with >98% degradation observed up to and including 6200 mM of MeOH. However, subsequent defluorination of the degraded PFOS was inhibited, with only 41% defluorination noted at 6200 mM of MeOH (Figure 4.2A). These results support

the hypothesis that, while PFOS degradation is initiated by aqueous electrons, its resultant defluorination is driven by a mix of oxidative and reductive radicals.

Degradation of PFOS in the presence of isopropanol was unaffected up to a concentration of 1300 mM of isopropanol (Figure 4.2B), with PFAS degradation decreasing at higher isopropanol concentrations. At 3300 mM of isopropanol, only 16% of PFOS was degraded. As was observed with methanol, isopropanol inhibits defluorination of PFOS at all concentrations, with only 7% defluorination occurring at 3300 mM of isopropanol (Figure 4.2B). These results further support the hypothesis that PFAS degradation is initiated by aqueous electrons (which is only inhibited at isopropanol concentrations >1300 mM, due to the generation of acetone, an aqueous electron scavenger), and PFAS defluorination is supported by both oxidative and reductive mechanisms (with the oxidative mechanisms being quenched in the presence of isopropanol and methanol).

The non-reactivity of aqueous electrons with alcohols like methanol and isopropanol is well studied (Hunt and Chase, 1977; Jortner et al., 1963; Okazaki and Freeman, 1978). Deister and Warneck reported the oxidative conversion of isopropanol to acetone in the UV/sulfite system, identifying the sulfite radical (SO_3^{-}) as being responsible for the reaction (Deister and Warneck, 1990).

4.3.3 Effect of Nitrate on PFAS Degradation and Defluorination

Both nitrate and nitrite have been identified as potent aqueous electron scavengers in the UV/sulfite system (Fennell et al., 2021), with several authors identifying complete inhibition of PFAS degradation until the nitrate/nitrite is removed from the reaction. The impact of nitrate on the degradation and defluorination of PFOS and 6:2 FTS can be seen in Figure 4.3.
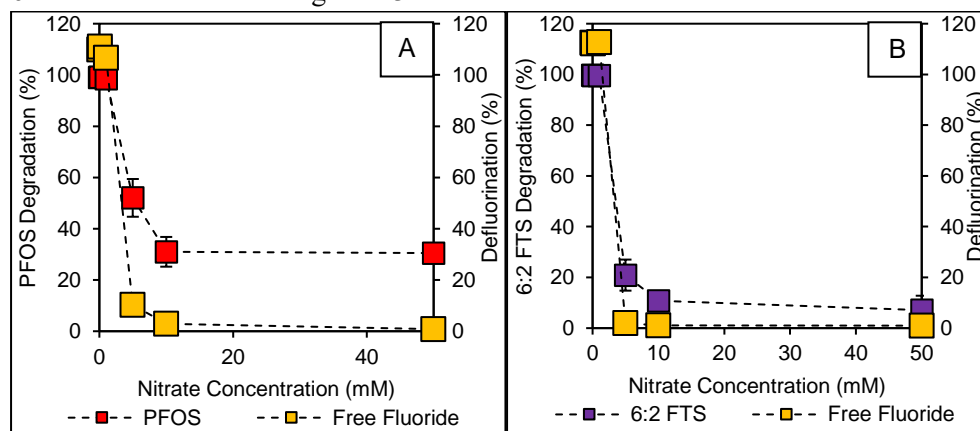
Figure 4.3 Degradation and defluorination of (A) PFOS and (B) 6:2 FTS with different concentrations of NO_3^{-} in the UV/S+I system (20 mM Na_2SO_3, 10 mM KI, 10 mM $NaHCO_3$,

150 mM NaOH, 4 hours). Data points are the average of triplicates. Error bars are the standard deviation of the triplicates. Some error bars are too small to be seen.

It was identified that both PFOS and 6:2 FTS were completely defluorinated in the presence of up to 1 mM nitrate, after which the extent of PFAS degradation and defluorination was substantially inhibited. Even at the highest nitrate concentration evaluated (50 mM), PFOS was degraded by approximately 30%, compared to only 7% degradation of 6:2 FTS. It is possible that different reactive iodine species were generated (e.g. I^-, I_2, I_3^-), which may have initiated conversion of PFOS to semi-volatile perfluoroalkyl iodide species (e.g. $C_8F_{17}I$) (O'Connor et al., 2023; Park et al., 2009; Vecitis et al., 2009). Visual inspection of the reaction cuvettes supports this hypothesis, as the solution with 10 mM and 50 mM nitrate had a characteristic iodine brown/yellow coloration, and the rubber cuvette lids were stained purple from iodine vapour.

These results suggest that UV/S+I system modifications would be required to degrade PFAS in nitrate-containing waters (>1 mM NO_3^-). Increasing the initial sulfite concentration, or adding more sulfite earlier in the UV-activation period, may be sufficient in eliminating nitrate from the solution. There are also several other processes that could be employed to remove nitrate, such as chemical denitrification using powdered aluminum or nano zero valent iron (nZVI) (Sharma and Chander Sobti, 2012; Siciliano, 2015).

4.3.4 Effect of Carbonate on PFAS Degradation and Defluorination

The impacts of different bicarbonate concentrations of the degradation of PFBS can be seen in Figure 4.4. PFBS degradation and defluorination were affected differently by the presence and concentration of carbonate. Without carbonate, ~8% PFBS was remaining after six hours of UV-irradiation. Similar rates of PFBS degradation and defluorination were observed in the presence of 10 mM CO_3^{2-}-amended DI water and unadjusted tap water (~ 1 mM $CaCO_3$).
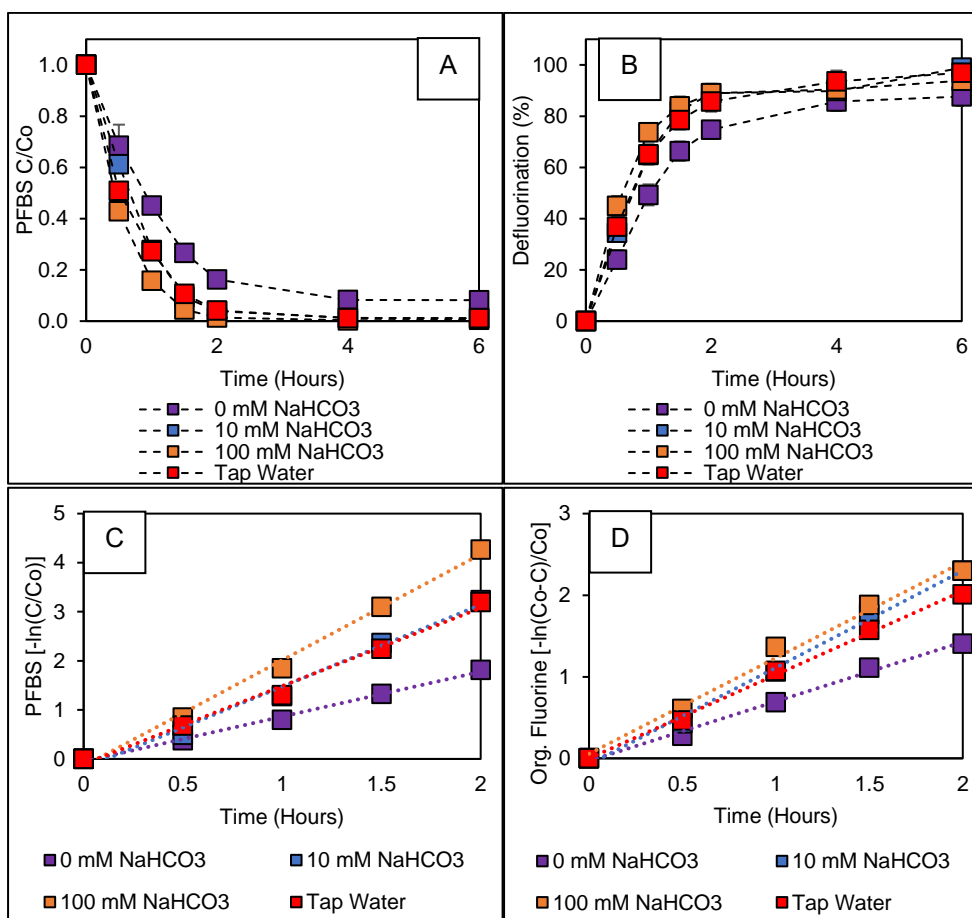
Figure 4.4 (A) Degradation of PFBS, (B) resultant defluorination, (C) first order rate law of PFBS degradation, and (D) first order rate law of resultant free fluoride generation in the UV/S+I system (50 mM Na$_2$SO$_3$, 10 mM KI, 150 mM NaOH) for six hours. Data points are the average of triplicates. Error bars are the standard deviation of the triplicates. Some error bars are too small to be seen.

In the first two hours of the reaction, the presence of 100 mM of CO$_3^{2-}$ resulted in a faster rate of PFAS degradation and defluorination, but correspondingly appeared to inhibit defluorination by the end of the six-hour treatment, although it is difficult to identify due to the similar extent of total defluorination (99±4% defluorination with 10 mM CO$_3^{2-}$, compared to 94±4% defluorination with 100 mM CO$_3^{2-}$).

It is hypothesized that, in the first two hours of the reaction, the higher concentration of carbonate promotes the longevity of generated aqueous electrons by quenching generated oxidative species (Amador et al., 2023; Busset et al., 2007; Liu et al., 2016; Medinas et al., 2007; Yan et al., 2019). However, as PFBS degradation proceeds and various polyfluorinated transformation products accumulate, they cannot be oxidatively defluorinated as effectively due to the same quenching by carbonate. It is important to note that this effect appears to be minor, as the end levels of defluorination are within one standard deviation of each other. Nevertheless, the

hardness of PFAS-impacted water should be considered when using the UV/S+I system, especially when considering carbonate's ability to buffer the pH of the system. Supplemental investigations have confirmed that a system pH of 12.5–13 is optimal, with decreases in PFAS degradation at hydroxide concentrations <50 mM and >150 mM (Figure B3).

4.3.5 Degradation of a Legacy and Modern AFFF Formulation

Previous work by O'Connor et al. investigated the degradation of an FTSaB-dominant AFFF foam using the UV/S+I system (10 mM SO_3^{2-}, 10 mM I^-, 10 mM HCO_3^-, 150 mM OH^-) (O'Connor et al., 2023). This was done to identify potential transformation products resulting from applied UV/S+I treatment. In this study, two diluted (1000x) AFFF formulations (3M and Ansul) were selected for investigation, with analysis focused on the degradation of initial parent compounds, high resolution analysis of transformation products, and identification of defluorination as a function of released free fluoride (Figure B5, B6). An overview of the results for the degradation of diluted 3M and Ansul formulations is presented in Figure 4.5.
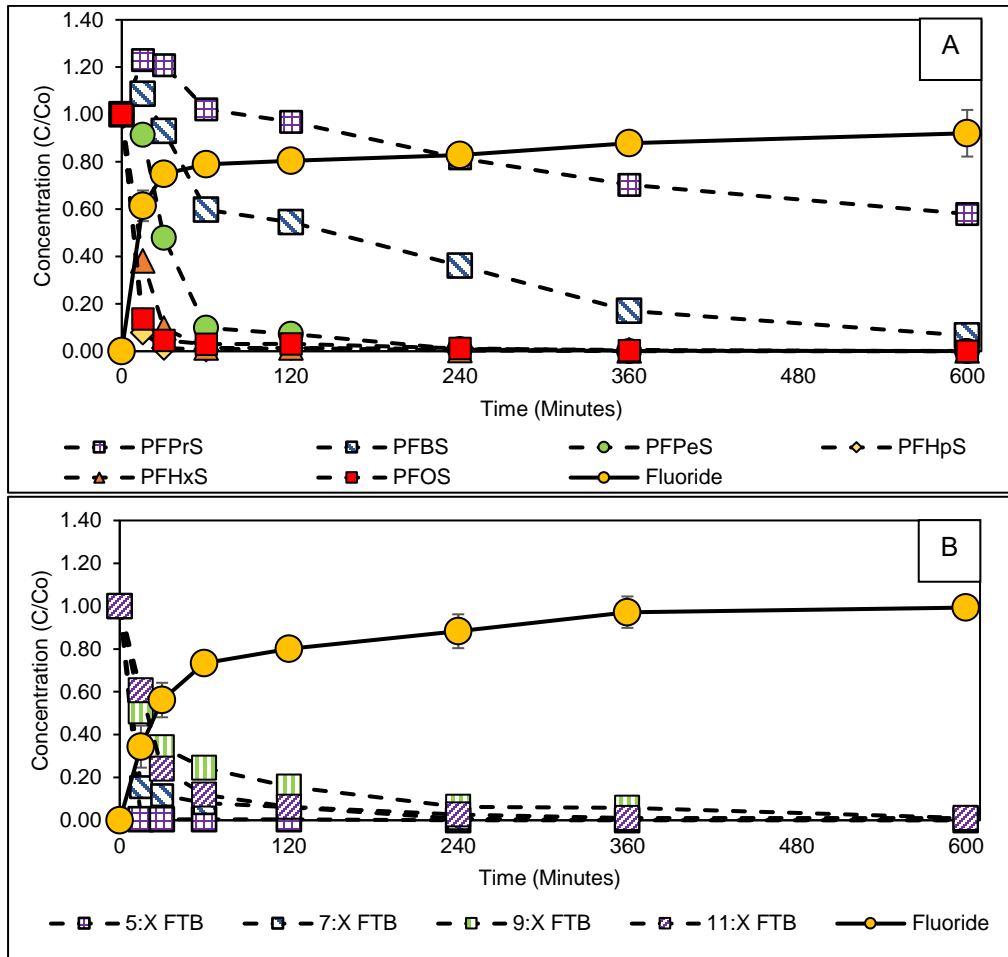
Figure 4.5 (A) Degradation of PFAS in a dilute (1000x) 3M formulation and (B) dilute (1000x) Ansul formulation, using the (20+10+10+10+10):10 UV/S+I system. (ΣPFAS$_{3M}$ C$_0$= ~700 µg/L, ΣPFAS$_{Ansul}$ C$_0$= ~250 µg/L, semi-quantified). The fluoride C/C$_0$ was calculated using the total reducible fluoride yield (appendix, Figure B4). Data points are the average of triplicates. Error bars are the standard deviation of the triplicates. Some error bars are too small to be seen.

Degradation of the PFSA-dominant 3M AFFF formulation resulted in rapid degradation of $\geq$C5 PFSAs, with PFBS and PFPrS having displayed a high degree of recalcitrance. Both PFBS and PFPrS also increased in concentration in the first hour of treatment, before eventually decreasing, suggesting the conversion of PFAS precursors was occurring (e.g. perfluorobutane sulfonamide). Visual inspection of the post-remediation chromatograms identified several previously identified (O'Connor et. al., 2023) transformation products, including -F/+H exchanged PFSAs. Overall, defluorination (based on the total reducible fluoride concentration determined using the UV/S+I system on a more diluted sample) was found to be 92±10% (Figure B5).

High resolution analysis of the FtB-dominant Ansul AFFF formulation identified the initial presence of fluorotelomer betaine compounds of various chain structures (X:3, X:1:2, 4:N, 6:N, 8:N FtB, where X=5, 7, 9, 11 or 1:2, and N=2, 4). Degradation of the 5:3 and 5:1:2 FtB compounds were fastest, with 9:3 and 9:1:2 FtB compounds being degraded the slowest. The presence of fluorotelomer amines (FtAms) were also detected in the initial Ansul formulation and were found to increase in concentration as the FtB compounds were degraded to FtAms. This conversion of betaine-containing fluorotelomers to their corresponding amine product has been noted in previous work (O'Connor et al., 2023), and has been hypothesized to follow aqueous electron attack of the nitrogen atom, resulting in C-N bond cleavage and reaction of the resulting PFAS amine radical with a hydrogen radical, to form the FtAm.

Identifying the extent of defluorination in the Ansul formulation is complicated by the major discrepancy between the TOP-derived organic fluorine concentration and the amount of fluoride generated following application of the UV/S+I system (Figure B6). When comparing to the TOP-derived organic fluorine concentration, defluorination was found to be 181±10%, indicating that a substantial amount of PFAS is unaccounted for in the TOP assay. To provide a better estimate as to the total amount of reducible organic fluorine present in the formulation, the UV/S+I system was applied to a series of a highly diluted AFFF samples (x10,000, n=6) with the hypothesis that the average free fluoride generated following the degradation of these samples would approach a 'true' total organic fluoride value. Using this reducible organic fluorine value, total defluorination was found to be 99±5%. A limitation of this approach is that using the same underlying technique (UV/S+I) to self-validate the defluorination extent is inappropriate, and future work would benefit from the use of other total organic fluorine measurement tools (e.g. combustion ion chromatography).

4.3.6 Effect of High PFAS Concentration on PFAS Degradation and Defluorination

Several studies, including this work, have identified successful degradation of PFAS present in dilute AFFF formulations using UV-ARP systems (Tenorio et al. 2020). One of the challenges in treating less diluted AFFF formulations is identifying the source of any reduced system effectiveness. The previous sections in the present study have identified that several species present within AFFF, such as butyl carbitol, methanol and isopropanol, can interfere with the UV/S+I system's effectiveness. However, it is also important to evaluate the effects of the high PFAS concentrations themselves. To this end, a sub-critical micelle concentration of PFBS (600 mg/L of PFBS) was subjected to destruction using a scaled-up, sulfite drip-fed UV/S+I system. This system was used as it allowed for a continuous addition of sulfite to the system for an extended duration (Figure 4.6).
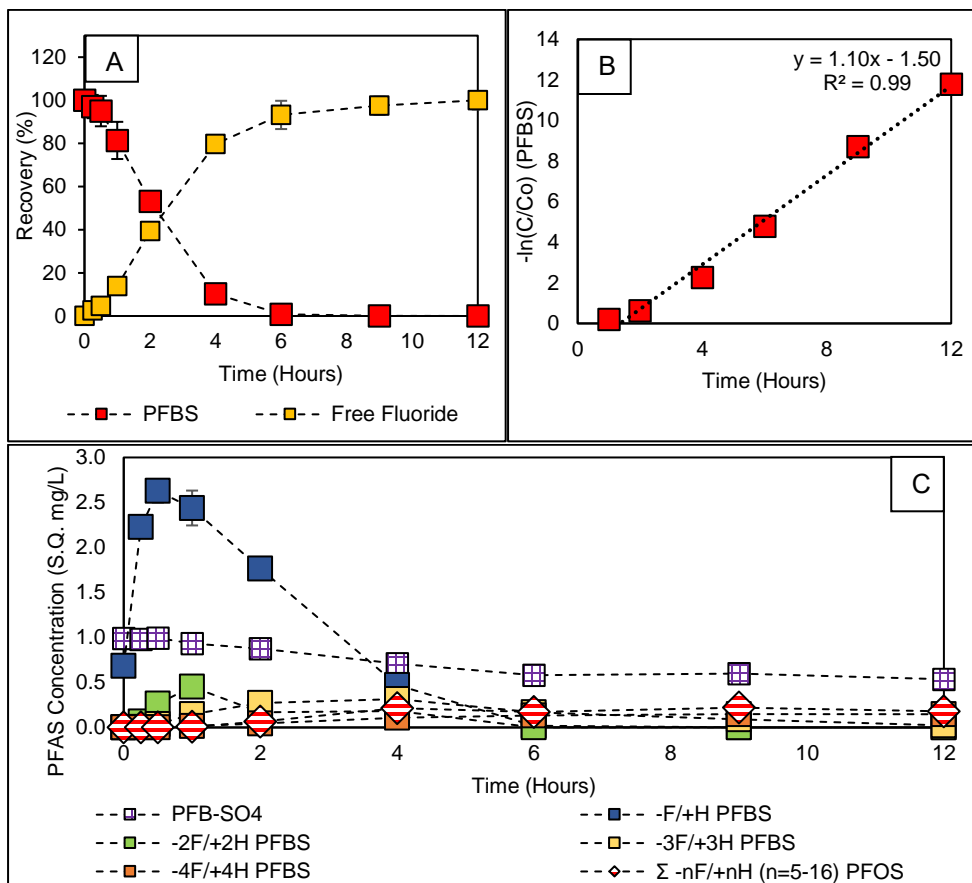
Figure 4.6 Destruction of PFBS (600 mg/L) in a 1L, UV/S+I system (20 mM Na_2SO_3, 10 mM KI, 10 mM $NaHCO_3$, 150 mM NaOH, with dropwise replenishment of Na_2SO_3 at a rate of 10 mM per hour), with (A) recovery of PFBS and free fluoride , (B) first order rate law of PFBS degradation, and (C) semi-quantified transformation products identified. Data points are the average of triplicates. Error bars are the standard deviation of the triplicates. Some error bars are too small to be seen.

After the initial lag period (likely due to the removal of oxygen by sulfite radicals), the destruction of PFBS follows a first-order rate constant of 1.10 h^{-1}, which is maintained for the remainder of the 12-hour remediation. This results in the degradation of >99.999% PFBS (600 mg/L to 4.5 µg/L) and a total defluorination of 97±4%. The ability of the system to maintain a first order rate constant is likely 0due to the dropwise replenishment of sulfite, equating to a total of 140 mM of Na_2SO_3 added over the course of the 12-hour treatment.

The first-order rate of PFBS degradation observed in the present study is slightly slower than previous work at a lower concentration, using a smaller volume system (1.10 h^{-1} compared to 1.46 h^{-1} in previous work (O'Connor et al., 2023)). The slower first-order rate in the present study could be attributable to the scaled-up volume of the system but may also be due to the higher concentration of PFBS (600 mg/L in this study, compared to 30 mg/L of PFBS in previous work). Work by Maza et al.

(2022) reported that the formation of PFAS aggregates at higher concentrations decreases the probability of reduction by aqueous electrons, albeit for reasons only partially understood (Maza et al., 2022). Given the high concentration of PFBS employed, it is possible that the formation of PFBS aggregates may be responsible for the reduced rate of destruction. Implementation of this technology under high PFAS concentration scenarios will need to balance the higher mass of PFAS destroyed with the reduced rate of PFAS destruction due to potential aggregation.

High resolution mass spectrometric analysis of the PFBS transformation products identified three different PFAS groups: perfluorobutane sulfate ($C_4F_9SO_4$), various -nF/+nH exchanged PFBS molecules, and -nF/+nH exchanged PFOS molecules. Perfluorobutane sulfate was identified to be a PFBS impurity, present in the initial (pre-remediated) solution at a semi-quantified concentration of ~ 1 mg/L (<0.2% initial PFBS concentration). Perfluorobutane sulfate was found to only undergo ~45% degradation over the 12-hour time period, suggesting that the presence of the sulfate functional group bestows a degree of recalcitrance. The presence of -nF/+nH exchanged PFBS products have been previously identified and followed expected trends for formation and subsequent destruction (O'Connor et al., 2023).

The most interesting observation was the formation of -F/+H exchanged PFOS molecules, with the number of -F/+H exchanges ranging from 8 to 14 (Figure A8, Table A3). These fluorinated transformation products were not previously identified in lower PFBS concentration investigations. Considering that neither PFOS nor any PFOS-related molecules were identified in the initial solution, it is hypothesized that these molecules were formed from two PFBS molecules first undergoing significant -F/+H exchange transformation, followed by a radical-induced chain addition. In-silico fragmentation analysis of the transformation products, using ddMS$_2$, as previously described (O'Connor et al., 2023; Patch et al., 2022) further reinforced the identification of the -F/+H exchanged PFOS transformation products, identifying several common fragments including SO_3F, SO_3H, and various C_nF_x moieties (Table A3).

These results indicate a diminishing return effect on overall PFAS destruction with respect to irradiation time. In terms of practical implications, the energy, reagent, and time investment associated with extended UV irradiation should be balanced against the advantageous use of secondary/tertiary treatment processes as a polishing step, such as granular activated carbon or ion exchange resin.

4.3.7 Mechanism for Oxidative Radical Generation

The results derived from the alcohol, butyl carbitol, nitrate, and bicarbonate experiments provide support for the postulated hypothesis of PFAS defluorination being at least partially driven by reaction with oxidative radicals. The strongest evidence for this is the observed degradation of PFOS at all concentrations of

methanol, with subsequent defluorination being hindered with increasing concentrations of methanol. If PFOS was both degraded and defluorinated only by aqueous electrons, then it would be unaffected by the presence of methanol. This mixed-radical mechanism for degradation/defluorination has been well studied in gamma/electron beam radiolysis studies but has not been fully explored in UV-ARP investigations (Patch et al., 2022; Trojanowicz et al., 2020, 2018; Zhang et al., 2014).

With the above mechanisms in mind, a simplified mixed-radical reaction mechanism has been proposed for the degradation and defluorination of PFAS in the UV/S+I system (Figure 4.7).
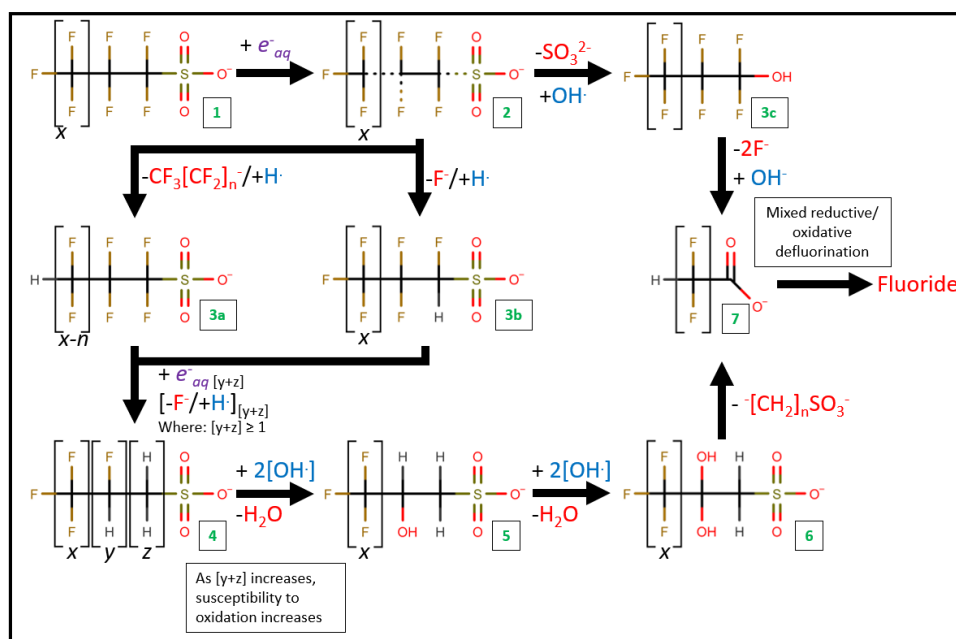
Figure 4.7 Proposed mechanism for aqueous electron-initiated degradation of PFAS, followed by subsequent mixed-mode reductive/oxidative defluorination. Green boxed numbers refer to steps.

This proposed mechanism is similar to mechanisms proposed in studies employing gamma irradiation, electron beam, or other mixed reductive/oxidative remediation technologies (Lassalle et al., 2021; Patch et al., 2022; Trojanowicz et al., 2020, 2019, 2018; Zhang et al., 2014). The novelty of this mechanism in the present work is the contribution of reductive and oxidative radicals present in the UV/S+I system towards the degradation and defluorination of PFAS, along with the aqueous electrons heretofore thought to be solely responsible for PFAS degradation/defluorination. It is important to state that the described reaction mechanism is simplified and does not represent the web of reaction pathways that can arise depending on initial and subsequent carbon attack.

As identified in previous work (O'Connor et al., 2023), PFAS degradation is initiated following attack by an aqueous electron, which can result in the cleavage of C-C, C-F, and C-S bonds (Figure 4.7; steps 1 and 2). Following C-C or C-F bond cleavage, the subsequent perfluoroalkyl radical will react with a hydrogen radical (or water) to generate a -F/+H PFAS transformation product (Figure 4.7; steps 3a and 3b). Given the high pH of the system (which typically scavenges hydrogen radicals), the source of the hydrogen radicals is not exactly known, but it may result from direct reaction of an aqueous electron with water (Deister and Warneck, 1990):

$$e_{aq}^- + H_2O \rightarrow H^\cdot + OH^- \qquad (10)$$
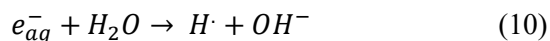
The single -F/+H exchanged PFAS will then react with additional aqueous electrons, repeating steps 1-3, generating a multiple -F/+H exchanged PFAS product (Figure 4.7, step 4). Using PFOS as an example, the transformation product will have a formula of either $F (CF_2)_x (CFH)_y (CH_2)_z SO_3^-$ (assuming only C-F bond cleavage), or $H (CF_2)_x (CFH)_y (CH_2)_z SO_3^-$ (assuming mix of C-F and C-C bond cleavages), where $[X+Y+Z] \leq 8$. Previous authors have identified the recalcitrance of -CH$_2$ and -CHF moieties to degradation by aqueous electron and have proposed the need for oxidation reactions to further drive defluorination of these transformation products (Bentel et al., 2020a, 2019a; Liu et al., 2021b; Zhang et al., 2014). Therefore, we propose as the proportion of -F/+H substitution increases (e.g. X+Y increases), the likelihood of degradation by hydroxyl radicals (or other oxidative species) increases (as discussed in equations 4-9) (Figure 4.7, step 5). Reaction with additional hydroxyl radicals may eventually result in enough -F/+OH substitutions to result in several different C-C chain cleavage mechanisms, which are not shown in Figure 4.7, but detailed in the literature, such as a diol conversion into a carboxylic acid, proposed for the TOP assay mechanisms (Zhang et al., 2021) (Figure 4.7; steps 6 and 7). However, as this aldol product was not identified in the present study, this is speculative at best and would be an appropriate area of future work.

4.4 Conclusions

This study investigated the effectiveness of the UV/S+I system in the presence of both well understood and less well understood reduction/oxidation radical scavengers, including the remediation of a highly concentrated PFBS solution, as well as two different diluted AFFF formulations.

These experiments were performed to provide insights into the possible role of radicals in the degradation and defluorination of PFAS, beyond that of the aqueous electron. This work builds on the postulations posed by previous studies, and challenges the standard simplified model that the UV/S+I system drives complete PFAS destruction using only aqueous electrons. The inhibition of PFOS defluorination, but not degradation, with increasing methanol concentration directly supports the hypothesis that oxidative radicals contribute to the destruction of the

highly recalcitrant -F/+H exchanged PFOS transformation products. This is further supported by subsequent scavenging investigations using isopropanol and butyl carbitol.

The results from the investigations of reduction/oxidation radical scavengers have practical implications for the implementation of UV/S+I as a scaled up, viable PFAS treatment technology. The impacts of alcohols, butyl carbitol, nitrate, bicarbonate, pH, high PFAS concentration on PFAS destruction, and the effectiveness of treating dilute, but nevertheless complex AFFF matrices identified the robustness of the UV/S+I system and the potential benefits of pre- or post-treatment technologies.

The conclusion of this work supports previous hypotheses that UV-ARP systems, in particular the UV/S+I system, is a complex remediation technology that initiates the destruction of PFAS through reductive processes, and drives subsequent defluorination through a synergistic combination of reductive and oxidative reactions. While the UV/S+I system shows strong promise for the effective destruction of PFAS under a variety of scenarios, it is critical to understand the impacts of different species present in different aqueous systems and, where necessary, modify the UV/S+I system to compensate for areas of increased complexity.

4.5 Acknowledgements

4.6 References

Abusallout, I., Wang, J., Hanigan, D., 2021. Emerging investigator series: rapid defluorination of 22 per- and polyfluoroalkyl substances in water using sulfite irradiated by medium-pressure UV. En-viron Sci (Camb) 7, 1552–1562. https://doi.org/10.1039/d1ew00221j

Amador, C.K., Cavalli, H., Tenorio, R., Tetu, H., Higgins, C.P., Vyas, S., Strathmann, T.J., 2023. In-fluence of Carbonate Speciation on Hydrated Electron Treatment Processes. Environ Sci Technol 57, 7849–7857. https://doi.org/10.1021/acs.est.2c09451

Barzen-Hanson, K.A., Roberts, S.C., Choyke, S., Oetjen, K., McAlees, A., Riddell, N., McCrindle, R., Ferguson, P.L., Higgins, C.P., Field, J.A., 2017. Discovery of 40 Classes of Per- and Polyfluoroal-kyl Substances in Historical Aqueous Film-Forming Foams (AFFFs) and AFFF-Impacted Groundwater. Environ Sci Technol. https://doi.org/10.1021/acs.est.6b05843

Bentel, M.J., Liu, Z., Yu, Y., Gao, J., Men, Y., Liu, J., 2020. Enhanced Degradation of Perfluorocar-boxylic Acids (PFCAs) by UV/Sulfite Treatment: Reaction Mechanisms and System Efficiencies at pH 12. Environ Sci Technol Lett 7, 351–357. https://doi.org/10.1021/acs.estlett.0c00236

Bentel, M.J., Yu, Y., Xu, L., Li, Z., Wong, B.M., Men, Y., Liu, J., 2019. Defluorination of Per- and Polyfluoroalkyl Substances (PFASs) with Hydrated Electrons: Structural Dependence and Impli-cations to PFAS Remediation and Management. Environ Sci Technol 53, 3718–3728. https://doi.org/10.1021/acs.est.8b06648

Buck, R.C., Franklin, J., Berger, U., Conder, J.M., Cousins, I.T., Voogt, P. De, Jensen, A.A., Kannan, K., Mabury, S.A., van Leeuwen, S.P.J., 2011. Perfluoroalkyl and polyfluoroalkyl substances in the environment: Terminology, classification, and origins. Integr Environ Assess Manag 7, 513–541. https://doi.org/10.1002/ieam.258

Busset, C., Mazellier, P., Sarakha, M., De Laat, J., 2007. Photochemical generation of carbonate radi-cals and their reactivity with phenol. J Photochem Photobiol A Chem 185, 127–132. https://doi.org/10.1016/j.jphotochem.2006.04.045

Cao, Y., Qiu, W., Li, J., Jiang, J., Pang, S., 2021. Review on UV/sulfite process for water and wastewater treatments in the presence or absence of O2. Science of the Total Environment 765, 142762. https://doi.org/10.1016/j.scitotenv.2020.142762

Das, T.N., 2001. Reactivity and role of SO5•- radical in aqueous medium chain oxidation of sulfite to sulfate and atmospheric sulfuric acid generation. Journal of Physical Chemistry A 105, 9142–9155. https://doi.org/10.1021/jp011255h

Deister, Ursula., Warneck, P., 1990. Photooxidation of sulfite (SO32) in aqueous solution. American Chemical Society 94, 2191–2198.

Fennell, B.D., Fowler, D., Mezyk, S.P., McKay, G., 2023. Reactivity of Dissolved Organic Matter with the Hydrated Electron: Implications for Treatment of

Chemical Contaminants in Water with Ad-vanced Reduction Processes. Environ Sci Technol 57, 7634–7643. https://doi.org/10.1021/acs.est.3c00909

Fennell, B.D., Mezyk, S.P., McKay, G., 2021. Critical Review of UV-Advanced Reduction Processes for the Treatment of Chemical Contaminants in Water. ACS Environmental Au. https://doi.org/10.1021/acsenvironau.1c00042

Guan, Y.H., Ma, J., Li, X.C., Fang, J.Y., Chen, L.W., 2011. Influence of pH on the formation of sul-fate and hydroxyl radicals in the UV/Peroxymonosulfate system. Environ Sci Technol 45, 9308–9314. https://doi.org/10.1021/es2017363

Harding-Marjanovic, K.C., Houtz, E.F., Yi, S., Field, J.A., Sedlak, D.L., Alvarez-Cohen, L., 2015. Aerobic Biotransformation of Fluorotelomer Thioether Amido Sulfonate (Lodyne) in AFFF-Amended Microcosms. Environ Sci Technol 49, 7666–7674. https://doi.org/10.1021/acs.est.5b01219

Houtz, E.F., Sedlak, D.L., 2012. Oxidative conversion as a means of detecting precursors to perfluoro-alkyl acids in urban runoff. Environ Sci Technol 46, 9342–9349. https://doi.org/10.1021/es302274g

Hunt, J.W., Chase, W.J., 1977. Temperature and solvent dependence of electron scavenging efficiency in polar liquids: water and alcohols. Can J Chem 55, 2080–2087. https://doi.org/10.1139/v77-289

Javed, H., Lyu, C., Sun, R., Zhang, D., Alvarez, P.J.J., 2020. Discerning the inefficacy of hydroxyl rad-icals during perfluorooctanoic acid degradation. Chemosphere 247. https://doi.org/10.1016/j.chemosphere.2020.125883

Jortner, J., Ottolenghi, M., Stein, G., 1963. The Formation of Solvated Electrons in the Photochemistry of the Phenolate Ion in Aqueous Solutions. J Am Chem Soc 85, 2712–2715. https://doi.org/10.1021/ja00901a007

Lassalle, J., Gao, R., Rodi, R., Kowald, C., Feng, M., Sharma, V.K., Hoelen, T., Bireta, P., Houtz, E.F., Staack, D., Pillai, S.D., 2021. Degradation of PFOS and PFOA in soil and groundwater samples by high dose Electron Beam Technology. Radiation Physics and Chemistry 189, 109705. https://doi.org/10.1016/j.radphyschem.2021.109705

Liu, T., Yin, K., Liu, C., Luo, J., Crittenden, J., Zhang, W., Luo, S., He, Q., Deng, Y., Liu, H., Zhang, D., 2018. The role of reactive oxygen species and carbonate radical in oxcarbazepine degradation via UV, UV/H2O2: Kinetics, mechanisms and toxicity evaluation. Water Res 147, 204–213. https://doi.org/10.1016/j.watres.2018.10.007

Liu, Y., He, X., Duan, X., Fu, Y., Fatta-Kassinos, D., Dionysiou, D.D., 2016. Significant role of UV and carbonate radical on the degradation of oxytetracycline in UV-AOPs: Kinetics and mecha-nism. Water Res 95, 195–204. https://doi.org/10.1016/j.watres.2016.03.011

Liu, Z., Bentel, M.J., Yu, Y., Ren, C., Gao, J., Pulikkal, V.F., Sun, M., Men, Y., Liu, J., 2021. Near-Quantitative Defluorination of Perfluorinated and Fluorotelomer

Carboxylates and Sulfonates with Integrated Oxidation and Reduction. Environ Sci Technol 55, 7052–7062. https://doi.org/10.1021/acs.est.1c00353

Liu, Z., Chen, Z., Gao, J., Yu, Y., Men, Y., Gu, C., Liu, J., 2022. Accelerated Degradation of Per-fluorosulfonates and Perfluorocarboxylates by UV/Sulfite + Iodide: Reaction Mechanisms and System Efficiencies. Environ Sci Technol 56, 3699–3709. https://doi.org/10.1021/acs.est.1c07608

Maza, W.A., Etz, B.D., Schutt, T.C., Chaloux, B.L., Breslin, V.M., Pate, B.B., Shukla, M.K., Owrut-sky, J.C., Epshteyn, A., 2022. Impact of Submicellar Aggregation on Reduction Kinetics of Per-fluorooctanoate by the Hydrated Electron. Environ Sci Technol Lett 9, 226–232. https://doi.org/10.1021/acs.estlett.1c01020

Medinas, D.B., Cerchiaro, G., Trindade, D.F., Augusto, O., 2007. The carbonate radical and related oxidants derived from bicarbonate buffer. IUBMB Life 59, 255–262. https://doi.org/10.1080/15216540701230511

O'Connor, N., Patch, D., Noble, D., Scott, J., Koch, I., Mumford, K.G., Weber, K., 2023. Forever no more : Complete mineralization of per - and poly fl uoroalkyl substances (PFAS) using an opti-mized UV / sulfite / iodide system. Science of the Total Environment 888, 164137. https://doi.org/10.1016/j.scitotenv.2023.164137

Okazaki, K., Freeman, G.R., 1978. Scavenging of electrons prior to solvation in liquid alcohols. Can J Chem 56, 2313–2323. https://doi.org/10.1139/v78-381

Olsen, G.W., Mair, D.C., Lange, C.C., Harrington, L.M., Church, T.R., Goldberg, C.L., Herron, R.M., Hanna, H., Nobiletti, J.B., Rios, J.A., Reagen, W.K., Ley, C.A., 2017. Per- and polyfluoroalkyl substances (PFAS) in American Red Cross adult blood donors, 2000–2015. Environ Res 157, 87–95. https://doi.org/10.1016/j.envres.2017.05.013

Park, H., Vecitis, C.D., Cheng, J., Choi, W., Mader, B.T., Hoffmann, M.R., 2009. Reductive defluori-nation of aqueous perfluorinated alkyl surfactants: Effects of ionic headgroup and chain length. Journal of Physical Chemistry A 113, 690–696. https://doi.org/10.1021/jp807116q

Patch, D., O'Connor, N., Koch, I., Cresswell, T., Hughes, C., Davies, J.B., Scott, J., O'Carroll, D., We-ber, K., 2022. Elucidating degradation mechanisms for a range of per- and polyfluoroalkyl sub-stances (PFAS) via controlled irradiation studies. Science of the Total Environment 832, 154941. https://doi.org/10.1016/j.scitotenv.2022.154941

Ross, A.B., Neta, P., 1982. Rate Constants for Reactions of Aliphatic Carbon-Centered Radicals in Aqueous Solution. National Bureau of Standards, National Standard Reference Data Series 1027.

Sharma, S.K., Chander Sobti, R., 2012. Nitrate Removal from Ground Water: A Review.

Siciliano, A., 2015. Use of nanoscale zero-valent iron (NZVI) particles for chemical denitrification un-der different operating conditions. Metals (Basel) 5, 1507–1519. https://doi.org/10.3390/met5031507

Sunderland, E.M., Hu, X.C., Dassuncao, C., Tokranov, A.K., Wagner, C.C., Allen, J.G., 2019. A re-view of the pathways of human exposure to poly- and perfluoroalkyl substances (PFASs) and pre-sent understanding of health effects. J Expo Sci Environ Epidemiol 29, 131–147. https://doi.org/10.1038/s41370-018-0094-1

Tenorio, R., Liu, J., Xiao, X., Maizel, A., Higgins, C.P., Schaefer, C.E., Strathmann, T.J., 2020. De-struction of Per-and Polyfluoroalkyl Substances (PFASs) in Aqueous Film-Forming Foam (AFFF) with UV-Sulfite Photoreductive Treatment. Environ Sci Technol 54, 6957–6967. https://doi.org/10.1021/acs.est.0c00961

Trojanowicz, M., Bartosiewicz, I., Bojanowska-Czajka, A., Kulisa, K., Szreder, T., Bobrowski, K., Nichipor, H., Garcia-Reyes, J.F., Nałęcz-Jawecki, G., Męczyńska-Wielgosz, S., Kisała, J., 2019. Application of ionizing radiation in decomposition of perfluorooctanoate (PFOA) in waters. Chemical Engineering Journal 357, 698–714. https://doi.org/10.1016/j.cej.2018.09.065

Trojanowicz, M., Bartosiewicz, I., Bojanowska-Czajka, A., Szreder, T., Bobrowski, K., Nałęcz-Jawecki, G., Męczyńska-Wielgosz, S., Nichipor, H., 2020. Application of ionizing radiation in de-composition of perfluorooctane sulfonate (PFOS) in aqueous solutions. Chemical Engineering Journal 379, 122303. https://doi.org/10.1016/j.cej.2019.122303

Trojanowicz, M., Bojanowska-Czajka, A., Bartosiewicz, I., Kulisa, K., 2018. Advanced Oxida-tion/Reduction Processes treatment for aqueous perfluorooctanoate (PFOA) and perfluorooc-tanesulfonate (PFOS) – A review of recent advances. Chemical Engineering Journal 336, 170–199. https://doi.org/10.1016/j.cej.2017.10.153

Vecitis, C.D., Park, H., Cheng, J., Mader, B.T., Hoffmann, M.R., 2009. Treatment technologies for aqueous perfluorooctanesulfonate (PFOS) and perfluorooctanoate (PFOA). Frontiers of Environ-mental Science and Engineering in China 3, 129–151. https://doi.org/10.1007/s11783-009-0022-7

Wang, Z., Buser, A.M., Cousins, I.T., Demattio, S., Drost, W., Johansson, O., Ohno, K., Patlewicz, G., Richard, A.M., Walker, G.W., White, G.S., Leinala, E., 2021. A New OECD Definition for Per- And Polyfluoroalkyl Substances. Environ Sci Technol 55, 15575–15578. https://doi.org/10.1021/acs.est.1c06896

Wilkinson, T. G., & Hamer, G. (2007). The microbial oxidation of mixtures of methanol, phenol, acetone and isopropanol with reference to effluent purification. Journal of Chemical Technology and Biotechnology, 29 (1), 56–67. https://doi:10.1002/jctb.503290110

Yan, S., Liu, Y., Lian, L., Li, R., Ma, J., Zhou, H., Song, W., 2019. Photochemical formation of car-bonate radical and its reaction with dissolved organic matters. Water Res 161, 288–296. https://doi.org/10.1016/j.watres.2019.06.002

Yang, L., He, L., Xue, J., Ma, Y., Xie, Z., Wu, L., Huang, M., Zhang, Z., 2020. Persulfate-based deg-radation of perfluorooctanoic acid (PFOA) and perfluorooctane sulfonate (PFOS) in aqueous solu-tion: Review on influences, mechanisms and prospective. J Hazard Mater. https://doi.org/10.1016/j.jhazmat.2020.122405

Zhang, Y., Liu, J., Ghoshal, S., Moores, A., 2021. Density Functional Theory Calculations Decipher Complex Reaction Pathways of 6:2 Fluorotelomer Sulfonate to Perfluoroalkyl Carboxylates Initi-ated by Hydroxyl Radical. Environ Sci Technol 55, 16655–16664. https://doi.org/10.1021/acs.est.1c05549

Zhang, Y., Liu, J., Ghoshal, S., Moores, A., n.d. Density functional theory calculations decipher com-plex reaction pathways of 6: 2 fluorotelomer sulfonate to perfluoroalkyl carboxylic acids initiated by hydroxyl radical, in: American Chemical Society Conference Spring 2021.

Zhang, Z., Chen, J.J., Lyu, X.J., Yin, H., Sheng, G.P., 2014. Complete mineralization of perfluorooc-tanoic acid (PFOA) by γ-irradiation in aqueous solution. Sci Rep 4, 1–6. https://doi.org/10.1038/srep07418

5. Conclusions and Recommendations

5.1 Developing a UV-ARP system capable of degrading and defluorinating PFAS

The primary goal of this research was to develop a UV light-activated ARP system capable of degrading and defluorinating a suite of different PFAS. Investigations into various photosensitizers and their effectiveness in destroying PFOS were undertaken. UV activated sulfite/iodide (UV/S+I) was identified to have the potential to destroy PFOS in aqueous matrices. The aqueous electron was identified as the main species responsible for degrading PFAS and the mechanism was discussed. The UV/S+I system was optimized to achieve complete defluorination of PFBS. From the work conducted and the results derived from this study, the following conclusions can be presented:

1. The UV/S+I system can achieve >90% defluorination of PFOS, PFOA, 6:2 FTS, and PFBS in deionized water. It was identified that 20 mM Na_2SO_3, 10 mM KI, 10 mM $NaHCO_3$, and 150 mM NaOH was required initially in the solution to degrade PFAS, and regular additions of SO_3^{2-} (10 mM every two hours) was required to sustain a first order rate of PFAS destruction.
2. Aqueous electrons are responsible for initial degradation of PFAS, capable of cleaving C-C, C-F, and C-S bonds, which was supported by the formation of different PFAS transformation products.
3. Several transformation products were identified following application of the UV/S, UV/I, and UV/S+I systems, including -F/+H, -F/+OH, $-CF_x/+H$ substituted transformation products of the parent compound, as well as PFCAs.
4. Transformation products, following their formation, were subsequently degraded by additional reaction time in the UV-activated systems.

5.2 Evaluating the effectiveness of the UV/S+I system at destroying PFAS in complex matrices

Investigations into the effectiveness of the UV/S+I system at degrading PFAS in more real-world (complex) matrices were undertaken. Organic matter and other potential scavengers that could reduce the effectiveness of PFAS destruction in an ARP system are naturally present in complex matrices. The roles of oxidizing species in the UV/S+I system were investigated by evaluating the effectiveness of the UV/S+I system in the presence of different radical scavengers. The UV/S+I system was further optimized for the destruction of 600 mg/L of PFBS in a 1 L system. From the work conducted and the results derived from this study, the following conclusions can be presented:

5. Methanol at concentrations up to ~6 M did not affect initial degradation of PFOS, but did result in a linear inhibition of PFOS defluorination.

6. Isopropanol at concentrations up to 1.3 M did not affect PFOS degradation but did inhibit defluorination. At isopropanol concentrations >1.3 M, both PFOS degradation and defluorination were inhibited. This is hypothesized to be due to the conversion of isopropanol to acetone, which scavenged aqueous electrons.

7. Butyl carbitol (BC) was found to impact both the degradation and defluorination of PFOS and 6:2 FTS, although 6:2 FTS was much more sensitive to increasing BC concentrations. For 6:2 FTS, it was hypothesized that BC scavenged oxidative radicals that may initiate 6:2 FTS degradation. For PFOS, it was hypothesized that high concentrations of BC may result in the formation of protective surfactant micelles or other supramolecular structures which inhibited degradation by aqueous electrons.

8. Nitrate at concentrations up to 1 mM did not affect the efficiency of the UV/S+I system (20 mM SO_3^{2-}, 10 mM I^-). At 5 mM of nitrate, PFOS destruction was partially inhibited, and at 10 mM of nitrate and higher, PFOS destruction was completely inhibited. 6:2 FTS experienced similar levels of inhibition at 5 mM and 10 mM of nitrate, although 6:2 FTS degradation was noticeably more inhibited.

9. Carbonate, either present from tap water or added as part of the experiment, was found to improve PFAS degradation compared to a carbonate-free system. Higher concentrations (100 mM CO_3^{2-}) were found to increase the rate of PFAS degradation but had a minimal effect on PFAS defluorination.

10. The UV/S+I system was found to be capable of degrading PFBS at a high concentration (600 mg/L), with a slight lag at the start of degradation (likely due to the presence of dissolved oxygen) and a defluorination of ~97% after 12 hours. The remaining 3% of organic fluorine was attributed to PFAS transformation products, including -F/+H PFBS, -F/+H PFOS (arising from radical chain combination), and -F/+H, +OH PFOS.

11. The above findings support the hypothesis that PFAS defluorination is initiated by aqueous electrons, and PFAS defluorination is driven by a mix of reductive and oxidative degradation mechanisms. Through the reaction of sulfite radicals with dissolved oxygen, several oxidative species can be generated including the sulfate radical, carbonate radical, and hydroxyl radical.

5.3 Recommendations

The research performed in this thesis has provided a detailed understanding of the UV/S+I system for remediating PFAS-impacted aqueous media. However, there are several limitations that have either been directly identified (e.g. nitrate) or postulated based on data and literature (e.g. dissolved organic matter) that require further investigation. Therefore, recommendations for future work include:

1. Employ techniques such as laser-flash photolysis to confirm the various reductive and oxidative radicals generated in the UV/S+I system.
2. Identify the concentration of sulfite required to overcome different initial concentrations of aqueous electron scavengers (e.g. nitrates, dissolved oxygen, iron).
3. Identify situations in which the UV/S+I system may be appropriately supported by a treatment train approach. For example:
   a. In aqueous systems that contain high amounts of dissolved organic matter, an oxidative pre-treatment may be used (e.g. UV-H_2O_2).
   b. A sorptive technology at the end of the UV/S+I system as a final polishing step (e.g. GAC, IXR) could be used.
4. Investigate the potential for other photosensitizers to be added to the UV/S+I system to further improve PFAS destruction efficiency, either directly (generating more aqueous electrons), or indirectly (regenerating iodide, or bypassing scavenging reactions).
5. Investigate the impacts of system scale-up on PFAS destruction efficacy, including scale-ups in volume, lamp wattage, and system complexity.

5.3 Thesis Conclusions

This thesis has resulted in the development of an optimized UV/S+I system capable of destroying high concentrations of PFAS in a short duration of time. The robustness of the system has been evaluated in the presence of several different reactive radical scavengers, providing both underlying mechanistic insights, as well as allowing for the prediction of system effectiveness based on different water parameters. It is the overall recommendation of this thesis that this work be further pursued for scale-up and commercialization so it can be added to the growing list of effective PFAS treatment options. Without additional optimization, this technology would excel for the flow-through destruction of high concentrations of PFCAs in simple and moderately complex aqueous matrices. It is hypothesized that the addition of an oxidative pre-treatment would further expand the effectiveness of the system to the treatment of fluorotelomer-dominant, complex aqueous matrices.

A. Appendix A

Supplemental Information

Forever No More: Complete mineralization of per- and polyfluoroalkyl substances (PFAS) using an optimized UV/sulfite/iodide system.

Natalia O'Connor†, David Patch†, Diana Noble†, Jennifer Scott†, Iris Koch†, Kevin G. Mumford ††, Kela Weber†*

† Department of Chemistry and Chemical Engineering, Royal Military College of Canada, Kingston, ON, Canada K7K 7B4.

††Department of Civil Engineering, Queen's University, Kingston, ON, Canada.

* Corresponding Author: Kela.Weber@rmc.ca

A.1 PFAS Analysis

Samples were diluted at least 10x with 1:1 water/methanol and analyzed on a ThermoFisher Exploris 120 Orbitrap mass spectrometer coupled to a Vanquish ultra-high-performance liquid chromatography (uHPLC) system using a 100 mm x 2.1 mm x 3.0 μm ACME C18 analytical column and paired guard column. Mobile phases consisted of 5 mM ammonium acetate in deionized (DI) water (A) and acetonitrile (B). The elution profile started at 90% A/10% B, transitioning to 100% B over 10 minutes, holding for 2 minutes, then equilibrating at starting conditions for 3 minutes, using a flow rate of 0.5 mL/min. A diverter valve was used to send the first minute of elution to waste to avoid heavy salt content impacting the MS. A heated electrospray ionization ion source was used, with a static spray voltage. Both positive and negative ion voltage were set to 3000 V. Gas was run in static mode, with a sheath gas of 50 (arbitrary units), aux gas of 10 (arbitrary units) and sweep gas of 1 (arbitrary units). The ion transfer tube temperature was set to 325°C, the vaporizer temperature was set to 350°C, and mild trapping was not used. The MS global settings were set to expect an LC peak width of 10 seconds, and the mass was calibrated before each sample injection using the RunStart EASY-IC ™ system.

Before samples were run, the uHPLC and mass spectrometer were flushed with 10% DI water/90% acetonitrile for a minimum of 1 hour, until baseline ion peak intensity was stable (indicating a clean sample path), and spray stability was <5%. The analysis method was set up with two 'experiments' (XCalibur ® software nomenclature for analytical protocols), one for positive mode analysis and one for negative mode analysis. Each experiment used an instrument resolution of 60,000, a scan range of 100-1000 m/z, an RF lens of 70%, a standard automatic gain control (AGC) target, an automatic maximum injection time mode setting, and had in-source fragmentation disabled. PFAS peak intensities were extracted using XCalibur ® software (Processing Setup and Quan Browser) and converted to concentration using an external calibration curve.

The external calibration curve ranged from 0.1 μg/L to 200 μg/L ($R^2 > 0.99$, detection limit of ~0.05 μg/L for each individual PFAS). Quantification limits were set to the lowest concentration of each calibration curve. With all samples being diluted by at least 10x, this equates to a method detection limit of 0.5 μg/L and method quantitation limit of 1 μg/L. 6:2 FtSaB and subsequent transformation products (excluding 6:2 FTS) were semi-quantified using the PFOSA calibration response.

Continuing calibration standards at two different concentrations (50 μg/L, 5 μg/L) were run every 20 samples to measure possible instrument drift. Recoveries of the standards were within a 95-105% range, indicating negligible instrument drift and acceptable control results (within 20% of theoretical values) (CCME 2016). Samples

were run in batches based on their concentration, with a minimum of four injection blanks (1:1 H_2O/MeOH) run between high concentration and low concentration batches, to monitor carry over effects. Sample carry over was found to be <0.1% of previous PFAS concentration and did not impact subsequent samples. The autosampler injection needle was cleaned between injections using the built-in flush program. The needle was washed for 10 seconds with flush solution (20% DI water, 35% isopropanol, 45% MeOH). Reagent blanks were run before and after each batch to track any contamination in the reagents. All blanks were found to be below PFAS detection limits. Precision was monitored using triplicates in cuvette experiments and duplicates in immersion experiments. Relative standard deviation for each experiment is indicated by error bars present in the figures. On average, RSDs were found to be less than 10% (1.0-9.8%), indicating good agreement between the replicates.

A.2 PFAS Transformation Product Identification

High concentration (>10 mg/L) degradation experiments for PFOS, PFOA, PFBS, 6:2 FTS and 6:2 FtSaB were performed to identify potential transformation products. Samples were analyzed under optimized chromatographic and mass spectrometer conditions specific to transformation product analysis. A brand new 150 mm x 2.1 mm x 3.0 μm ACME C18 analytical column was only used for these high concentration experiments. Initial chromatographic conditions were set to 95% mobile phase A (10 mM ammonium acetate, HPLC-MS grade, in LCMS grade water) and 5% mobile phase B (LCMS grade acetonitrile) for 1 minute, then transitioned to 80% B to 13 minutes, then held until 15 minutes, and then back to initial conditions for three minutes. Ten method blank samples were run before any sample acquisition to clean the sample path and provide a representative background chromatogram. The Exploris 120 Orbitrap was tuned with Pierce ™ FlexMix ™ in both positive and negative mode before each batch of samples. The mass spectrometer was run under similar conditions as for target PFAS analysis, except with a Full Scan resolution of 120,000, scan range of 100-600, and 60,000 ddMS$_2$ resolution. Initial ddMS$_2$ scans were triggered by a peak intensity of >1.0 x 10^6, and analyzed again using a target ddMS$_2$ scan based on the suspected transformation products.

Following acquisition, transformation products were identified using Background Subtracter (Thermo Fisher Scientific), FreeStyle, Processing Setup, and Quan Browser (all Thermo Fisher Scientific software tools). For each degradation experiment, a background blank chromatogram and unirradiated PFAS control chromatogram were collected. Chromatograms from each active experiment were blank subtracted and visually inspected for any new peaks. Following initial peak identification (*e.g.* -F/+H PFOS), a homologue series search was performed using Isotope Simulation in Freestyle. If possible, these products were compared to known

masses of byproducts found in the literature and an in-house database of degradation products identified in previous work ((Banayan Esfahani and Mohseni, 2022; Bentel et al., 2020b; Liu et al., 2021b; Patch et al., 2022). A small number of potential transformation products were not included if their retention time aligned perfectly with a substituted PFCA, as PFCAs fragment readily in the electrospray and may yield false positives. Where possible, ddMS$_2$ fragmentation spectra were used to confirm the identity of transformation products. The use of ddMS$_2$ fragmentation was limited due to either low intensity of transformation products, or difficulty in achieving in-silico fragmentation (*e.g.* -F$_n$/+H$_n$ PFSAs). Identified transformation products and their homologues were then programmed into a Processing Setup method, which was used to process all samples across the kinetic time series of active experiments. Processed data was then inspected with Quan Browser, and exported to Microsoft Excel for additional processing, including semi-quantitation. Transformation products were semi-quantified using the instrument response of the original PFAS or the closest homologue based on pKa. For example, -F/+H PFOS, -2F/+2H PFOS, and -3F/+3H PFOS were quantified with PFOS, but -4F/+4H PFOS and beyond were quantified with 6:2 FTS.

$$Semi-Quantified\ TP\ Concentration$$
$$=\frac{TP\ Instrument\ Response}{Original\ PFAS\ Instrument\ Response}$$

Identified transformation products were assigned a confidence level based on several criteria (Schymanski et al., 2014). PFCAs were assigned a confidence level of 1, due to the ability to confirm these compounds with reference standards, MS$_2$ fragmentation, and retention time matching. -4F/+4H PFOS was assigned a confidence level of 2, due to the confirmation with a 6:2 FTS reference standard, and similar MS$_2$ fragmentation. However, multiple chromatographic peaks of -4F/+4H PFOS complicated retention time matching, as one peak did match but others did not. Transformation products that were able to undergo ddMS$_2$ fragmentation providing more than three characteristic PFAS fragments (typically CF$_3$, C$_3$F$_5$, SO$_3$F, C$_4$F$_7$), and whose retention time followed a pattern similar to other homologues were assigned a confidence of 3. Transformation products that could not provide MS$_2$ fragmentation information but still aligned with either previous homologues or were expected based on experimental set-up and previous work were assigned a confidence of 4.

A.3 Fluoride Analysis

Samples were analyzed using a fluoride ion-selective electrode (Fisher Scientific Accumet Fluoride Electrode) coupled to a pH/ISE meter (Mettler Toledo) to determine total fluoride content in the samples. This was done by taking 1 mL of the aqueous sample and mixing it with 1 mL of total ionic strength adjustment buffer

(TISAB, Fisher Scientific) and adjusting the final pH to 5.5 with acetic acid. Fluoride probe measurements were quantified using a six-point external calibration curve prepared using a standardized fluoride calibration solution (Hach, 10±0.2 mg/L, Fisher Scientific) (Figure A4). The calibration curve was made from 0.05 mg F^-/L to 5 mg F^-/L. Calibration curves exhibited strong linearity ($R^2 > 0.999$) across the concentration ranges. Minimum detection limit was set at the lowest calibration level (0.05 mg F^-/L) and the minimum quantitation limit was set at 5 times the detection limit (0.25 mg/L). Samples were diluted so the concentration of fluoride by the end of the reaction would be between 1-5 mg/L.

Accuracy was established using matrix-spiked samples, which were found to be within 10% of the expected spike concentration. Precision was monitored with experimental replicates and RSDs were found to be, on average, below 10% and deemed acceptable. The resultant defluorination values were mathematically derived by dividing the fluoride measurement by the theoretical maximum fluoride assuming complete defluorination of the given PFAS at the initial concentration.

$$Defluorination = \frac{Fluoride\ Measured\ at\ T\ (x)}{Theoretical\ Organic\ Fluoride\ at\ T(0)} * 100\%$$

A.4 Volume-Normalized Photon Irradiance to the Solution at 254 nm

The volume-normalized photon irradiance to the solution ($mJ\ s^{-1}\ L^{-1}$) to the reaction solutions were calculated for the cuvette and 250 mL beaker experiments respectively using iodide/iodate actinometry (Banayan Esfahani and Mohseni, 2022; Bolton and Stefan, 2002; Chen et al., 2022; Fennell et al., 2021; Li et al., 2012; Tenorio et al., 2020). An actinometry solution containing 0.6 M KI (9.96 g), 0.1 M KIO_3 (2.14 g), and 0.01 M $Na_2B_4O_7$ (0.201 g) was prepared to 100 mL with deionized water and used within four hours of preparation. The UV lamp was turned on and warmed up for 10 minutes before actinometry experiments. The formation of triiodide was measured at 352 nm using a UV-vis spectrophotometer, and all photons entering the solution were assumed to be totally absorbed by the opaque (at 254 nm) solution (Thermo Fisher Scientific Genesys 20). Samples were taken at regular intervals for the first five minutes of the reaction, and the slope (absorbance vs seconds) was converted into concentration (molarity vs seconds) by dividing the absorbance by the molar absorptivity of triiodide at 254 nm ($27600\ M^{-1}\ cm^{-1}$) and the pathlength of the cuvette (1 cm) (Figure A1).
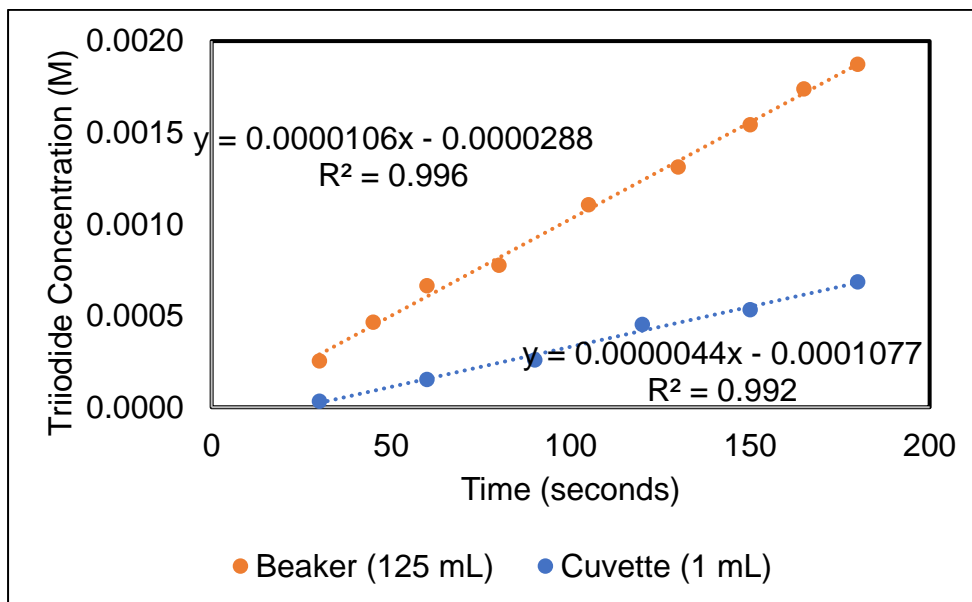
Figure A1 Formation of triiodide as a function of time in the beaker and cuvette experiments.

Volume-normalized photon irradiance (P_I) (mJ s^{-1} L^{-1}) by the 36 W lamp to the cuvette and beaker reactors (referred to by other authors as a photon flux) was calculated in accordance with the below formula.

$$P_I = \frac{d[I_3^-]}{dt} * \frac{1}{\Phi} * U_{254nm}$$

Where $d[I_3^-]/dt$ is the rate of triiodide formation for cuvette (4.38 x 10^{-6} M s^{-1}) or beaker (1.06 x 10^{-5} M s^{-1}), Φ is the quantum yield of triiodide at 22°C (0.69 moles Einstein $^{-1}$), and U_{254nm} is the molar photon energy at 254 nm (472,000 J/Ein). Therefore, the volume-normalized photon irradiance was calculated at 3.01 J s^{-1} L^{-1} and 7.26 J s^{-1} L^{-1} for the cuvette and beaker reactors respectively (6.01 mJ s^{-1} and 907 mJ s^{-1} for the 0.002L and 0.125L cuvette and beaker systems respectively). The geometry of beaker system can be seen below (Figure A2).
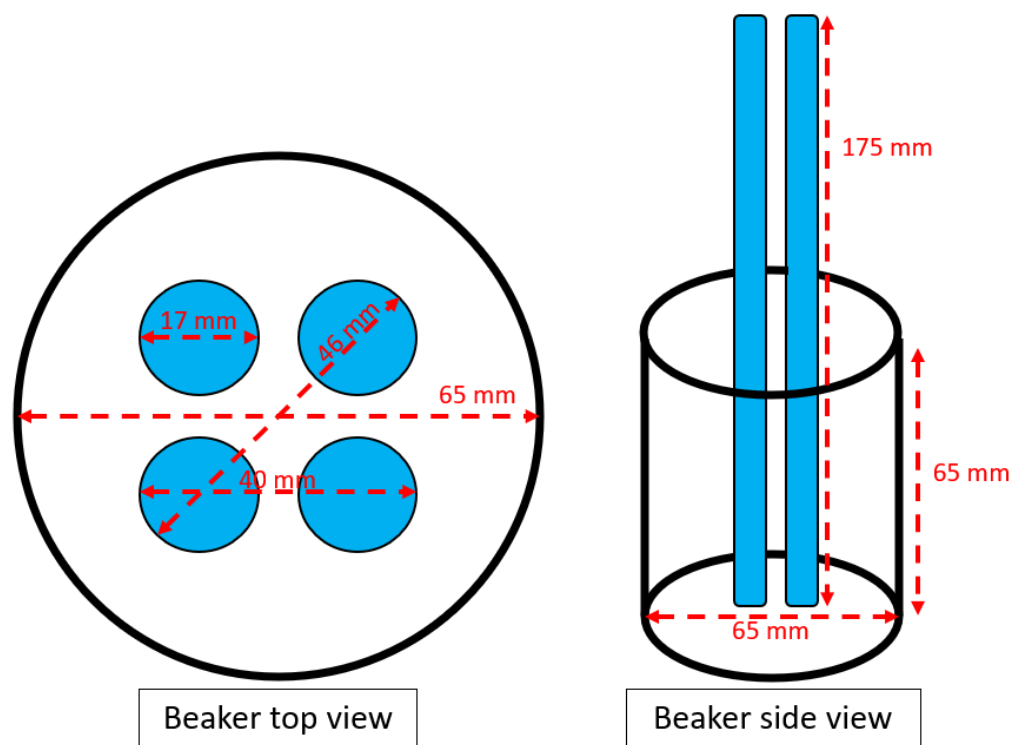
Figure A2 Beaker geometry system used in this study for the 125 mL beaker degradation experiments.

Table A1 Summary of recent UV-ARP publications, including PFAS degradation/defluorination rates.

Author	Year	PFAS	Destruction (Defluorination)	Time (h)	Parent Compound Decay k (h⁻¹)	Reactor Type	Lamp Strength (W)	SO_3^{2-} (mM)	I^- (mM)	HCO_3^- (mM)	pH	EE/O (kW h m⁻³)	Note
Qu	2010	PFOA (0.025 mM)	(94%)	14	0.44	Quartz jacket immersed in a beaker	15	0	0.025	0	9	N/A	N/A
Gu	2016	PFOS (32 µM)	(60%)	0.5	7.08	High pressure UV lamp with reflector, shutter, and timer	250 (unknown UV distribution)	10	0	0	9.2	N/A	N/A
Bao	2018	PFOA	(~80%)	6	2.46	Quartz tubes with lamps rotating around tubes	14 (16 lamps)	20	0	0	10	N/A	Rayonet RPR-200 Photoreactor
Bao	2018	GenX	(90%)	6	2.028								
Bao	2019	PFOS	(85%)	2	3 (mM⁻¹ h⁻¹)	Quartz tubes with lamps rotating around tubes	14 (16 lamps)	20	0	0	10	N/A	Rayonet RPR-200 Photoreactor
Bentel	2019	PFOS (0.025 mM)	(57%)	48	N/A	Quartz jacket immersed in beaker, cooled	18	10	0	5	9.5	N/A	2.9 cm effective path length
Bentel	2019	PFOA (0.025 mM)	(57%)	48	N/A								
Bentel	2020	PFOA (0.025 mM)	(52%)	24	0.56	Quartz jacket immersed in beaker, cooled	18	10	0	5	9.5	122	2.9 cm effective path length
Bentel	2020	PFOA (0.025 mM)	(93%)	8	4.38						12	15.8	
Tenorio	2020	PFOS (70 µg/L)	98% (53%)*	49	0.08	Quartz jacket immersed in beaker, cooled	18	10	0	5	9.5	N/A	2.85 cm effective path length
Abusallout	2021	PFOS (2 mg/L)	(65%)	0.5	1.88	Quartz tubes placed 3 cm from lamp	450 (40-48% between 200-400 nm)	10	0	0	12	32	1.6 cm effective path length
Abusallout	2021	PFOA (2 mg/L)	(82%)	0.5	3.70							16	
Liu	2021	PFOS (0.025 mM)	(30%)	24	N/A	Quartz jacket immersed in beaker, cooled	18	10	0	5	9.5	N/A	2.9 cm effective path length
Liu	2021	PFOA (0.025 mM)	(52%)	24									
Liu	2021	6:2 FTS (0.025 mM)	(35%)	24									
Liu	2021	PFOS (0.025 mM)	(80%)	8							12		
Liu	2021	PFOA (0.025 mM)	(93%)	8									
Liu	2021	6:2 FTS (0.025 mM)	(76%)	24									
Esfahani	2022	PFOS (0.1 mg/L)	0.44	9.6	N/A	Collimated beam reactor, 29 cm away from sample cell	24	10	0	0	12	N/A	N/A
Liu	2022	PFOS (0.025 mM)	(84%)	24	0.78	Quartz jacket immersed in beaker, cooled	18	10	0	5	12	88.8	2.9 cm effective path length
Liu	2022	PFOA (0.025 mM)	(39%)	1	5.2							13.2	
Liu	2022	PFBS (0.025 mM)	(43%)	24	0.05							1320	
Liu	2022	PFOS (0.025 mM)	(92%)	24	1.90				2			36.6	
Liu	2022	PFOA (0.025 mM)	(88%)	1	15.4							4.2	
Liu	2022	PFBS (0.025 mM)	(78%)	24	0.19							366	

Table A2 Reagent concentrations used in all the experiments in this study. The asterisked value is semi-quantified using PFOSA instrument response.

Phase 1 - Initial Reagent Selection (Cuvette) (September 2021, Repeated March 2023)							
Name	PFAS	PFAS Co (mg/L)	Sulfite (mM)	Iodide (mM)	Phenol (mM)	Bicarbonate (mM)	Hydroxide (mM)
Control	PFOS/PFOA	10 mg/L PFOS	0	0	0	10	150
Sulfite			10	0	0		
Iodide			0	10	0		
Phenol			0	0	10		
Sulfide/Iodide			10	10	0		
Sulfite/Phenol			10	0	10		
Iodide/Phenol			0	10	10		
Sulfite/Iodide/Phenol			10	10	10		

Phase 2 - UV/Sulfite/Iodide (Beaker, Immersion) (November 2021-September 2022)					
PFAS	PFAS Co (mg/L)	Sulfite (mM)	Iodide (mM)	Bicarbonate (mM)	Hydroxide (mM)
PFOS	1	10	10	10	150
PFOA	1				
6:2 FTS	1				
PFBS	30				
6:2 FtSaB	0.7*				

Phase 3 - UV/Sulfite/Iodide Optimization (Cuvette) (October 2022-March 2023)						
Name	PFAS	PFAS Co (mg/L)	Sulfite (mM)	Iodide (mM)	Bicarbonate (mM)	Hydroxide (mM)
Control	PFBS	20-30	0	0	0	0
Standard Treatment			10	10	10	150
20 mM Iodide T0			10	20	10	150
20 mM Sulfite T0			20	10	10	150
50 mM Sulfite T0			50	20	10	150
10 mM Sulfite at 2h and 4h			10+10+10	10	10	150
20 mM Sulfite T0 + 10 mM sulfite at 2, 4 hours			20+10+10	10	10	150

Phase 4 - UV/Sulfite/Iodide Optimized (Cuvette) (October 2022)					
PFAS	PFAS Co (mg/L)	Sulfite (mM)	Iodide (mM)	Bicarbonate (mM)	Hydroxide (mM)
PFBS	30	20+10+10+10+10	10	10	150

Phase 4b - UV/Sulfite/Iodide Optimized (1L Beaker, Immersion) (March 2023)					
PFAS	PFAS Co (mg/L)	Sulfite (mM)	Iodide (mM)	Bicarbonate (mM)	Hydroxide (mM)
PFBS	11	20+10+10+10	10	10	150
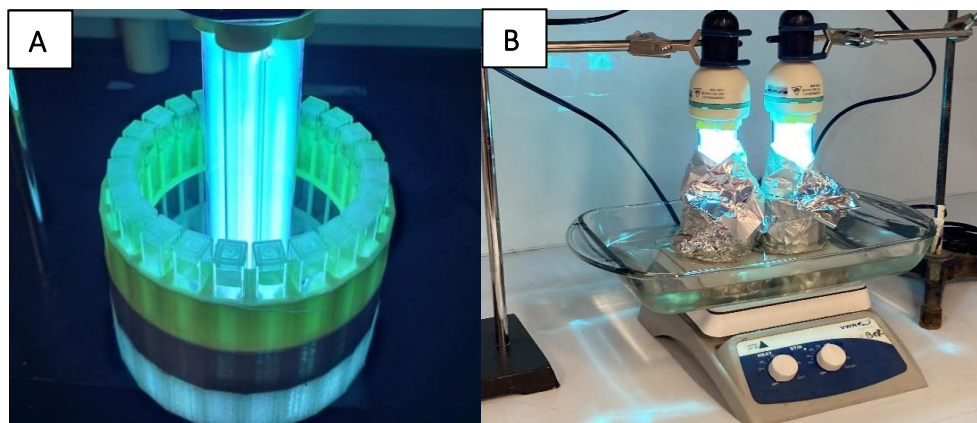
Figure A3 PFAS irradiation set-ups using UV-transmissible cuvettes (left) and beakers (right).
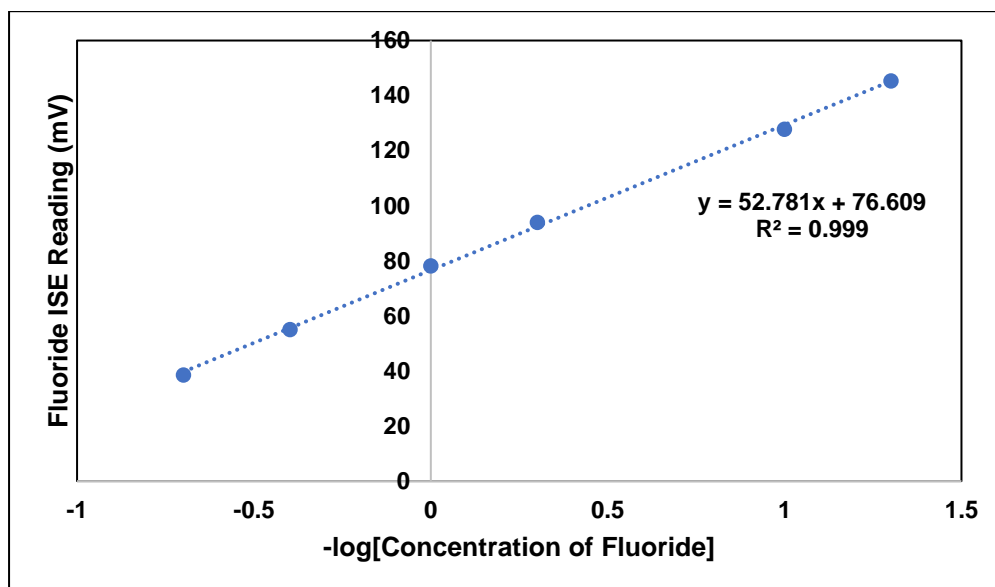
Figure A4 Sample of six-point external calibration curve used to quantify free fluoride measurements in TISAB-amended, pH 5.5 adjusted samples.
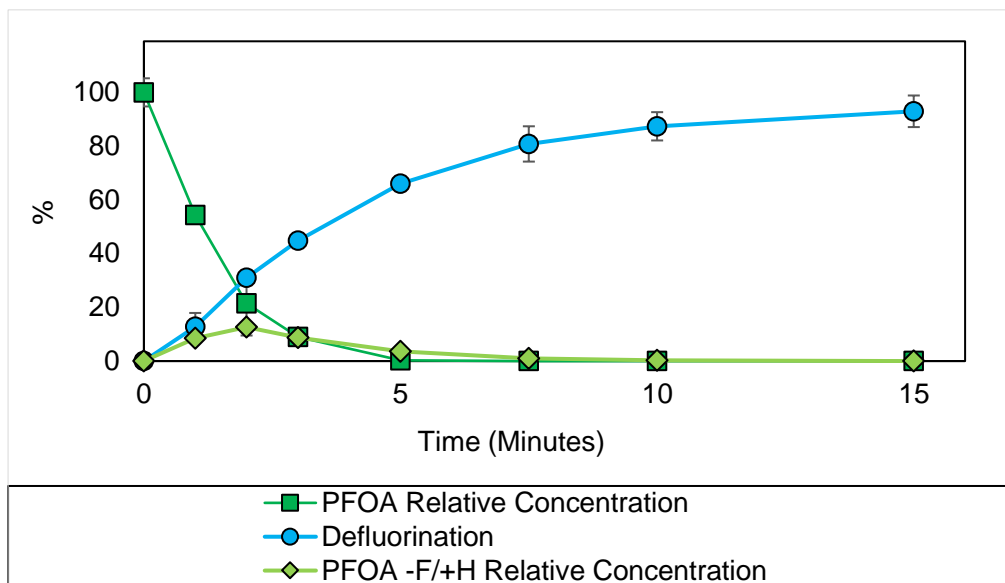
Figure A5 Identification of -F/+H exchanged PFOA following exposure to UV/sulfite/iodide system.
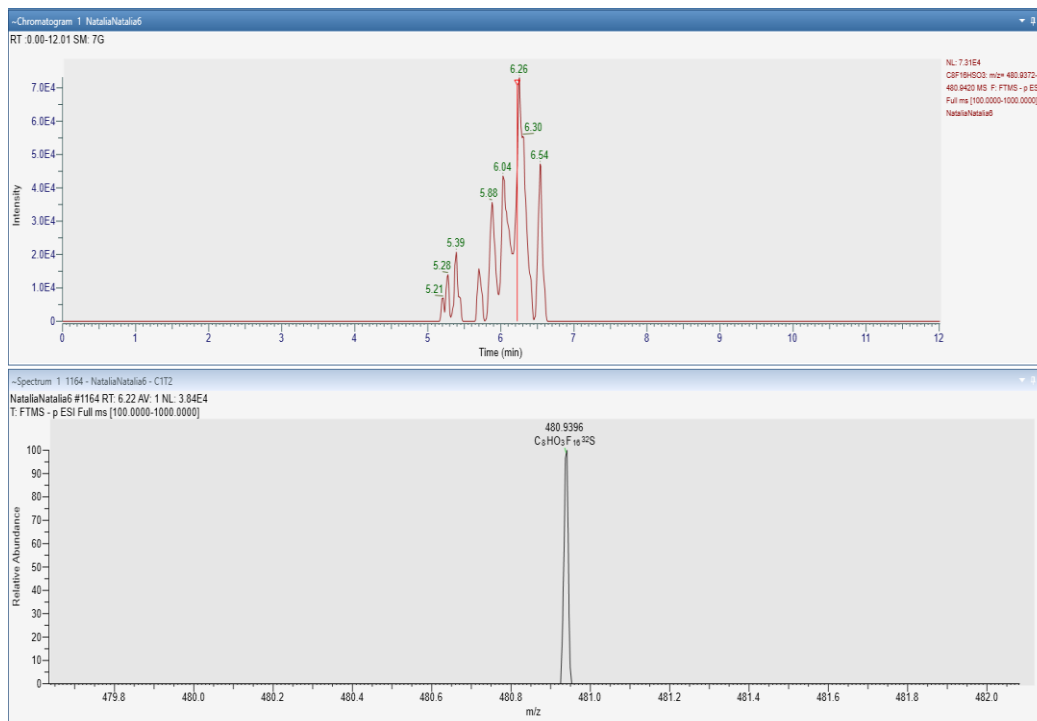
Figure A6 Chromatograms for -F/+H PFOS in the UV/sulfite/iodide system employed in this study, showing eight different isomeric peaks. Chromatogram has been smoothed using gaussian 7 in Freestyle (ThermoFisher).
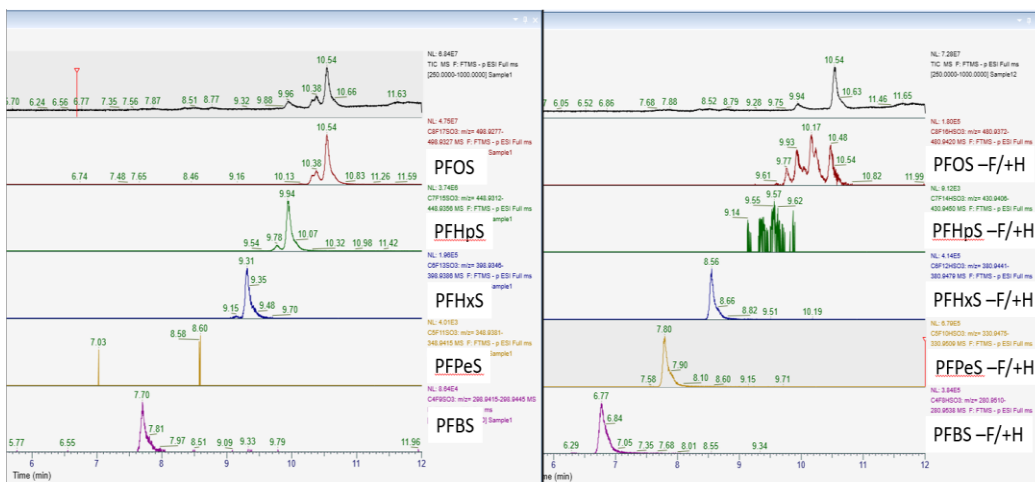
Figure A7 Chromatograms for C4-C8 PFSAs (left, control sample) and the associated -F/+H C4-C8 PFSAs (right, UV/sulfite system).
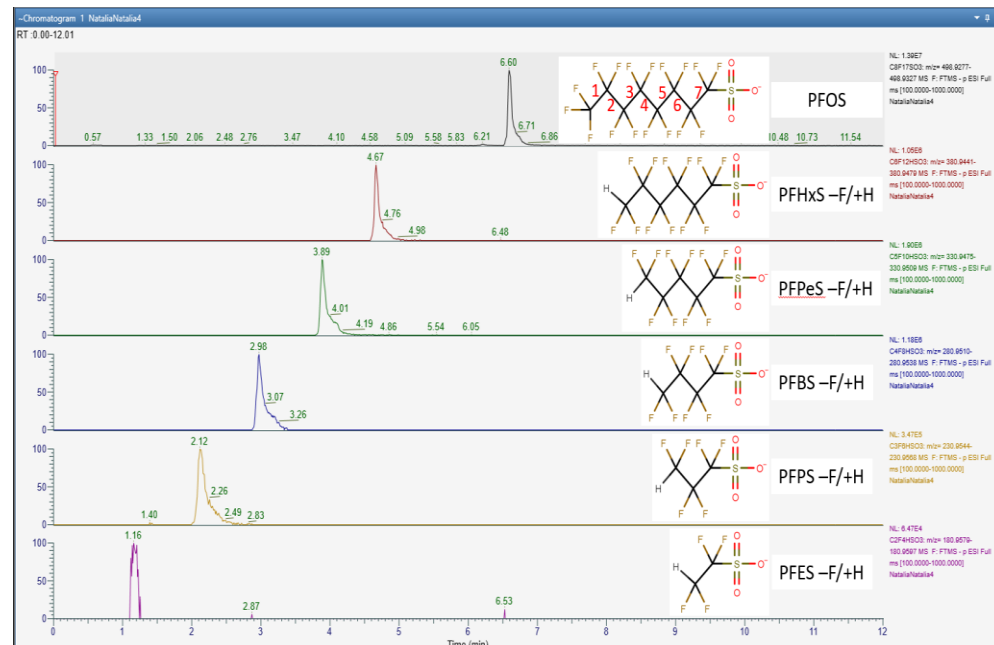
Figure A8 Chromatograms for -F/+H C2-C8 PFSAs formed from C-C bond cleavage of PFOS.
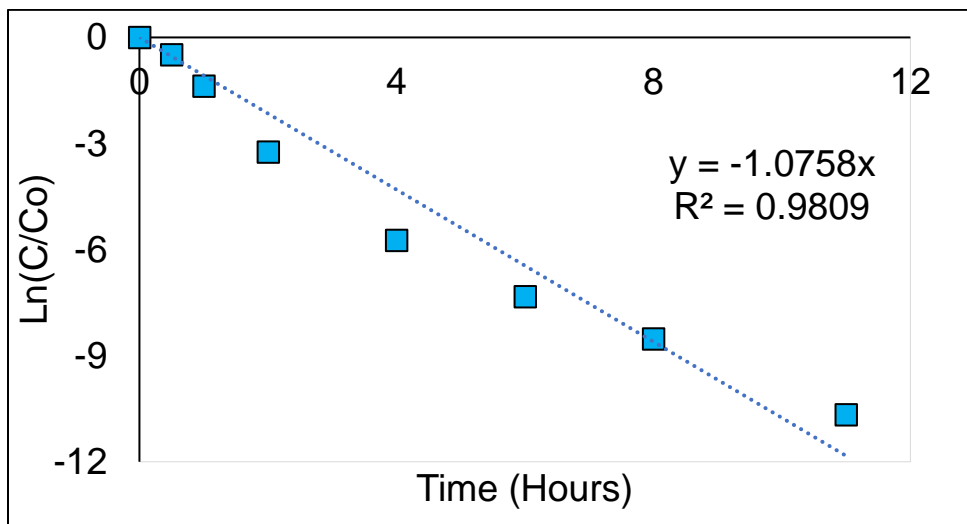
Figure A9 First order degradation of PFBS using an optimized UV/sulfite/iodide system (20 mM SO_3^{2-}, 10 mM I^-, 10 mM HCO_3^-, 150 mM OH^-, 11 hours total irradiation) and 10 mM sulfite added at 2, 4, 6, and 8 hours (60 mM sulfite total). Error bars are the standard deviation of cuvette triplicates. Some error bars are too small to be seen.
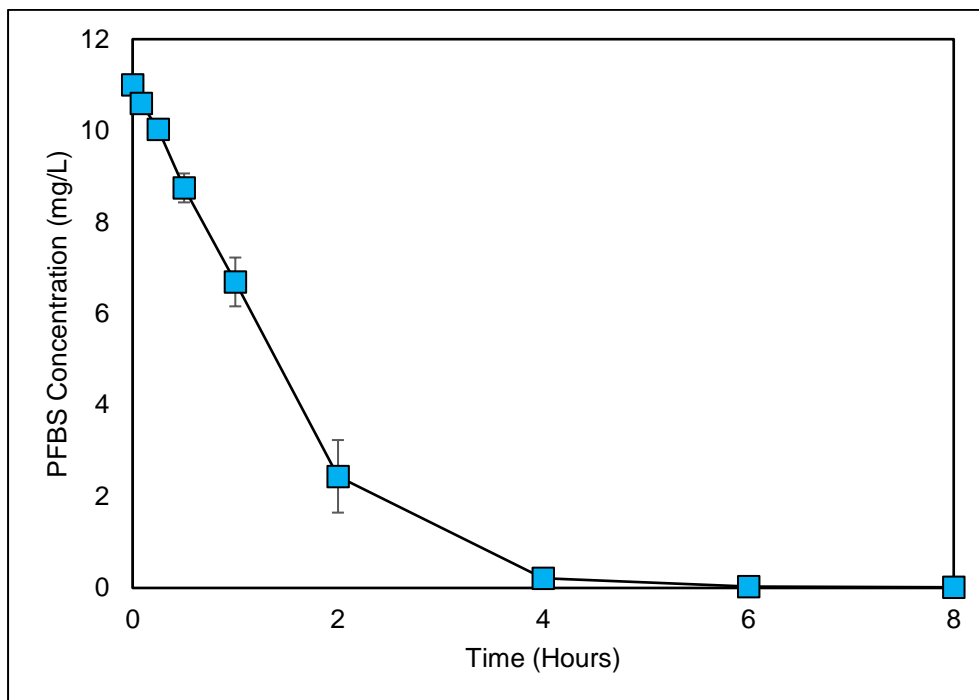
Figure A10 Degradation of 11 mg/L PFBS in a 1 liter beaker (800 mL of water) using an optimized UV/sulfite/iodide system (20 mM SO_3^{2-}, 10 mM I^-, 10 mM HCO_3^-, 150 mM OH^-, 8 hours total irradiation) and 10 mM sulfite added at 2, 4 and 6 hours (50 mM sulfite total). Error bars are the standard deviation of the beaker replicates. Some error bars are too small to be seen.
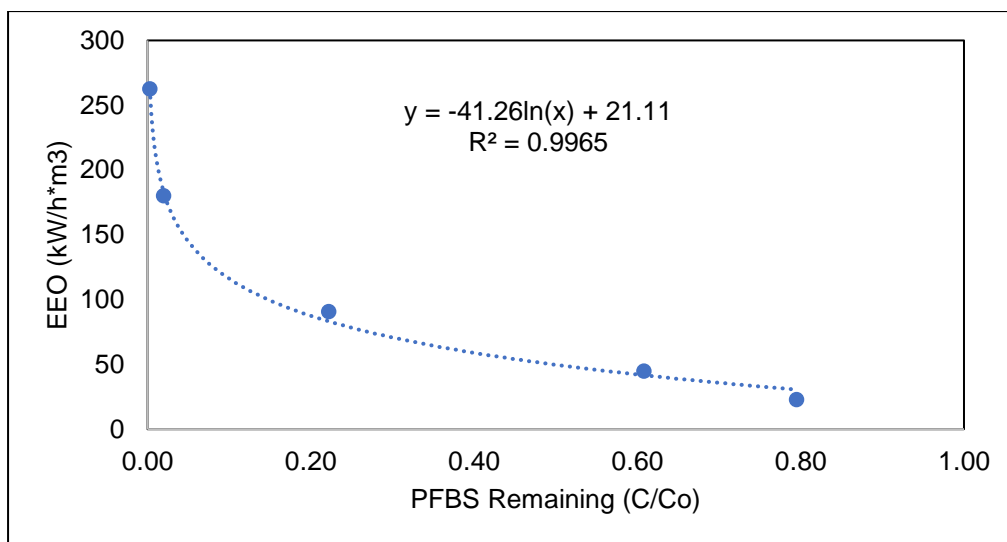
Figure A11 E_{EO} values calculated as a function of PFBS remaining in the system during 11 mg/L PFBS degradation in a 1-liter beaker (800 mL of water) using the optimized UV/sulfite/iodide system (20 mM SO_3^{2-}, 10 mM I^-, 10 mM HCO_3^-, 150 mM OH^-, 8 hours total irradiation) and 10 mM sulfite added at 2, 4 and 6 hours (50 mM sulfite total). Used to calculate the E_{EO} value at C/Co = 0.1.

Table A3 Transformation products identified following degradation of PFOS, PFOA, PFBS.

|	PFAS Compound	PFAS Group	Molecular Formula [M-H]	Measured Mass	Theoretical Mass	Delta [ppm]	Matched Isotopes	Missed Isotopes	Pattern Cov [%]	Confidence Level (Schymanski Scale)	Confidence Level (Charbonnet Scale)
Initially Present	PFBS	PFSA	C4F9SO3	298.9431	298.94299	0.37	3	2	98.68	1	1a
	PFHxS		C6F13SO3	398.9365	398.9366	-0.25	3	2	99.09	1	1a
	PFHpS		C7F15SO3	448.9331	448.93341	-0.69	5	0	100	1	1a
	PFOS		C8F17SO3	498.9295	498.93022	-1.44	5	0	99.2	1	1a
PFOS Transformation Product	PFPA	PFCA	C3F5O2	262.9761	262.97601	0.34	1	0	100	1	1a
	PFBA		C4F7O2	212.9794	212.9792	0.94	1	0	100	1	1a
	PFPeA		C5F9O2	262.976	262.97601	-0.04	1	0	100	1	1a
	PFHxA		C6F11O2	312.9729	312.97281	0.29	1	1	93.91	1	1a
	PFHpA		C7F13O2	362.9695	362.96962	-0.33	2	0	100	1	1a
	PFOA -F/+H		C8F14HO2	394.9761	394.97585	0.63	3	0	100	3	3
	PFOA		C8F15O2	412.9665	412.96643	0.17	2	1	99.44	1	1a
	PFES -F/+H	PFSA -F/+H	C2F4HSO3	180.9587	180.9588	-0.55	1	0	100	4	4
	PFPS -F/+H		C3F6HSO3	230.9557	230.95561	0.39	3	0	100	4	4
	PFBS -F/+H		C4F8HSO3	280.9524	280.95241	-0.04	6	0	99.09	3	2c
	PFBS -2F/+2H		C4F7H2SO3	262.9619	262.96184	0.23	3	1	95.26	3	3
	PFBS -3F/+3H		C4F6H3SO3	244.9713	244.97126	0.16	1	0	100	4	4
	PFBS -4F/+4H		C4F5H4SO3	226.9806	226.98068	-0.35	1	0	100	4	4
	PFBS -5F/+5H		C4F4H5SO3	208.99	208.9901	-0.48	1	0	100	4	4
	PFBS -6F/+6H		C4F3H6SO3	190.9996	190.99952	0.42	1	2	91.87	4	4
	PFPeS -F/+H		C5F10HSO3	330.949	330.94922	-0.66	5	0	100	3	2c
	PFHxS -F/+H		C6F12HSO3	380.9458	380.94603	-0.60	5	0	100	3	2c
	PFHpS -F/+H		C7F14HSO3	N/A	N/A	N/A	N/A	N/A	N/A	3	N/A
	PFOS -F/+H	PFOS -F/+H	C8F16HSO3	480.9399	480.9396	0.54	2	1	95.86	3	2c
	PFOS -2F/+2H		C8F15H2SO3	462.9494	462.9491	0.73	3	0	100	3	2c
	PFOS -3F/+3H		C8F14H3SO3	N/A	N/A	N/A	N/A	N/A	N/A	3	N/A
	PFOS -4F/+4H		C8F13H4SO3	426.9677	426.9679	-0.47	1	0	100	2	2c
	PFOS -5F/+5H		C8F12H5SO3	408.977	408.9773	-0.73	1	0	100	4	4
	PFOS -6F/+6H		C8F11H6SO3	390.9868	390.9868	0.13	1	0	100	4	4
	PFOS -7F/+7H		C8F10H7SO3	372.9961	372.9962	-0.27	1	0	100	4	4
	PFOS -8F/+8H		C8F9H8SO3	355.0056	355.0056	0.00	1	1	91.68	4	4
	PFOS -9F/+9H		C8F8H9SO3	337.0147	337.0150	-0.89	1	0	100	4	4
	PFOS -10F/+10H		C8F7H10SO3	319.0244	319.0244	0.00	1	0	100	4	4
	PFOS -11F/+11H		C8F6H11SO3	301.0337	301.0339	-0.66	1	0	100	4	4
	PFOS -12F/+12H		C8F5H12SO3	283.0434	283.0433	0.35	1	0	100	4	4
	PFOS -13F/+13H		C8F4H13SO3	265.053	265.0527	1.13	1	0	100	4	4
	PFHpS -F/+OH	PFSA -F/+OH	C7F14OHSO3	446.9379	446.93775	0.34	4	1	99.7	3	3b
	PFOS -F/+OH		C8F16OHSO3	496.9341	496.93455	-0.91	5	0	100	3	2c
	PFOS -2F/+H, OH		C8F15HOHSO3	478.9436	478.944	-0.84	3	1	99	4	4
	PFOS -2F/+OH, OH		C8F15(OH)2SO3	494.9387	494.93889	-0.38	5	0	98.85	4	4
	PFOS Alkene	PFOS Alkene	C8F15SO3	460.9336	460.93341	0.41	1	2	87.78		4
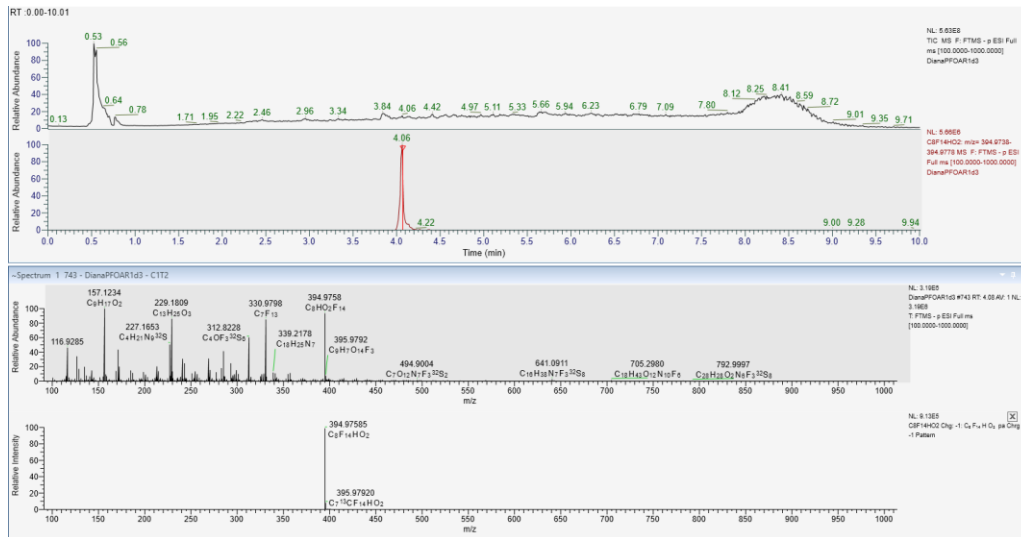
Figure A12 Chromatogram of -F/+H exchanged PFOA in negative mode (m/z 397.9758 observed, m/z 394.97585 theoretical) with C_7F_{13} fragment (m/z 330.9798).
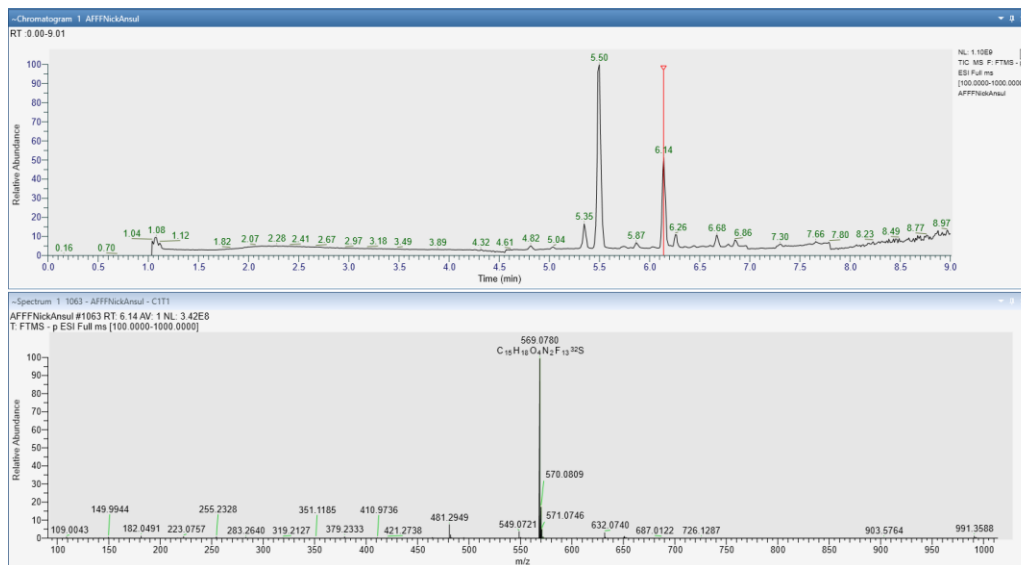
Figure A13 Chromatogram of 6:2 FtSaB in negative mode (m/z 569.0780 observed, m/z 569.0785 theoretical).
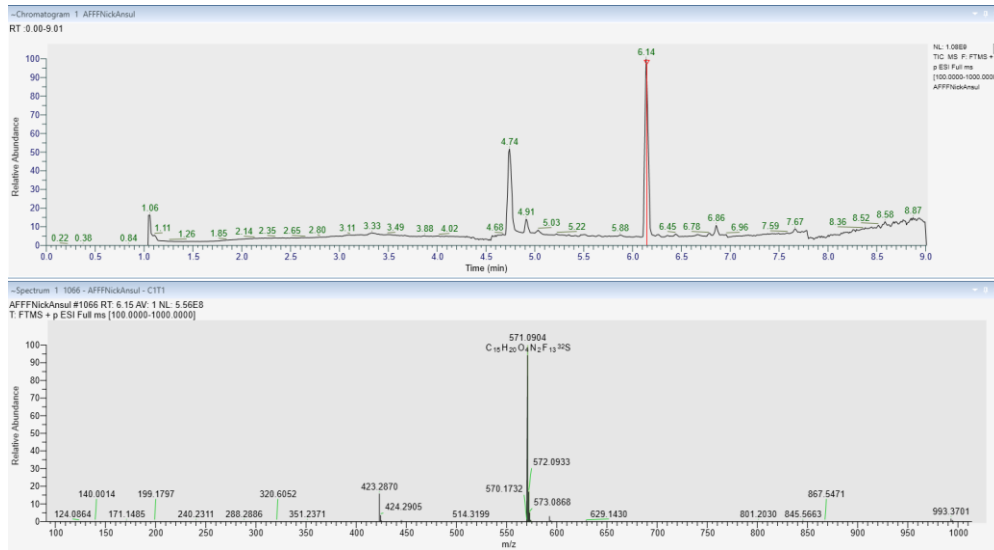
Figure A14 Chromatogram of 6:2 FtSaB in positive mode (m/z 571.0904 observed, m/z 571.0931 theoretical).
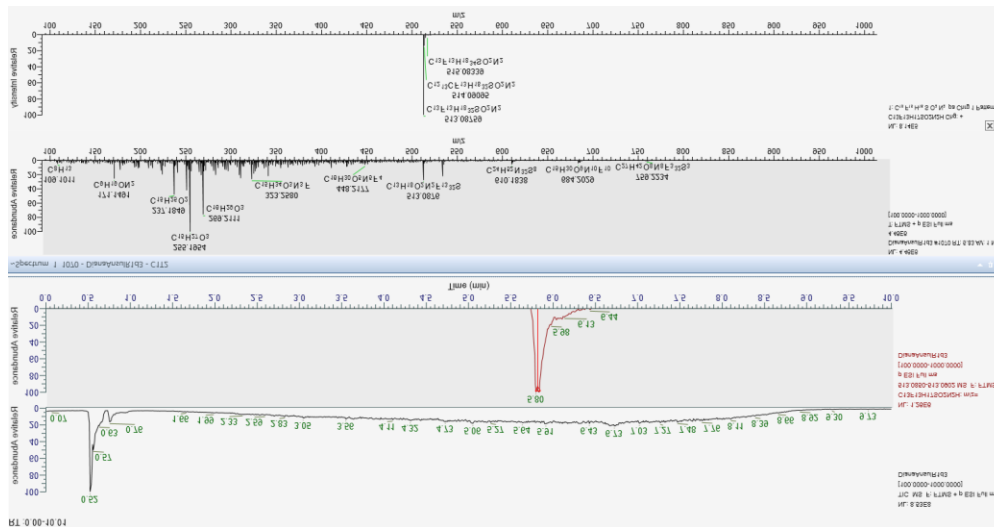
Figure A15 Chromatogram of 6:2 FtSaAm in positive mode (m/z 513.0876 observed, m/z 513.08759 theoretical).
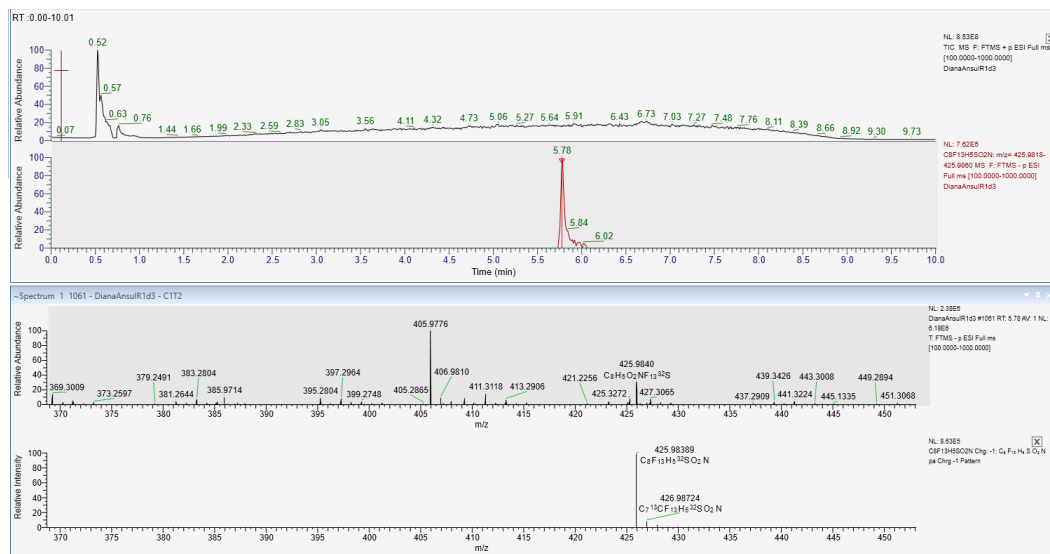
Figure A16 Chromatogram of 6:2 FtSAm in negative mode (m/z 425.9840 observed, m/z 425.98389 theoretical).
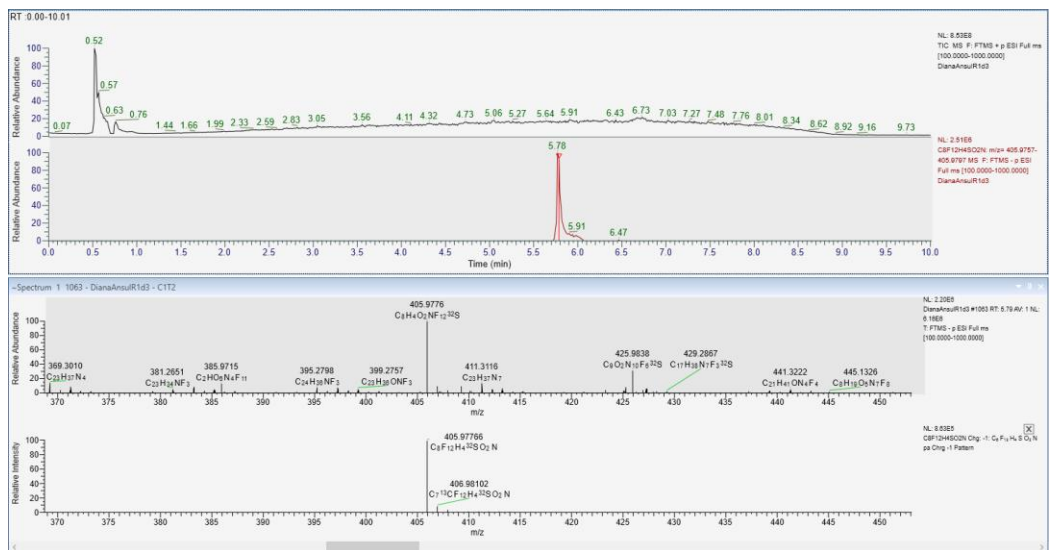
Figure A17 Chromatogram of 6:2 FtuSAm in negative mode (m/z 405.9776 observed, m/z 405.97766 theoretical).

Figure A18 -nF/+nH PFOS following degradation of PFOS in the UV/sulfite/iodide system.

Figure A19 -F/+OH PFOS following degradation of PFOS in the UV/sulfite/iodide system.

Table A4 ddMS$_2$ fragments identified from the -F/+OH PFOS transformation product.

Fragment	Mass	#1	#2	#3	#4	Common Fragments	Unique Fragments
$C_8F_{16}SO_3OH$	496.9344	X	X	X	X	All	
$C_8F_{15}SO_4$	476.9284	X	X	X	X	All	
$C_7F_{13}SO_4$	426.9317	X	X	X	X	All	
$C_8F_{16}OH$	416.9778	X	X	X	X	All	
$C_8F_{15}O$	396.9713	X	X	?			
$C_6F_{10}SO_4$	357.9362		X				2
C_7F_{13}	330.9798	X	X	X			
$C_5F_{10}SO_3$	329.9413	X					1
$C_5F_9SO_4H$	327.9457			X			3
$C_5F_9SO_3$	310.9431	X	?				1
$C_5F_8SO_4$	307.9395			X			3
C_6F_{11}	280.9829	X	X	X			
$C_4F_8SO_3H$	280.9523		X				2
$C_4F_8SO_3$	279.9446		X				2
$C_4F_7SO_4$	276.9406				X		4
$C_4F_7SO_3$	260.9462		X				2
$C_4F_6SO_4$	257.9428				X		4
C_5F_9O	246.9813	X	X	X			
C_5F_9	230.9861	X	X	X			
$C_3F_6SO_3H$	230.9555			X			3
$C_3F_6SO_3$	229.9478	X		X			
C_4F_7O	196.9844	X	X		X		
C_4F_7	180.9893	X	X	X	X	All	
C_3F_7	168.9893	X	X	X			
$C_2F_3SO_3$	160.9525				X		4
C_3F_5O	146.9875	X	X	X	X	All	
C_3F_5	130.9925	X	X	X	X	All	
$C_2F_3O_2$	112.9855			X	X		
SO_3F	98.9557	X	X	X			
C_2F_3O	96.9906	?			X		
SO_2F	82.9608	X	X	X	X	All	
SO_3	79.9573	X	X	X	X	All	

A.5 References

Banayan Esfahani, E., Mohseni, M., 2022. Fluence-based photo-reductive decomposition of PFAS us-ing vacuum UV (VUV) irradiation: Effects of key parameters and decomposition mechanism. J Environ Chem Eng 10, 107050. https://doi.org/10.1016/j.jece.2021.107050

Bentel, M.J., Liu, Z., Yu, Y., Gao, J., Men, Y., Liu, J., 2020. Enhanced Degradation of Perfluorocar-boxylic Acids (PFCAs) by UV/Sulfite Treatment: Reaction Mechanisms and System Efficiencies at pH 12. Environ Sci Technol Lett 7, 351–357. https://doi.org/10.1021/acs.estlett.0c00236

Bolton, J.R., Stefan, M.I., 2002. Fundamental photochemical approach to the concepts of fluence (UV dose) and electrical energy efficiency in photochemical degradation reactions. Research on Chemi-cal Intermediates 28, 857–870. https://doi.org/10.1163/15685670260469474

Chen, G., Liu, S., Shi, Q., Gan, J., Jin, B., Men, Y., Liu, H., 2022. Hydrogen-polarized vacuum ultravi-olet photolysis system for enhanced destruction of perfluoroalkyl substances. Journal of Hazard-ous Materials Letters 3, 100072. https://doi.org/10.1016/j.hazl.2022.100072

Fennell, B.D., Mezyk, S.P., McKay, G., 2021. Critical Review of UV-Advanced Reduction Processes for the Treatment of Chemical Contaminants in Water. ACS Environmental Au. https://doi.org/10.1021/acsenvironau.1c00042

Li, X., Liu, G., Fang, J., Yue, S., Guan, Y., Chen, L., Liu, X., 2012. Efficient Reductive Dechlorination of Monochloroacetic Acid by Sulfite/UV Process 7342.

Liu, Z., Bentel, M.J., Yu, Y., Ren, C., Gao, J., Pulikkal, V.F., Sun, M., Men, Y., Liu, J., 2021. Near-Quantitative Defluorination of Perfluorinated and Fluorotelomer Carboxylates and Sulfonates with Integrated Oxidation and Reduction. Environ Sci Technol 55, 7052–7062. https://doi.org/10.1021/acs.est.1c00353

Patch, D., O'Connor, N., Koch, I., Cresswell, T., Hughes, C., Davies, J.B., Scott, J., O'Carroll, D., We-ber, K., 2022. Elucidating degradation mechanisms for a range of per- and polyfluoroalkyl sub-stances (PFAS) via controlled irradiation studies. Science of the Total Environment 832, 154941. https://doi.org/10.1016/j.scitotenv.2022.154941

Schymanski, E.L., Jeon, J., Gulde, R., Fenner, K., Ruff, M., Singer, H.P., Hollender, J., 2014. Identify-ing small molecules via high resolution mass spectrometry: Communicating confidence. Environ Sci Technol 48, 2097–2098. https://doi.org/10.1021/es5002105

Tenorio, R., Liu, J., Xiao, X., Maizel, A., Higgins, C.P., Schaefer, C.E., Strathmann, T.J., 2020. De-struction of Per-and Polyfluoroalkyl Substances (PFASs) in Aqueous Film-Forming Foam (AFFF) with UV-Sulfite Photoreductive Treatment. Environ Sci Technol 54, 6957–6967. https://doi.org/10.1021/acs.est.0c00961

B. Appendix B

Supplemental Information

Investigating the UV/Sulfite + Iodide System to Mineralize Per and Polyfluoroalkyl Substances (PFAS) in the Presence of Complex Matrices: Implications for Treatment of AFFF Concentrates

Natalia O'Connor†, David Patch†, Michael Bentel†††, Iris Koch†, Kevin G. Mumford ††, Kela Weber†*

† Department of Chemistry and Chemical Engineering, Royal Military College of Canada, Kingston, ON, Canada K7K 7B4.

††Department of Civil Engineering, Queen's University, Kingston, ON, Canada.

†††Department

* Corresponding Author: Kela.Weber@rmc.ca

B.1 UV Irradiation – Cuvette and Beaker Systems

Investigations into the effects of methanol, isopropanol, butyl carbitol, alkalinity (pH and bicarbonate), and nitrate were performed in a cuvette reactor system described in previous work (O'Connor et al., 2023). In brief, PFAS and other reagents were sampled into 4 mL UV-transmissible cuvettes (Brandtech ®, VWR) and amended to a final concentration of 50 mM Na_2SO_3, 10 mM KI, 10 mM $NaHCO_3$ (unless otherwise stated), and 150 mM NaOH (unless otherwise stated). The cuvettes were them capped, inversion mixed, and placed 3.5 cm away from a pre-heated, 36-watt, 254 nm UV lamp (Coospider CTUV, 3 J s^{-1} L^{-1}). After irradiation, samples were amended with acetic acid to a final concentration of 1% (v/v) and prepared for either fluoride or PFAS analysis (see below).

Investigations into the degradation of dilute AFFF samples were performed in the same cuvette / UV reactor system, but were amended with 20 mM Na_2SO_3, 10 mM KI, 10 mM $NaHCO_3$, and 150 mM NaOH. Additional amendments of 10 mM Na_2SO_3 were added every two hours for the duration of the irradiation. Samples were then neutralized and prepared for analysis as previously described.

Investigation into the degradation of a high concentration PFBS solution (600 mg/L) was performed in a beaker reactor set-up. PFBS was prepared from a powder directly into the beaker and amended with 20 mM Na_2SO_3, 10 mM KI, 10 mM $NaHCO_3$, and 150 mM NaOH before being diluted to the 800 mL mark with MilliQ ® deionized water. The water level was then marked, before adding a magnetic stir bar and mixing the solution for one hour.

A 1 M solution of Na_2SO_3 was prepared in deionized water and loaded into an automated syringe pump, calibrated to deliver 10 mM of Na_2SO_3 per hour dropwise. After one hour of equilibration through mixing, the UV lamp (not on) was immersed into the beaker with an aluminum foil lid, and a second line indicating the new water level was made. Three 1mL sub-samples of the solution were then taken (t=0 concentration), after which point the UV lamp was turned on, the syringe pump started, and triplicate samples were taken at each time point for a 12 hour period. System temperature steadily increased at a rate of ~8°C per hour, before stabilizing at 52±3°C. After the 12-hour period the final volume of the system was determined (after cooling to room temperature) using a graduated cylinder and, alongside the volumes taken during sampling, used to calculate the overall system dilution (due to dropwise addition of Na_2SO_3) or concentration (due to evaporative loss of water). Overall dilution due to system volume change was found to be < 4% after 12 hours.

B.2 Alcohol Enhancement Factor on F-ISE Measurements

Initial fluoride analysis of alcohol-amended solutions identified a total free fluoride concentration higher than theoretically possible. It was hypothesized that different concentrations of isopropanol and methanol were affecting the accuracy of the ion selective electrode measurements. To evaluate this, a 1 mg/L F$^-$ solution was prepared and amended with different concentrations of either isopropanol or methanol (up to 6.25 % v/v, the highest alcohol concentration after sample preparation for F-ISE analysis).
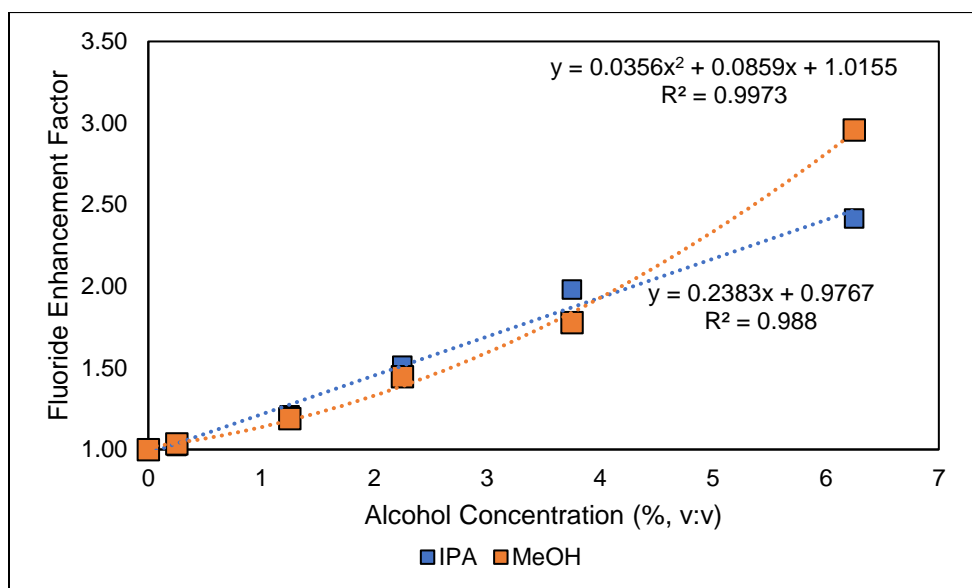
Figure B1 Fluoride enhancement factor as a function of isopropanol or methanol concentration.

Fluoride concentrations in the methanol/isopropanol interferent trials were corrected based on the above data.
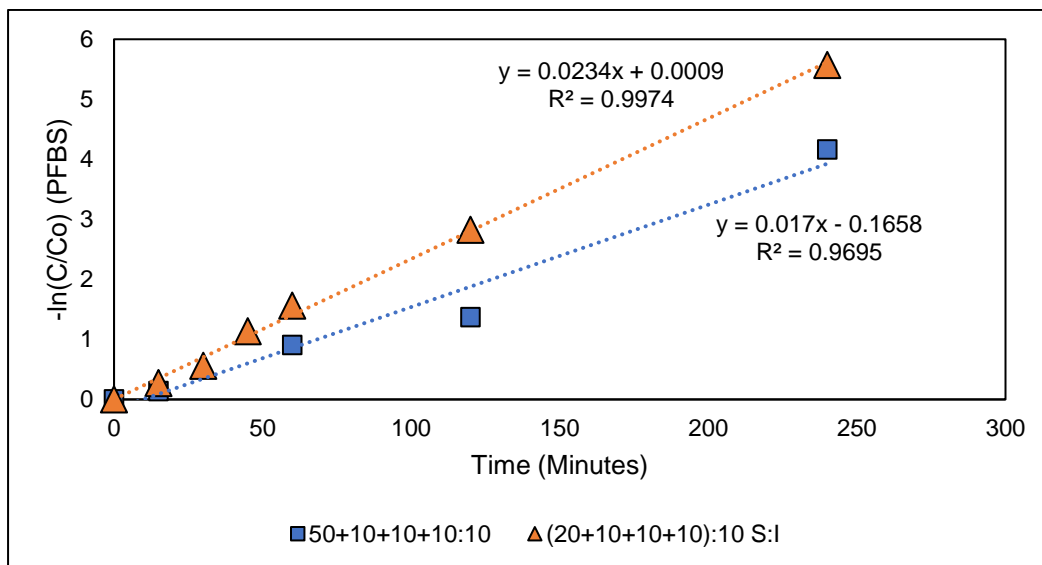
Figure B2 First order rate of PFBS degradation using the optimized (20+10+10+10):10 S: I system, compared to (50+10+10+10):10 S:I system.

B.3 Effect of NaOH Concentration on PFAS Degradation and Defluorination

Several authors have identified a general increase in PFAS degradation at higher pH in different UV-ARP systems (Bentel et al., 2020a, 2019a). However, there may exist a very specific optimum in the hydroxide concentration of the system, and by extension the system pH. To explore this, PFBS was degraded in the UV/S+I system at different concentrations of hydroxide (Figure B3).
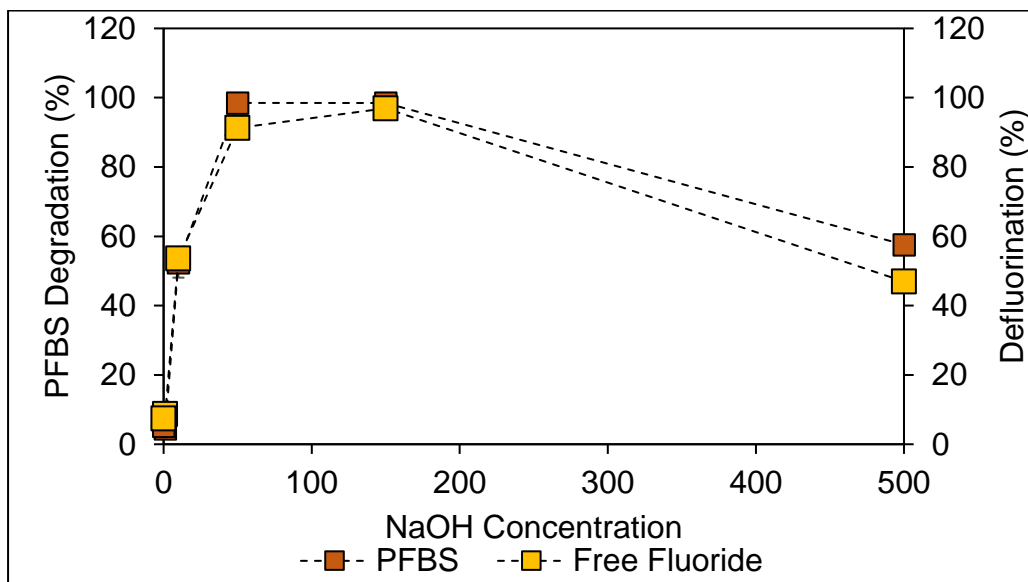
Figure B3 PFBS degradation and defluorination at different concentrations of NaOH in the UV/S+I system (50 mM Na_2SO_3, 10 mM KI, 10 mM $NaHCO_3$) for six hours. Error bars are too small to be shown.

The five concentrations of NaOH explored in this study (0, 1, 10, 50, 150, 500 mM NaOH) correspond to an initial pH of 8.2, 9.2, 11, 12.5, 13, and 13.5 respectively. Degradation and defluorination reached a maximum at 150 mM of NaOH, corresponding to >99% degradation and 97% defluorination. This aligns well with trends observed by previous authors, who identified an increase in UV-ARP effectiveness when transitioning from pH 9.2 to >12 (Bentel et al., 2020a, 2019a). This is due to removal of common aqueous electron scavengers present at neutral pHs, such as protons and protonated oxyanions/oxyanion radicals (e.g. bisulfite, bicarbonate). PFBS degradation was found to decrease at 500 mM of NaOH, with only 58% degradation observed (47% defluorination). The exact reason for this is not well understood but could be due to the enhanced ionic strength of the system interfering with aqueous electron generation/solvation.

These results identify an optimal range for hydroxide concentration of 50–150 mM, which has implications for the remediation of highly buffered natural waters or systems. The role of atmospheric deposition of CO_2 must also be considered, especially when systems are scaled up in size and interface surface area increases relative to the volume of the system. These results indicate that careful monitoring of pH is critical to ensure system effectiveness, and scaled up system designs should prioritize closed systems with minimal headspace to mitigate CO_2 deposition.

B3.1 Characterization of AFFF Formulations

Previous studies have investigated the use of UV-activated processes to destroy PFAS in several matrices, including DI water, simulated sea water, and AFFF (Bentel et al., 2020a; Z. Liu et al., 2022; O'Connor et al., 2023; Tenorio et al., 2020). The treatment of AFFF is of particular importance due to it being a source of high concentrations of PFAS, and the need to treat large stockpiles of the products as more organizations are legislated to change from C_8 AFFF to C_6 AFFF, and eventually to fluorine free foam (F_3) AFFF formulations. In this work, four AFFF compounds were initially selected for investigation, including a 3M-dominant formulation (3M), a fluorotelomer-betaine dominant formulation (FtB), a fluorotelomer sulfonamido betaine formulation (FtSaB), and a mixed 6:2 fluorotelomer formulation. The AFFF formulations were diluted and analyzed using both target analysis, a UV-activated TOP assay (Patch et al., 2024), and subjected to the UV/S+I system to identify an approximate measure of the total reducible organic fluorine in the system (Figure B4). The concentration of free fluoride in the 3M sample was found to be 58±1 µM, agreeing well with the organic fluorine determined using the UV-TOP assay (53±2 µM). The concentrations of free fluoride in the Ansul, National Foam, and Solberg AFFFs were found to be 44 µM, 24 µM, and 39 µM respectively, surpassing the UV-TOP assay derived organic fluorine concentrations by 73-84%. This suggests that, without a secondary total fluoride determination tool (such as combustion ion chromatography), achieving mass balance closure and examining overall destruction efficiency will be reliant on the total organic fluorine concentration determined by the UV/S+I system.
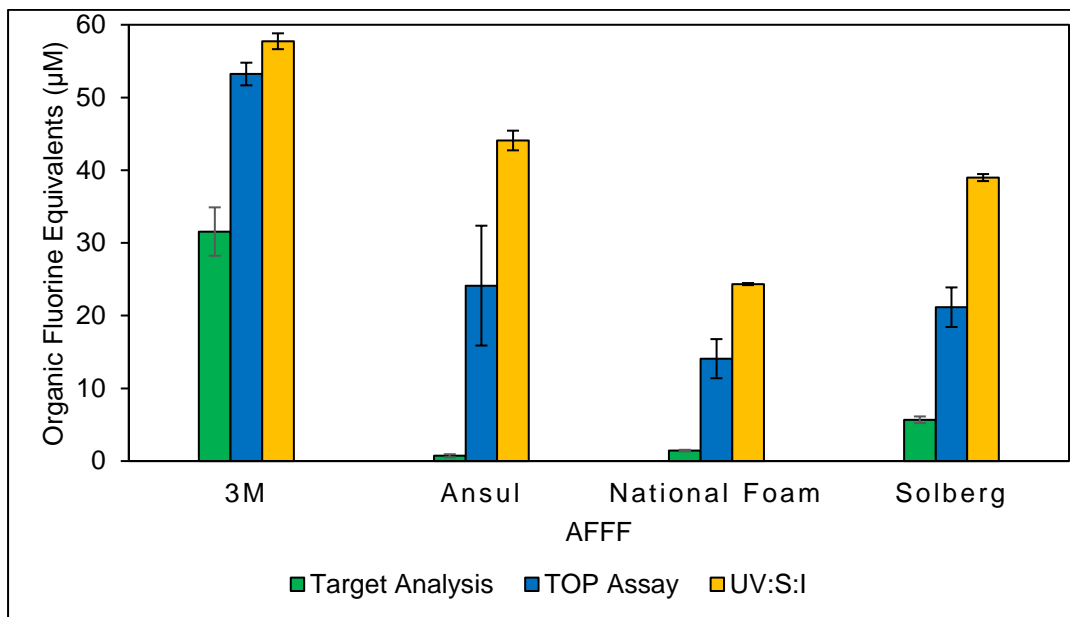
Figure B4 Concentration of PFAS represented in organic fluorine equivalents (μM of fluorine) for four AFFF formulations (10,000x dilution) following targeted analysis, application of the TOP assay, and application of the sub-optimal 50:10 UV/S+I assay.

B.4 Degradation of a Legacy AFFF Formulation

Previous work by O'Connor et al. investigated the degradation of an FtSaB-dominant AFFF foam using the unoptimized UV/S+I system (10 mM SO_3^{2-}, 10 mM I^-, 10 mM HCO_3^-, 150 mM OH^-) (O'Connor et al., 2023). This was done to identify potential transformation products resulting from applied UV-ARP treatment. In this study, two AFFF formulations (3M and Ansul) were selected for investigation, with analysis focused on the degradation of initial parent compounds, high resolution analysis of transformation products, and identification of defluorination as a function of released free fluoride (Figure B5).

Figure B5 Concentration of PFAS parent compounds (top left), rate of PFAS degradation (top right), PFAS transformation products (middle), and free fluoride (bottom) generated following the degradation of 10,000x diluted 3M using the (20+10+10+10+10):10 UV/S+I system. [PFOS] C_0 = 500 µg/L. [ΣPFSA] C_0 = 700 µg/L.

Target analysis of the diluted 3M solution identified an initial concentration of ~700 µg/L of total PFSAs, with most of that concentration being PFOS (500 µg/L). The rate of PFAS degradation was found to be inversely proportional to the PFAS chain length, with PFOS being degraded the fastest, and perfluoropropane sulfonic acid (PFPrS) being degraded the slowest. This is likely due to the higher recalcitrance of short- and ultra-short-chain PFSAs, as well as the lower initial concentration of PFPrS (11 µg/L) relative to PFOS. Both PFBS and PFPrS increased in concentration in the first 30 minutes of UV-S+I, before decreasing back to the initial concentration at 60 min and decreasing further afterwards. This is likely due to the degradation of PFBS and PFPrS-precursors (e.g. perfluorobutane sulfonamide).

Visual inspection of the chromatograms post-remediation identified several previously identified transformation products, such as -F/+H exchanged PFSAs.

125

Other previously identified transformation products were also identified, but not communicated due to low abundance. Overall, shorter-chain PFSAs (PFPeS, PFBS, PFPrS) were found to have the highest relative and longest-lived -F/+H exchanged products. Whereas both PFBS and -F/+H PFBS underwent >90% degradation by 10 hours, only 42±4% of PFPrS was degraded by the same time, further highlighting the recalcitrance of the ultra-short chain PFAS. The generation of free fluoride was found to align well with the destruction of PFOS, with the fluoride plateauing by two hours, then slowly increasing as the more recalcitrant shorter-chain PFSAs and -F/+H PFSAs were subsequently degraded. The final concentration of free fluoride after 10 h of degradation with the theoretical organic fluorine determined by the UV-TOP assay.

The results of this experiment identify that a significant amount of ECF-derived PFAS can be degraded using UV/S+I. As can be seen by the presence of PFPrS after 10 h of reduction, there are highly recalcitrant PFAS in low intensity that remain undegraded, supporting the previous suggestion that the use of a polishing treatment step after UV/S+I may be an appropriate part of a remediation strategy for highly complex matrices or highly recalcitrant PFAS.

B.5 Degradation of a Modern AFFF Formulation

The degradation of fluorotelomer betaine-dominated AFFF (Ansul) was evaluated using LC-HRMS, to allow for direct tracking of the different fluorotelomer betaine structures with respect to duration of degradation in the UV/S+I system. Based on previous studies, it was expected that the degradation of the fluorotelomer compounds would be slower than PFOS, but faster than short-chain PFSAs like PFBS and PFPrS (O'Connor et al., 2023) (Figure B6).
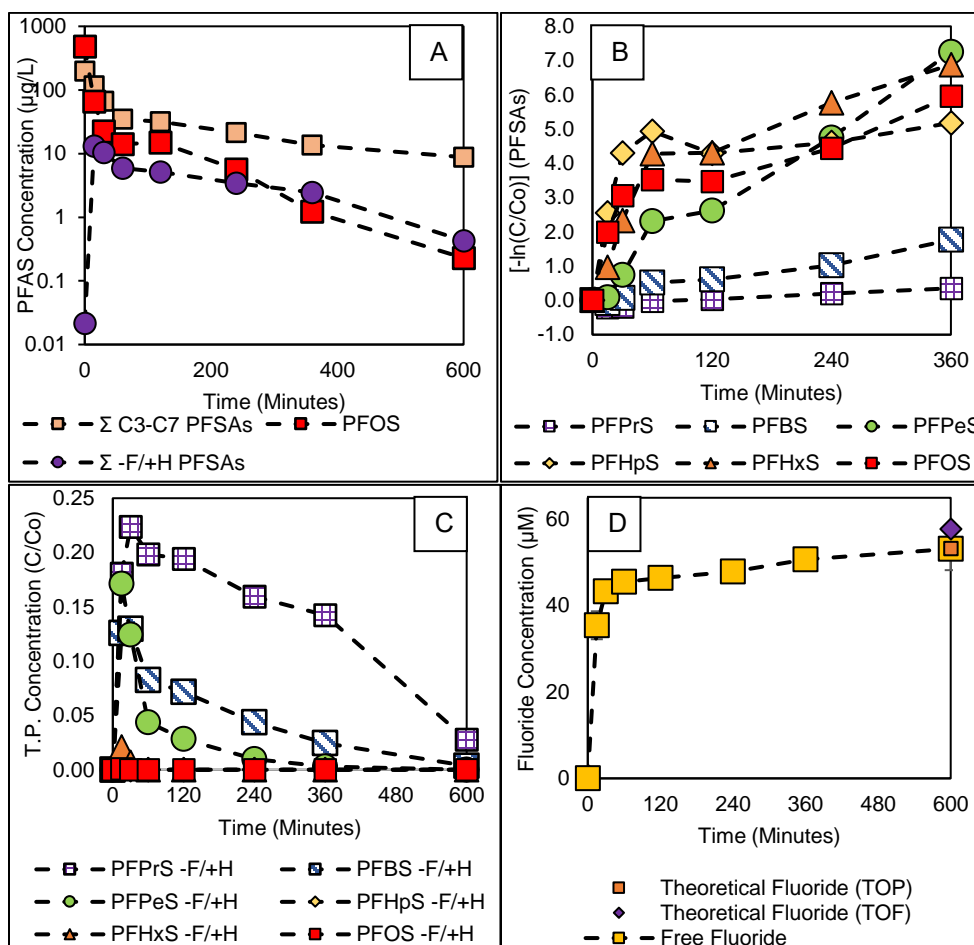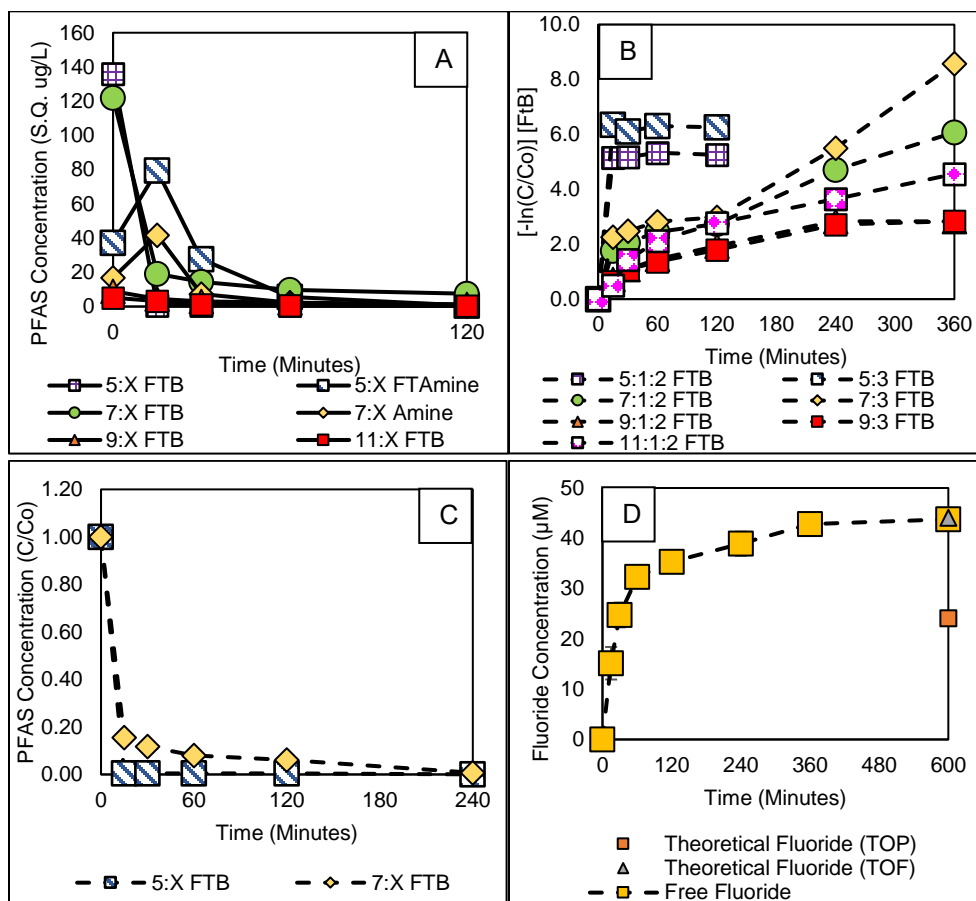

Figure B6 Concentration of PFAS parent compounds (top left), rate of PFAS degradation (top right), PFAS transformation products (bottom left), and free fluoride (bottom right) generated following the degradation of 10,000x diluted Ansul using the (20+10+10+10+10):10 UV/S+I system. [ΣFtB (Semi-Quantified)] = 250 µg/L.

Target analysis of the dilute Ansul solution identified the initial presence of 5:1:2 FtB, 7:1:2 FtB, 5:3 FtB, 7:3 FtB, 4:N FtB, 6:N FtB, 8:N FtB (N=2 or 4), 9:X FtB, and 11:X FtB (X=3, or 1:2). Before UV/S+I treatment, trace amounts of 5:X and 7:X fluorotelomer amine were also detected; these are dealkylated transformation products of fluorotelomer betaine. Application of the UV/S+I system resulted in

127

degradation of all identified FtB parent compounds. The rate of FtB degradation generally decreases with increasing chain length, which is the opposite phenomenon from that observed with the PFSAs. However, degradation of 11:1:2 FtB appears to be faster than its corresponding 9:1:2 counterpart, indicating a potential peak recalcitrance at the C_9 fluorotelomer chain length.

As identified in earlier work, a common transformation product of amine-containing fluorotelomers (e.g. FtSaB) is the resultant de-alkylated product (O'Connor et al., 2023); for FtSaB specifically, the resultant degradation product is the fluorotelomer sulfonamido amide (FtSAAm) (O'Connor et al. 2023). In the present study, it was hypothesized that the degradation of fluorotelomer betaine would yield the corresponding de-alkylated fluorotelomer amine (FtAm). High resolution mass spectrometric analysis of the time points revealed the presence of FtAm at time 0, which then increased over time (for the first 15 minutes), before subsequently being degraded to non-detectable concentrations by 4 hours. The presence of FtAm in the initial formulation may indicate either an ageing of the formulation, potentially caused by abiotic transformation, or an impurity present in the original synthesis. Unlike PFBS and the 3M AFFF formulation, there were no PFAS transformation products identified at the conclusion of UV/S+I treatment, suggesting that complete or near-complete destruction of fluorotelomer AFFF formulations is easier to achieve compared to electrochemical fluorination (ECF) derived formulations.

1. -6F/+6H PFBS, -5F/+5H PFBS
2. -7F/+7H PFBS
3. -12F/+12H PFPe-Sulfate ($C_7H_{12}F_4SO_4$)
4. -4F/+4H PFBS
5. -3F/+3H PFBS
6. -14F/+14H PFOS
7. -11F/+11H PFOS
8. -F/+H PFB-Sulfate ($C_4F_8HSO_4$)
9. -8F/+8H PFOS
10. PFB-Sulfate ($C_4F_9SO_4$)
11. -10F/+10H PFOS
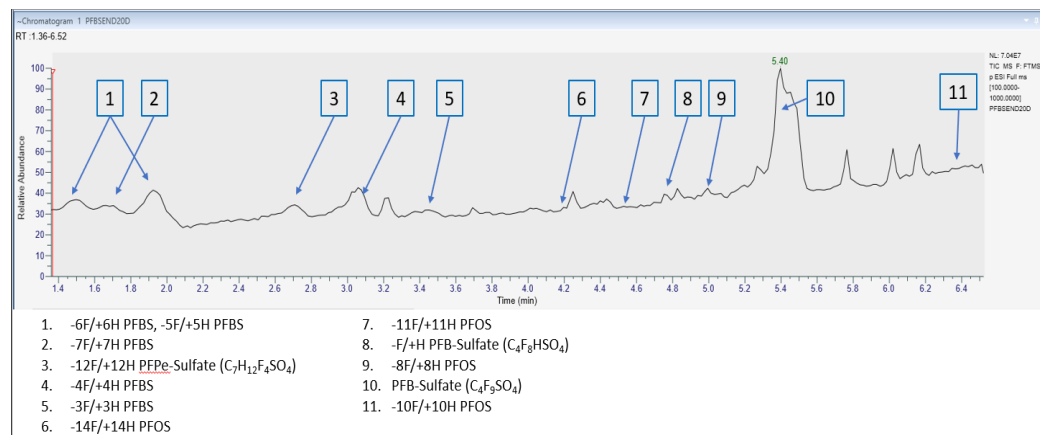
Figure B7 Identification of PFAS transformation products following destruction of PFBS (C_0=600 mg/L) in the UV/S+I system (20 mM Na_2SO_3, additional spikes of 10 mM Na_2SO_3/hour fed dripwise. 10 mM KI, 10 mM $NaHCO_3$, 150 mM NaOH).

Table B1 Identified transformation products following degradation of 600 mg/L PFBS in the UV/S+I system.

Parent Molecule	Formula (-)	Mass	Fragment 1	Fragment 2	Fragment 3
-7F/+7H PFBS	C4F2H7SO3	173.009	SO3		
-F/+H PFES	C2F4HSO3	180.9588	SO3		
-4F/+4F Unsaturated PFBS	C4F3H4SO3	188.9856	SO3H	SO3	
-6F/+6H PFBS	C4F3H6SO3	190.9996	SO3		
-5F/+5H PFBS	C4F4H5SO3	208.9902	SO3	SO3H	
-4F/+4H PFBS	C4F5H4SO3	226.9808	SO3	SO3H	C4F3H2O
-14F/+14H PFOS	C8F3H14SO3	247.0622	SO3	SO3H	
-11F/+11H PFOS	C8F6H11SO3	301.0338	SO3		
PFB-Sulfate	C4F9SO4	314.9379	C2F5O	CF3	SO3F
-11F/+5H, +2OH PFOS	C8F6H5(OH)2SO3	328.9927	SO3	SO3H	SO3F
-8F/+8H PFOS	C8F9H8SO3	355.0063	SO3	SO3H	
-6F/+4H, +2OH PFOS	C8F9H4(OH)2SO3	384.9796	SO3H	C5F7	C4F6OH
			C8F5O2	C8F7(OH)2	C8F9H2(OH)2
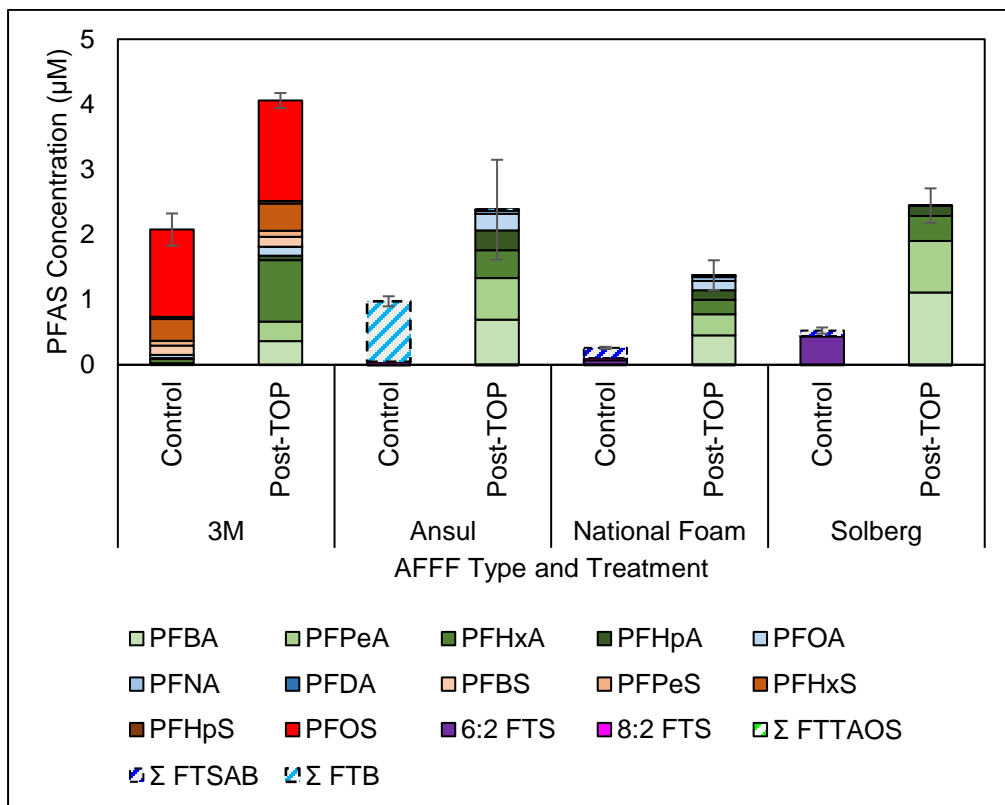
Figure B8 High resolution analysis of four AFFF samples, pre- and post-oxidation. Concentrations of FtTAoS, FtSaB, and FtB were semi-quantified using 6:2 FTS.

Generation of Oxidative Radicals in the UV/S+I System

$$SO_3^{2-} + h\nu \rightarrow \mathbf{SO_3^{-\cdot}} + e_{aq}^-$$
$$SO_3^{-\cdot} + O_2 \rightarrow \mathbf{SO_5^{-\cdot}}$$
$$SO_5^{-\cdot} + SO_3^{2-} \rightarrow \mathbf{SO_4^{-\cdot}} + SO_4^{2-}$$
$$2SO_5^{-\cdot} \rightarrow \mathbf{2SO_4^{-\cdot}} + O_2$$
$$SO_4^{-\cdot} + OH^- \rightarrow SO_4^{2-} + \mathbf{OH^\cdot}$$
$$SO_4^{-\cdot} + CO_3^{2-} \rightarrow SO_4^{2-} + \mathbf{CO_3^{-\cdot}}$$
$$OH^\cdot + CO_3^{2-} \rightarrow OH^- + \mathbf{CO_3^{-\cdot}}$$
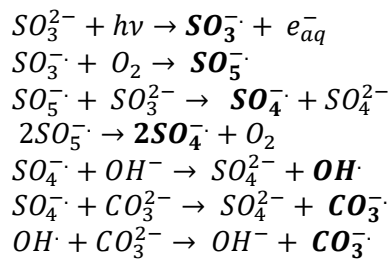
Table B2 Elementary reactions involved in the UV/S+I system.

Elementary Reaction	*Φ*	*ε (M⁻¹ cm⁻¹)*	*e⁻aq Scavenging (k)*	*E° (V)*
Primary Photosensitizers				
$SO_3^{2-} + UV \rightarrow SO_3^{\cdot-} + e^-_{aq}$	0.12	18-20	$<1.5 \times 10^6$	0.73
$I^- + H_2O + UV \rightarrow I^\cdot + e^-_{aq}$	0.17-0.29	162-220	$5.3 \times 10^{10}*$	0.35

Table B3 Elementary reactions involved in the UV/S+I system.

Eq	*Elementary Reaction*	*Bimolecular Rate Constant (k) (M⁻¹ s⁻¹)*	*Reference*
Photoinitiated Chain Autoxidation of Sulfur (IV) (Removal of O₂)			
1	$SO_3^{\cdot-} + O_2 \rightarrow SO_5^{\cdot-}$	1.5×10^9	(Li et al., 2014)
2	$SO_5^{\cdot-} + SO_5^{\cdot-} \rightarrow 2SO_4^{\cdot-} + O_2$	$10^6\text{-}10^8$	(Das, 2001)
3	$SO_5^{\cdot-} + SO_3^{2-} \rightarrow SO_4^{\cdot-} + SO_4^{2-}$	1.3×10^7	(Ross and Neta, 1982)
4	$SO_5^{\cdot-} + SO_3^{2-} \rightarrow SO_3^{\cdot-} + SO_5^{2-}$	1.3×10^7	(Deister and Warneck, 1990)

Table B4 Elementary reactions involved in the UV/S+I system.

Eq	Elementary Reaction	Bimolecular Rate Constant (k) ($M^{-1} s^{-1}$)	Reference
Generated Oxidative Species			
5	$SO_4^{-\cdot} + OH^- \rightarrow SO_4^{2-} + OH^\cdot$	6.5×10^7	(Guan et al., 2011)
6	$CO_3^{2-} + SO_4^{-\cdot} \rightarrow CO_3^{-\cdot} + SO_4^{2-}$	6.1×10^6	(Liu et al., 2016; Ross and Neta, 1982)
7	$CO_3^{2-} + OH^\cdot \rightarrow CO_3^{-\cdot} + OH^-$	3.2×10^8	(Yan et al., 2019)
8	$e^-_{aq} + H_2O \rightarrow H^\cdot + OH^-$	27	(Deister and Warneck, 1990)

Table B5 Elementary reactions involved in the UV/S+I system.

Eq	Elementary Reactions	Rate Constant ($M^{-1}s^{-1}$)	Reference
UV/Iodide			
9	$I^- + H_2O + UV \leftrightarrow I^\cdot H_2O^{-*}$		(Qu et al., 2010)
10	$I^\cdot H_2O^{-*} \rightarrow (I^\cdot, e^-_{aq}) + H_2O$		(Qu et al., 2010)
11	$(I^\cdot, e^-_{aq}) \rightarrow I^\cdot + e^-_{aq}$		(Qu et al., 2010)
12	$I^\cdot + I^- \rightarrow I_2^{-\cdot}$	1.2×10^4	(Park et al., 2011)
13	$I^\cdot + I^\cdot \rightarrow I_2$	1.0×10^{10}	(Park et al., 2011)
14	$I^\cdot + I_2^{-\cdot} \rightarrow I_3^-$	6.4×10^9	(Park et al., 2011)
15	$I_2^{-\cdot} + I_2^{-\cdot} \leftrightarrow I_3^- + I^-$	3.2×10^9	(Park et al., 2011)
16	$I^- + I_2 \rightarrow I_3^-$	7.2×10^2	(Park et al., 2011)

17	$e^-_{aq} + I_2 \rightarrow I_2^{\bullet-}$	5.3×10^{10}	(Park et al., 2011)
18	$e^-_{aq} + I_2^{\bullet-} \rightarrow 2I^-$	9.0×10^{10}	(Yu et al., 2018)
19	$e^-_{aq} + I_3^- \rightarrow I^- + I_2^{\bullet-}$	3.5×10^{10}	(Park et al., 2011)
UV/Sulfite			
20	$SO_3^{2-} + UV \rightarrow SO_3^{\bullet-} + e^-_{aq}$		(Yu et al., 2018)
21	$2SO_3^{\bullet-} \rightarrow S_2O_6^{2-}$	1.1×10^9	(Ren et al., 2021; Yu et al., 2018)
22	$2SO_3^{\bullet-} + H_2O \rightarrow SO_4^{2-} + H^+ + HSO_3^-$		(Yu et al., 2018)
UV/Sulfite/Iodide			
23	$I^{\bullet} + SO_3^{2-} \rightarrow I^- + SO_3^{\bullet-}$	1.4×10^9	(Yu et al., 2018)
24	$I^{\bullet} + HSO_3^- \rightarrow I^- + H^+ + SO_3^{\bullet-}$	6.3×10^8	(Yu et al., 2018)
25	$I_2^{\bullet-} + SO_3^{2-} \rightarrow 2I^- + SO_3^{\bullet-}$	1.9×10^8	(Yu et al., 2018)
26	$I_2^{\bullet-} + HSO_3^- \rightarrow 2I^- + H^+ + SO_3^{\bullet-}$	1.1×10^6	(Yu et al., 2018)
27	$I_3^- + SO_3^{2-} \rightarrow 2I^- + ISO_3^-$	2.9×10^8	(Yu et al., 2018)
28	$I_3^- + HSO_3^{2-} \rightarrow 2I^- + H^+ + ISO_3^-$	1.5×10^7	(Yu et al., 2018)
29	$I_2 + SO_3^{2-} \rightarrow ISO_3^- + I^-$	3.1×10^9	(Yu et al., 2018)
30	$I_2 + HSO_3^- \rightarrow ISO_3^- + I^- + H^+$	1.7×10^9	(Yu et al., 2018)
31	$ISO_3^- + H_2O \rightarrow SO_4^{2-} + I^- + 2H^+$	8.5×10^6 (s^{-1})	(Yu et al., 2018)

Table B6 Elementary reactions involved in the UV/S+I system.

Common e^-_{aq} Scavengers			
32	$e^-_{aq} + O_2 \rightarrow O_2^{\bullet-}$	1.9×10^{10}	(Park et al., 2011)
33	$e^-_{aq} + O_2^{\bullet-} \rightarrow O_2^-$		
34	$e^-_{aq} + H^+ \rightarrow H^{\bullet}$	2.3×10^{10}	(Park et al., 2011)
35	$H^{\bullet} + OH^- \rightarrow e^-_{aq} + H_2O$	2.2×10^7	(Yu et al., 2018)
36	$e^-_{aq} + NO_3^- \rightarrow NO_3^{2-\bullet} + H_2O \rightarrow NO_2^- + 2OH^-$	1.0×10^{10}	(Ren et al., 2021)
37	$e^-_{aq} + H_2CO_3 \rightarrow H^{\bullet} + HCO_3^-$	2.2×10^9	(Amador et al., 2023)
38	$e^-_{aq} + HCO_3^- \rightarrow H^{\bullet} + CO_3^{2-}$	2.2×10^6	(Amador et al., 2023)
39	$e^-_{aq} + CO_3^{2-} \rightarrow$	1.0×10^5	(Amador et al., 2023)
Common Oxidation Scavengers			
40	$OH^{\bullet} + CH_3OH$ (Methanol)	9.7×10^8	(Guan et al., 2011)
41	$SO_4^{\bullet-} + IPA \rightarrow SO_4^{2-} + Acetone + H^+$	8.5×10^7	(Deister and Warneck, 1990)

B.6 References

Abercrombie, S.A., de Perre, C., Choi, Y.J., Tornabene, B.J., Sepúlveda, M.S., Lee, L.S., Hoverman, J.T., 2019. Larval amphibians rapidly bioaccumulate poly- and perfluoroalkyl substances. Ecotoxicol Environ Saf 178, 137–145. https://doi.org/10.1016/j.ecoenv.2019.04.022

Abunada, Z., Alazaiza, M.Y.D., Bashir, M.J.K., 2020. An overview of per- and polyfluoroalkyl substances (Pfas) in the environment: Source, fate, risk and regulations. Water (Switzerland) 12, 1–28. https://doi.org/10.3390/w12123590

Abusallout, I., Wang, J., Hanigan, D., 2021a. Emerging investigator series: Rapid defluorination of 22 per- And polyfluoroalkyl substances in water using sulfite irradiated by medium-pressure UV. Environ Sci (Camb) 7, 1552–1562. https://doi.org/10.1039/d1ew00221j

Abusallout, I., Wang, J., Hanigan, D., 2021b. Emerging investigator series: rapid defluorination of 22 per- and polyfluoroalkyl substances in water using sulfite irradiated by medium-pressure UV. Environ Sci (Camb) 7, 1552–1562. https://doi.org/10.1039/d1ew00221j

Amador, C.K., Cavalli, H., Tenorio, R., Tetu, H., Higgins, C.P., Vyas, S., Strathmann, T.J., 2023. Influence of Carbonate Speciation on Hydrated Electron Treatment Processes. Environ Sci Technol 57, 7849–7857. https://doi.org/10.1021/acs.est.2c09451

Bachman, B.F., Zhu, D., Bandy, J., Zhang, L., Hamers, R.J., 2022. Detection of Aqueous Solvated Electrons Produced by Photoemission from Solids Using Transient Absorption Measurements. ACS Measurement Science Au 2, 46–56. https://doi.org/10.1021/acsmeasuresciau.1c00025

Backe, W.J., Day, T.C., Field, J.A., 2013. Zwitterionic, cationic, and anionic fluorinated chemicals in aqueous film forming foam formulations and groundwater from U.S. military bases by nonaqueous large-volume injection HPLC-MS/MS. Environ Sci Technol 47, 5226–5234. https://doi.org/10.1021/es3034999

Banayan Esfahani, E., Mohseni, M., 2022. Fluence-based photo-reductive decomposition of PFAS using vacuum UV (VUV) irradiation: Effects of key parameters and decomposition mechanism. J Environ Chem Eng 10, 107050. https://doi.org/10.1016/j.jece.2021.107050

Banzhaf, S., Filipovic, M., Lewis, J., Sparrenbom, C.J., Barthel, R., 2017. A review of contamination of surface-, ground-, and drinking water in Sweden by perfluoroalkyl and polyfluoroalkyl substances (PFASs). Ambio 46, 335–346. https://doi.org/10.1007/s13280-016-0848-8

Bao, Y., Deng, S., Jiang, X., Qu, Y., He, Y., Liu, L., Chai, Q., Mumtaz, M., Huang, J., Cagnetta, G., Yu, G., 2018. Degradation of PFOA Substitute: GenX (HFPO-DA Ammonium Salt): Oxidation with UV/Persulfate or Reduction with UV/Sulfite? Environ Sci Technol 52, 11728–11734. https://doi.org/10.1021/acs.est.8b02172

Barry, V., Winquist, A., Steenland, K., 2013. Perfluorooctanoic acid (PFOA) exposures and incident cancers among adults living near a chemical plant. Environ Health Perspect 121, 1313–1318. https://doi.org/10.1289/ehp.1306615

Barzen-Hanson, K.A., Davis, S.E., Kleber, M., Field, J.A., 2017a. Sorption of Fluorotelomer Sulfonates, Fluorotelomer Sulfonamido Betaines, and a Fluorotelomer Sulfonamido Amine in National Foam Aqueous Film-Forming Foam to Soil. Environ Sci Technol 51, 12394–12404. https://doi.org/10.1021/acs.est.7b03452

Barzen-Hanson, K.A., Roberts, S.C., Choyke, S., Oetjen, K., McAlees, A., Riddell, N., McCrindle, R., Ferguson, P.L., Higgins, C.P., Field, J.A., 2017b. Discovery of 40 Classes of Per- and Polyfluoroalkyl Substances in Historical Aqueous Film-Forming Foams (AFFFs) and AFFF-Impacted Groundwater. Environ Sci Technol. https://doi.org/10.1021/acs.est.6b05843

Battye, N.J., Patch, D.J., Roberts, D.M.D., O'Connor, N.M., Turner, L.P., Kueper, B.H., Hulley, M.E., Weber, K.P., 2022. Use of a horizontal ball mill to remediate per- and polyfluoroalkyl substances in soil. Science of The Total Environment 835, 155506. https://doi.org/https://doi.org/10.1016/j.scitotenv.2022.155506

Bentel, M.J., Liu, Z., Yu, Y., Gao, J., Men, Y., Liu, J., 2020a. Enhanced Degradation of Perfluorocarboxylic Acids (PFCAs) by UV/Sulfite Treatment: Reaction Mechanisms and System Efficiencies at pH 12. Environ Sci Technol Lett 7, 351–357. https://doi.org/10.1021/acs.estlett.0c00236

Bentel, M.J., Liu, Z., Yu, Y., Gao, J., Men, Y., Liu, J., 2020b. Enhanced Degradation of Perfluorocarboxylic Acids (PFCAs) by UV/Sulfite Treatment: Reaction Mechanisms and System Efficiencies at pH 12.

Environ Sci Technol Lett 7, 351–357.
https://doi.org/10.1021/acs.estlett.0c00236

Bentel, M.J., Yu, Y., Xu, L., Li, Z., Wong, B.M., Men, Y., Liu, J., 2019a.
Defluorination of Per- and Polyfluoroalkyl Substances (PFASs) with
Hydrated Electrons: Structural Dependence and Implications to PFAS
Remediation and Management. Environ Sci Technol 53, 3718–3728.
https://doi.org/10.1021/acs.est.8b06648

Bentel, M.J., Yu, Y., Xu, L., Li, Z., Wong, B.M., Men, Y., Liu, J., 2019b.
Defluorination of Per- and Polyfluoroalkyl Substances (PFASs) with
Hydrated Electrons: Structural Dependence and Implications to PFAS
Remediation and Management. Environ Sci Technol 53, 3718–3728.
https://doi.org/10.1021/acs.est.8b06648

Boisvert, G., Sonne, C., Rigét, F.F., Dietz, R., Letcher, R.J., 2019.
Bioaccumulation and biomagnification of perfluoroalkyl acids and
precursors in East Greenland polar bears and their ringed seal prey.
Environmental Pollution 252, 1335–1343.
https://doi.org/10.1016/j.envpol.2019.06.035

Bolan, N., Sarkar, B., Yan, Y., Li, Q., Wijesekara, H., Kannan, K., Tsang,
D.C.W., Schauerte, M., Bosch, J., Noll, H., Ok, Y.S., Scheckel, K.,
Kumpiene, J., Gobindlal, K., Kah, M., Sperry, J., Kirkham, M.B.,
Wang, H., Tsang, Y.F., Hou, D., Rinklebe, J., 2021. Remediation of
poly- and perfluoroalkyl substances (PFAS) contaminated soils – To
mobilize or to immobilize or to degrade? J Hazard Mater 401.
https://doi.org/10.1016/j.jhazmat.2020.123892

Bolton, J.R., Stefan, M.I., 2002. Fundamental photochemical approach to
the concepts of fluence (UV dose) and electrical energy efficiency in
photochemical degradation reactions. Research on Chemical
Intermediates 28, 857–870.
https://doi.org/10.1163/15685670260469474

Boschloo, G., Hagfeldt, A., 2009. Characteristics of the iodide/triiodide
redox mediator in dye-sensitized solar cells. Acc Chem Res 42, 1819–
1826. https://doi.org/10.1021/ar900138m

Brusseau, M.L., Anderson, R.H., Guo, B., 2020. PFAS concentrations in
soils: Background levels versus contaminated sites. Science of the
Total Environment 740, 140017.
https://doi.org/10.1016/j.scitotenv.2020.140017

Bruton, T.A., Sedlak, D.L., 2017. Treatment of Aqueous Film-Forming Foam by Heat-Activated Persulfate under Conditions Representative of in Situ Chemical Oxidation. Environ Sci Technol 51, 13878–13885. https://doi.org/10.1021/acs.est.7b03969

Buck, R.C., Franklin, J., Berger, U., Conder, J.M., Cousins, I.T., Voogt, P. de, Jensen, A.A., Kannan, K., Mabury, S.A., van Leeuwen, S.P.J., 2011a. Perfluoroalkyl and polyfluoroalkyl substances in the environment: Terminology, classification, and origins. Integr Environ Assess Manag 7, 513–541. https://doi.org/10.1002/ieam.258

Buck, R.C., Franklin, J., Berger, U., Conder, J.M., Cousins, I.T., Voogt, P. De, Jensen, A.A., Kannan, K., Mabury, S.A., van Leeuwen, S.P.J., 2011b. Perfluoroalkyl and polyfluoroalkyl substances in the environment: Terminology, classification, and origins. Integr Environ Assess Manag 7, 513–541. https://doi.org/10.1002/ieam.258

Buck, R.C., Korzeniowski, S.H., Laganis, E., Adamsky, F., 2021. Identification and classification of commercially relevant per- and poly-fluoroalkyl substances (PFAS). Integr Environ Assess Manag 17, 1045–1055. https://doi.org/10.1002/ieam.4450

Burgess, A.E., Davidson, J.C., 2012. A kinetic-equilibrium study of a triiodide concentration maximum formed by the persulfate-iodide reaction. J Chem Educ 89, 814–816. https://doi.org/10.1021/ed200055t

Busset, C., Mazellier, P., Sarakha, M., De Laat, J., 2007. Photochemical generation of carbonate radicals and their reactivity with phenol. J Photochem Photobiol A Chem 185, 127–132. https://doi.org/10.1016/j.jphotochem.2006.04.045

Butt, C.M., Muir, D.C.G., Mabury, S.A., 2014. Biotransformation pathways of fluorotelomer-based polyfluoroalkyl substances: A review. Environ Toxicol Chem 33, 243–267. https://doi.org/10.1002/etc.2407

Buxton, G. V., Greenstock, C.L., Helman, W.P., Ross, A.B., 1988. Critical Review of rate constants for reactions of hydrated electrons, hydrogen atoms and hydroxyl radicals ($\cdot$OH/$\cdot$O$-$ in Aqueous Solution. J Phys Chem Ref Data 17, 513–886. https://doi.org/10.1063/1.555805

Cao, Y., Qiu, W., Li, J., Jiang, J., Pang, S., 2021. Review on UV/sulfite process for water and wastewater treatments in the presence or absence of O2. Science of the Total Environment 765, 142762. https://doi.org/10.1016/j.scitotenv.2020.142762

Chen, G., Liu, S., Shi, Q., Gan, J., Jin, B., Men, Y., Liu, H., 2022. Hydrogen-polarized vacuum ultraviolet photolysis system for enhanced destruction of perfluoroalkyl substances. Journal of Hazardous Materials Letters 3, 100072. https://doi.org/10.1016/j.hazl.2022.100072

Coggan, T.L., Anumol, T., Pyke, J., Shimeta, J., Clarke, B.O., 2019. A single analytical method for the determination of 53 legacy and emerging per- and polyfluoroalkyl substances (PFAS) in aqueous matrices. Anal Bioanal Chem 411, 3507–3520. https://doi.org/10.1007/s00216-019-01829-8

Conte, L., Gambaretto, G.P., 2004. Electrochemical fluorination: State of the art and future tendences. J Fluor Chem 125, 139–144. https://doi.org/10.1016/j.jfluchem.2003.07.002

Cousins, I.T., Dewitt, J.C., Glüge, J., Goldenman, G., Herzke, D., Lohmann, R., Ng, C.A., Scheringer, M., Wang, Z., 2020. The high persistence of PFAS is sufficient for their management as a chemical class. Environ Sci Process Impacts 22, 2307–2312. https://doi.org/10.1039/d0em00355g

D'Agostino, L.A., Mabury, S.A., 2014. Identification of novel fluorinated surfactants in aqueous film forming foams and commercial surfactant concentrates. Environ Sci Technol 48, 121–129. https://doi.org/10.1021/es403729e

Das, T.N., 2001. Reactivity and role of SO5•- radical in aqueous medium chain oxidation of sulfite to sulfate and atmospheric sulfuric acid generation. Journal of Physical Chemistry A 105, 9142–9155. https://doi.org/10.1021/jp011255h

Das, T.N., Huie, R.E., Neta, P., 1999. Reduction potentials of SO3 center dot-, SO5 center dot-, and S4O6 center dot 3- radicals in aqueous solution. Journal of Physical Chemistry A 103, 3581–3588.

Deister, Ursula., Warneck, P., 1990. Photooxidation of sulfite (SO32) in aqueous solution. American Chemical Society 94, 2191–2198.

Dombrowski, P.M., Kakarla, P., Caldicott, W., Chin, Y., Sadeghi, V., Bogdan, D., Barajas-Rodriguez, F., Chiang, S.Y.D., 2018a. Technology review and evaluation of different chemical oxidation conditions on treatability of PFAS. Remediation 28, 135–150. https://doi.org/10.1002/rem.21555

Dombrowski, P.M., Kakarla, P., Caldicott, W., Chin, Y., Sadeghi, V., Bogdan, D., Barajas-Rodriguez, F., Chiang, S.Y.D., 2018b. Technology review and evaluation of different chemical oxidation conditions on treatability of PFAS. Remediation 28, 135–150. https://doi.org/10.1002/rem.21555

Duchesne, A.L., Brown, J.K., Patch, D.J., Major, D., Weber, K.P., Gerhard, J.I., 2020. Remediation of PFAS-Contaminated Soil and Granular Activated Carbon by Smoldering Combustion. Environ Sci Technol 54, 12631–12640. https://doi.org/10.1021/acs.est.0c03058

Environmental Working Group (EWG), 2019. For 50 years, polluters knew pfas chemicals were dangerous but hid risks from public 1–26.

Fennell, B.D., Fowler, D., Mezyk, S.P., McKay, G., 2023. Reactivity of Dissolved Organic Matter with the Hydrated Electron: Implications for Treatment of Chemical Contaminants in Water with Advanced Reduction Processes. Environ Sci Technol 57, 7634–7643. https://doi.org/10.1021/acs.est.3c00909

Fennell, B.D., Mezyk, S.P., McKay, G., 2021a. Critical Review of UV-Advanced Reduction Processes for the Treatment of Chemical Contaminants in Water. ACS Environmental Au. https://doi.org/10.1021/acsenvironau.1c00042

Fennell, B.D., Mezyk, S.P., McKay, G., 2021b. Critical Review of UV-Advanced Reduction Processes for the Treatment of Chemical Contaminants in Water. ACS Environmental Au. https://doi.org/10.1021/acsenvironau.1c00042

Fennell, B.D., Odorisio, A., Mckay, G., 2022. Quantifying Hydrated Electron Transformation Kinetics in UV-Advanced Reduction Processes Using the Re-,UV Method. Environ Sci Technol 56, 10329–10338. https://doi.org/10.1021/acs.est.2c02003

Glüge, J., Scheringer, M., Cousins, I.T., Dewitt, J.C., Goldenman, G., Herzke, D., Lohmann, R., Ng, C.A., Trier, X., Wang, Z., 2020. An overview of the uses of per- And polyfluoroalkyl substances (PFAS). Environ Sci Process Impacts 22, 2345–2373. https://doi.org/10.1039/d0em00291g

Gu, J., Ma, J., Jiang, J., Yang, L., Yang, J., Zhang, J., Chi, H., Song, Y., Sun, S., Tian, W.Q., 2017. Hydrated electron (eaq−) generation from

phenol/UV: Efficiency, influencing factors, and mechanism. Appl Catal B 200, 585–593. https://doi.org/10.1016/j.apcatb.2016.07.034

Guan, Y.H., Ma, J., Li, X.C., Fang, J.Y., Chen, L.W., 2011. Influence of pH on the formation of sulfate and hydroxyl radicals in the UV/Peroxymonosulfate system. Environ Sci Technol 45, 9308–9314. https://doi.org/10.1021/es2017363

Harding-Marjanovic, K.C., Houtz, E.F., Yi, S., Field, J.A., Sedlak, D.L., Alvarez-Cohen, L., 2015a. Aerobic Biotransformation of Fluorotelomer Thioether Amido Sulfonate (Lodyne) in AFFF-Amended Microcosms. Environ Sci Technol 49, 7666–7674. https://doi.org/10.1021/acs.est.5b01219

Harding-Marjanovic, K.C., Houtz, E.F., Yi, S., Field, J.A., Sedlak, D.L., Alvarez-Cohen, L., 2015b. Aerobic Biotransformation of Fluorotelomer Thioether Amido Sulfonate (Lodyne) in AFFF-Amended Microcosms. Environ Sci Technol 49, 7666–7674. https://doi.org/10.1021/acs.est.5b01219

Hori, H., Nagaoka, Y., Sano, T., Kutsuna, S., 2008. Iron-induced decomposition of perfluorohexanesulfonate in sub- and supercritical water. Chemosphere 70, 800–806. https://doi.org/10.1016/j.chemosphere.2007.07.015

Hori, H., Yamamoto, A., Hayakawa, E., Taniyasu, S., Yamashita, N., Kutsuna, S., Kiatagawa, H., Arakawa, R., 2005. Efficient decomposition of environmentally persistent perfluorocarboxylic acids by use of persulfate as a photochemical oxidant. Environ Sci Technol 39, 2383–2388. https://doi.org/10.1021/es0484754

Houtz, E.F., Higgins, C.P., Field, J.A., Sedlak, D.L., 2013. Persistence of Per fl uoroalkyl Acid Precursors in AFFF-Impacted Groundwater and Soil.

Houtz, E.F., Sedlak, D.L., 2012a. Oxidative conversion as a means of detecting precursors to perfluoroalkyl acids in urban runoff. Environ Sci Technol 46, 9342–9349. https://doi.org/10.1021/es302274g

Houtz, E.F., Sedlak, D.L., 2012b. Oxidative conversion as a means of detecting precursors to perfluoroalkyl acids in urban runoff. Environ Sci Technol 46, 9342–9349. https://doi.org/10.1021/es302274g

Houtz, E.F., Sutton, R., Park, J.S., Sedlak, M., 2016. Poly- and perfluoroalkyl substances in wastewater: Significance of unknown

precursors, manufacturing shifts, and likely AFFF impacts. Water Res 95, 142–149. https://doi.org/10.1016/j.watres.2016.02.055

Hunt, J.W., Chase, W.J., 1977. Temperature and solvent dependence of electron scavenging efficiency in polar liquids: water and alcohols. Can J Chem 55, 2080–2087. https://doi.org/10.1139/v77-289

Hutchinson, S., Rieck, T., Wu, X.L., 2020. Advanced PFAS precursor digestion methods for biosolids. Environmental Chemistry 17, 558–567. https://doi.org/10.1071/EN20008

Javed, H., Lyu, C., Sun, R., Zhang, D., Alvarez, P.J.J., 2020. Discerning the inefficacy of hydroxyl radicals during perfluorooctanoic acid degradation. Chemosphere 247. https://doi.org/10.1016/j.chemosphere.2020.125883

Jian, J.M., Guo, Y., Zeng, L., Liang-Ying, L., Lu, X., Wang, F., Zeng, E.Y., 2017. Global distribution of perfluorochemicals (PFCs) in potential human exposure source–A review. Environ Int 108, 51–62. https://doi.org/10.1016/j.envint.2017.07.024

Jortner, J., Ottolenghi, M., Stein, G., 1963. The Formation of Solvated Electrons in the Photochemistry of the Phenolate Ion in Aqueous Solutions. J Am Chem Soc 85, 2712–2715. https://doi.org/10.1021/ja00901a007

Joudan, S., Mabury, S.A., 2022. Aerobic biotransformation of a novel highly functionalized polyfluoroether-based surfactant using activated sludge from a wastewater treatment plant. Environ Sci Process Impacts 24, 62–71. https://doi.org/10.1039/d1em00358e

Kim, S.K., Kannan, K., 2007. Perfluorinated acids in air, rain, snow, surface runoff, and lakes: Relative importance of pathways to contamination of urban lakes. Environ Sci Technol 41, 8328–8334. https://doi.org/10.1021/es072107t

Kleywegt, S., Raby, M., McGill, S., Helm, P., 2020. The impact of risk management measures on the concentrations of per- and polyfluoroalkyl substances in source and treated drinking waters in Ontario, Canada. Science of the Total Environment 748, 141195. https://doi.org/10.1016/j.scitotenv.2020.141195

Kugler, A., Dong, H., Li, C., Gu, C., Schaefer, C.E., Choi, Y.J., Tran, D., Spraul, M., Higgins, C.P., 2021. Reductive defluorination of Perfluorooctanesulfonic acid (PFOS) by hydrated electrons generated

upon UV irradiation of 3-Indole-acetic-acid in 12-Aminolauric-Modified montmorillonite. Water Res 200, 117221. https://doi.org/10.1016/j.watres.2021.117221

Kwok, K.Y., Yamazaki, E., Yamashita, N., Taniyasu, S., Murphy, M.B., Horii, Y., Petrick, G., Kallerborn, R., Kannan, K., Murano, K., Lam, P.K.S., 2013. Transport of Perfluoroalkyl substances (PFAS) from an arctic glacier to downstream locations: Implications for sources. Science of the Total Environment 447, 46–55. https://doi.org/10.1016/j.scitotenv.2012.10.091

Lang, J.R., Allred, B.M.K., Field, J.A., Levis, J.W., Barlaz, M.A., 2017. National Estimate of Per- and Polyfluoroalkyl Substance (PFAS) Release to U.S. Municipal Landfill Leachate, Environmental Science and Technology. https://doi.org/10.1021/acs.est.6b05005

Lassalle, J., Gao, R., Rodi, R., Kowald, C., Feng, M., Sharma, V.K., Hoelen, T., Bireta, P., Houtz, E.F., Staack, D., Pillai, S.D., 2021. Degradation of PFOS and PFOA in soil and groundwater samples by high dose Electron Beam Technology. Radiation Physics and Chemistry 189, 109705. https://doi.org/10.1016/j.radphyschem.2021.109705

Lee, H., Deon, J., Mabury, S.A., 2010. Biodegradation of polyfluoroalkyl phosphates as a source of perfluorinated acids to the environment. Environ Sci Technol 44, 3305–3310. https://doi.org/10.1021/es9028183

Lee, H., Mabury, S.A., 2014. Global Distribution of Polyfluoroalkyl and Perfluoroalkyl Substances and their Transformation Products in Environmental Solids. Transformation Products of Emerging Contaminants in the Environment: Analysis, Processes, Occurrence, Effects and Risks 797–826. https://doi.org/10.1002/9781118339558.ch27

Lesmeister, L., Lange, F.T., Breuer, J., Biegel-Engler, A., Giese, E., Scheurer, M., 2021. Extending the knowledge about PFAS bioaccumulation factors for agricultural plants – A review. Science of the Total Environment 766, 142640. https://doi.org/10.1016/j.scitotenv.2020.142640

Li, C., Hoffman, M.Z., 1999. One-Electron Redox Potentials of Phenols in Aqueous Solution. Journal of Physical Chemistry B 103, 6653–6656. https://doi.org/10.1021/jp983819w

Li, R., Munoz, G., Liu, Y., Sauvé, S., Ghoshal, S., Liu, J., 2019. Transformation of novel polyfluoroalkyl substances (PFASs) as co-contaminants during biopile remediation of petroleum hydrocarbons. J Hazard Mater 362, 140–147. https://doi.org/10.1016/j.jhazmat.2018.09.021

Li, X., Fang, J., Liu, G., Zhang, S., Pan, B., Ma, J., 2014. Kinetics and efficiency of the hydrated electron-induced dehalogenation by the sulfite/UV process. Water Res 62, 220–228. https://doi.org/10.1016/j.watres.2014.05.051

Li, X., Liu, G., Fang, J., Yue, S., Guan, Y., Chen, L., Liu, X., 2012. Efficient Reductive Dechlorination of Monochloroacetic Acid by Sulfite/UV Process 7342.

Liu, C., Liu, J., 2016. Aerobic biotransformation of polyfluoroalkyl phosphate esters (PAPs) in soil. Environmental Pollution 212, 230–237. https://doi.org/10.1016/j.envpol.2016.01.069

Liu, J., Wang, N., Szostek, B., Buck, R.C., Panciroli, P.K., Folsom, P.W., Sulecki, L.M., Bellin, C.A., 2010. 6-2 Fluorotelomer alcohol aerobic biodegradation in soil and mixed bacterial culture. Chemosphere 78, 437–444. https://doi.org/10.1016/j.chemosphere.2009.10.044

Liu, M., Munoz, G., Vo Duy, S., Sauvé, S., Liu, J., 2022. Per- and Polyfluoroalkyl Substances in Contaminated Soil and Groundwater at Airports: A Canadian Case Study. Environ Sci Technol 56, 885–895. https://doi.org/10.1021/acs.est.1c04798

Liu, S., Junaid, M., Zhong, W., Zhu, Y., Xu, N., 2020. A sensitive method for simultaneous determination of 12 classes of per- and polyfluoroalkyl substances (PFASs) in groundwater by ultrahigh performance liquid chromatography coupled with quadrupole orbitrap high resolution mass spectrometry. Chemosphere 251, 126327. https://doi.org/10.1016/j.chemosphere.2020.126327

Liu, T., Yin, K., Liu, C., Luo, J., Crittenden, J., Zhang, W., Luo, S., He, Q., Deng, Y., Liu, H., Zhang, D., 2018. The role of reactive oxygen species and carbonate radical in oxcarbazepine degradation via UV, UV/H2O2: Kinetics, mechanisms and toxicity evaluation. Water Res 147, 204–213. https://doi.org/10.1016/j.watres.2018.10.007

Liu, Y., He, X., Duan, X., Fu, Y., Fatta-Kassinos, D., Dionysiou, D.D., 2016. Significant role of UV and carbonate radical on the degradation of

oxytetracycline in UV-AOPs: Kinetics and mechanism. Water Res 95, 195–204. https://doi.org/10.1016/j.watres.2016.03.011

Liu, Z., Bentel, M.J., Yu, Y., Ren, C., Gao, J., Pulikkal, V.F., Sun, M., Men, Y., Liu, J., 2021a. Near-Quantitative Defluorination of Perfluorinated and Fluorotelomer Carboxylates and Sulfonates with Integrated Oxidation and Reduction. Environ Sci Technol 55, 7052–7062. https://doi.org/10.1021/acs.est.1c00353

Liu, Z., Bentel, M.J., Yu, Y., Ren, C., Gao, J., Pulikkal, V.F., Sun, M., Men, Y., Liu, J., 2021b. Near-Quantitative Defluorination of Perfluorinated and Fluorotelomer Carboxylates and Sulfonates with Integrated Oxidation and Reduction. Environ Sci Technol 55, 7052–7062. https://doi.org/10.1021/acs.est.1c00353

Liu, Z., Chen, Z., Gao, J., Yu, Y., Men, Y., Gu, C., Liu, J., 2022. Accelerated Degradation of Perfluorosulfonates and Perfluorocarboxylates by UV/Sulfite + Iodide: Reaction Mechanisms and System Efficiencies. Environ Sci Technol 56, 3699–3709. https://doi.org/10.1021/acs.est.1c07608

Longpré, D., Lorusso, L., Levicki, C., Carrier, R., Cureton, P., 2020. PFOS, PFOA, LC-PFCAS, and certain other PFAS: A focus on Canadian guidelines and guidance for contaminated sites management. Environ Technol Innov 18, 100752. https://doi.org/10.1016/j.eti.2020.100752

Mahinroosta, R., Senevirathna, L., 2020. A review of the emerging treatment technologies for PFAS contaminated soils. J Environ Manage 255, 109896. https://doi.org/10.1016/j.jenvman.2019.109896

Martin, D., Munoz, G., Mejia-Avendaño, S., Duy, S.V., Yao, Y., Volchek, K., Brown, C.E., Liu, J., Sauvé, S., 2019. Zwitterionic, cationic, and anionic perfluoroalkyl and polyfluoroalkyl substances integrated into total oxidizable precursor assay of contaminated groundwater. Talanta 195, 533–542. https://doi.org/10.1016/j.talanta.2018.11.093

Masoner, J.R., Kolpin, D.W., Cozzarelli, I.M., Smalling, K.L., Bolyard, S.C., Field, J.A., Furlong, E.T., Gray, J.L., Lozinski, D., Reinhart, D., Rodowa, A., Bradley, P.M., 2020. Landfill leachate contributes per-/poly-fluoroalkyl substances (PFAS) and pharmaceuticals to municipal wastewater. Environ Sci (Camb) 6, 1300–1311. https://doi.org/10.1039/d0ew00045k

Maza, W.A., Etz, B.D., Schutt, T.C., Chaloux, B.L., Breslin, V.M., Pate, B.B., Shukla, M.K., Owrutsky, J.C., Epshteyn, A., 2022. Impact of Submicellar Aggregation on Reduction Kinetics of Perfluorooctanoate by the Hydrated Electron. Environ Sci Technol Lett 9, 226–232. https://doi.org/10.1021/acs.estlett.1c01020

Medinas, D.B., Cerchiaro, G., Trindade, D.F., Augusto, O., 2007. The carbonate radical and related oxidants derived from bicarbonate buffer. IUBMB Life 59, 255–262. https://doi.org/10.1080/15216540701230511

Merino, N., Qu, Y., Deeb, R.A., Hawley, E.L., Hoffmann, M.R., Mahendra, S., 2016. Degradation and Removal Methods for Perfluoroalkyl and Polyfluoroalkyl Substances in Water. Environ Eng Sci 33, 615–649. https://doi.org/10.1089/ees.2016.0233

Mifkovic, M., van Hoomissen, D.J., Vyas, S., 2022. Conformational distributions of helical perfluoroalkyl substances and impacts on stability. J Comput Chem 43, 1656–1661. https://doi.org/10.1002/jcc.26967

Milley, S.A., Koch, I., Fortin, P., Archer, J., Reynolds, D., Weber, K.P., 2018. Estimating the number of airports potentially contaminated with perfluoroalkyl and polyfluoroalkyl substances from aqueous film forming foam: A Canadian example. J Environ Manage 222, 122–131. https://doi.org/10.1016/j.jenvman.2018.05.028

Nabb, D.L., Szostek, B., Himmelstein, M.W., Mawn, M.P., Gargas, M.I., Sweeney, L.M., Stadler, J.C., Buck, R.C., Fasano, W.J., 2007. In vitro metabolism of 8-2 fluorotelomer alcohol: Interspecies comparisons and metabolic pathway refinement. Toxicological Sciences 100, 333–344. https://doi.org/10.1093/toxsci/kfm230

Naidu, R., Nadebaum, P., Fang, C., Cousins, I., Pennell, K., Conder, J., Newell, C.J., Longpré, D., Warner, S., Crosbie, N.D., Surapaneni, A., Bekele, D., Spiese, R., Bradshaw, T., Slee, D., Liu, Y., Qi, F., Mallavarapu, M., Duan, L., McLeod, L., Bowman, M., Richmond, B., Srivastava, P., Chadalavada, S., Umeh, A., Biswas, B., Barclay, A., Simon, J., Nathanail, P., 2020. Per- and poly-fluoroalkyl substances (PFAS): Current status and research needs. Environ Technol Innov 19. https://doi.org/10.1016/j.eti.2020.100915

Nakayama, S.F., Yoshikane, M., Onoda, Y., Nishihama, Y., Iwai-Shimada, M., Takagi, M., Kobayashi, Y., Isobe, T., 2019. Worldwide trends in

tracing poly- and perfluoroalkyl substances (PFAS) in the environment. TrAC - Trends in Analytical Chemistry 121, 115410. https://doi.org/10.1016/j.trac.2019.02.011

Nickerson, A., Rodowa, A.E., Adamson, D.T., Field, J.A., Kulkarni, P.R., Kornuc, J.J., Higgins, C.P., 2021. Spatial Trends of Anionic, Zwitterionic, and Cationic PFASs at an AFFF-Impacted Site. Environ Sci Technol 55, 313–323. https://doi.org/10.1021/acs.est.0c04473

O'Connor, N., Patch, D., Noble, D., Scott, J., Koch, I., Mumford, K.G., Weber, K., 2023. Forever no more : Complete mineralization of per - and poly fl uoroalkyl substances (PFAS) using an optimized UV / sulfite / iodide system. Science of the Total Environment 888, 164137. https://doi.org/10.1016/j.scitotenv.2023.164137

Okazaki, K., Freeman, G.R., 1978. Scavenging of electrons prior to solvation in liquid alcohols. Can J Chem 56, 2313–2323. https://doi.org/10.1139/v78-381

Okazoe, T., 2009. Overview on the history of organofluorine chemistry from the viewpoint of material industry. Proc Jpn Acad Ser B Phys Biol Sci 85, 276–289. https://doi.org/10.2183/pjab.85.276

Olsen, G.W., Mair, D.C., Lange, C.C., Harrington, L.M., Church, T.R., Goldberg, C.L., Herron, R.M., Hanna, H., Nobiletti, J.B., Rios, J.A., Reagen, W.K., Ley, C.A., 2017. Per- and polyfluoroalkyl substances (PFAS) in American Red Cross adult blood donors, 2000–2015. Environ Res 157, 87–95. https://doi.org/10.1016/j.envres.2017.05.013

Park, H., Vecitis, C.D., Cheng, J., Choi, W., Mader, B.T., Hoffmann, M.R., 2009. Reductive defluorination of aqueous perfluorinated alkyl surfactants: Effects of ionic headgroup and chain length. Journal of Physical Chemistry A 113, 690–696. https://doi.org/10.1021/jp807116q

Park, H., Vecitis, C.D., Cheng, J., Dalleska, N.F., Mader, B.T., Hoffmann, M.R., 2011. Reductive degradation of perfluoroalkyl compounds with aquated electrons generated from iodide photolysis at 254 nm. Photochemical and Photobiological Sciences 10, 1945–1953. https://doi.org/10.1039/c1pp05270e

Patch, D., O'Connor, N., Koch, I., Cresswell, T., Hughes, C., Davies, J.B., Scott, J., O'Carroll, D., Weber, K., 2022. Elucidating degradation mechanisms for a range of per- and polyfluoroalkyl substances (PFAS)

via controlled irradiation studies. Science of the Total Environment 832, 154941. https://doi.org/10.1016/j.scitotenv.2022.154941

Patch, D., O'Connor, N., Vereecken, T., Murphy, D., Munoz, G., Ross, I., Glover, C., Scott, J., Koch, I., Sauvé, S., Liu, J., Weber, K., 2024. Advancing PFAS characterization: Enhancing the total oxidizable precursor assay with improved sample processing and UV activation. Science of The Total Environment 909, 168145. https://doi.org/10.1016/j.scitotenv.2023.168145

Pickard, H.M., Criscitiello, A.S., Persaud, D., Spencer, C., Muir, D.C.G., Lehnherr, I., Sharp, M.J., de Silva, A.O., Young, C.J., 2020. Ice Core Record of Persistent Short-Chain Fluorinated Alkyl Acids: Evidence of the Impact From Global Environmental Regulations. Geophys Res Lett 47. https://doi.org/10.1029/2020GL087535

Pickard, H.M., Ruyle, B.J., Thackray, C.P., Chovancova, A., Dassuncao, C., Becanova, J., Vojta, S., Lohmann, R., Sunderland, E.M., 2022. PFAS and Precursor Bioaccumulation in Freshwater Recreational Fish: Implications for Fish Advisories. Environ Sci Technol 56, 15573–15583. https://doi.org/10.1021/acs.est.2c03734

Qu, Y., Zhang, C., Li, F., Chen, J., Zhou, Q., 2010. Photo-reductive defluorination of perfluorooctanoic acid in water. Water Res 44, 2939–2947. https://doi.org/10.1016/j.watres.2010.02.019

Rappazzo, K.M., Coffman, E., Hines, E.P., 2017. Exposure to perfluorinated alkyl substances and health outcomes in children: A systematic review of the epidemiologic literature. Int J Environ Res Public Health 14, 1–22. https://doi.org/10.3390/ijerph14070691

Remde, A., Debus, R., 1996. Biodegradability of fluorinated surfactants under aerobic and anaerobic conditions. Chemosphere 32, 1563–1574. https://doi.org/10.1016/0045-6535(96)00066-5

Ren, Z., Bergmann, U., Leiviskä, T., 2021. Reductive degradation of perfluorooctanoic acid in complex water matrices by using the UV/sulfite process. Water Res 205. https://doi.org/10.1016/j.watres.2021.117676

Ross, A.B., Neta, P., 1982. Rate Constants for Reactions of Aliphatic Carbon-Centered Radicals in Aqueous Solution. National Bureau of Standards, National Standard Reference Data Series 1027.

Ruan, T., Lin, Y., Wang, T., Jiang, G., Wang, N., 2015. Methodology for studying biotransformation of polyfluoroalkyl precursors in the environment. TrAC - Trends in Analytical Chemistry 67, 167–178. https://doi.org/10.1016/j.trac.2014.11.017

Sauer, M.C., Crowell, R.A., Shkrob, I.A., 2004. Electron photodetachment from aqueous anions. 1. Quantum yields for generation of hydrated electron by 193 and 248 nm laser photoexcitation of miscellaneous inorganic anions. Journal of Physical Chemistry A 108, 5490–5502. https://doi.org/10.1021/jp049722t

Schymanski, E.L., Jeon, J., Gulde, R., Fenner, K., Ruff, M., Singer, H.P., Hollender, J., 2014. Identifying small molecules via high resolution mass spectrometry: Communicating confidence. Environ Sci Technol 48, 2097–2098. https://doi.org/10.1021/es5002105

Shahsavari, E., Rouch, D., Khudur, L.S., Thomas, D., Aburto-Medina, A., Ball, A.S., 2021. Challenges and Current Status of the Biological Treatment of PFAS-Contaminated Soils. Front Bioeng Biotechnol 8, 1–15. https://doi.org/10.3389/fbioe.2020.602040

Sharma, S.K., Chander Sobti, R., 2012. Nitrate Removal from Ground Water: A Review.

Siciliano, A., 2015. Use of nanoscale zero-valent iron (NZVI) particles for chemical denitrification under different operating conditions. Metals (Basel) 5, 1507–1519. https://doi.org/10.3390/met5031507

Southerland, E., Birnbaum, L.S., 2023. What Limits Will the World Health Organization Recommend for PFOA and PFOS in Drinking Water? Environ Sci Technol 57, 7103–7105. https://doi.org/10.1021/acs.est.3c02260

Stoiber, T., Evans, S., Naidenko, O. V., 2020. Disposal of products and materials containing per- and polyfluoroalkyl substances (PFAS): A cyclical problem. Chemosphere 260, 127659. https://doi.org/10.1016/j.chemosphere.2020.127659

Suja, F., Pramanik, B.K., Zain, S.M., 2009. Contamination, bioaccumulation and toxic effects of perfluorinated chemicals (PFCs) in the water environment: A review paper. Water Science and Technology 60, 1533–1554. https://doi.org/10.2166/wst.2009.504

Sunderland, E.M., Hu, X.C., Dassuncao, C., Tokranov, A.K., Wagner, C.C., Allen, J.G., 2019a. A review of the pathways of human exposure to

poly- and perfluoroalkyl substances (PFASs) and present understanding of health effects. J Expo Sci Environ Epidemiol 29, 131–147. https://doi.org/10.1038/s41370-018-0094-1

Sunderland, E.M., Hu, X.C., Dassuncao, C., Tokranov, A.K., Wagner, C.C., Allen, J.G., 2019b. A review of the pathways of human exposure to poly- and perfluoroalkyl substances (PFASs) and present understanding of health effects. J Expo Sci Environ Epidemiol 29, 131–147. https://doi.org/10.1038/s41370-018-0094-1

Surya Prakash, G.K., Wang, F., 2012. Fluorine: The new kingpin of drug discovery. Chimica Oggi/Chemistry Today 30, 30–36.

Tenorio, R., Liu, J., Xiao, X., Maizel, A., Higgins, C.P., Schaefer, C.E., Strathmann, T.J., 2020. Destruction of Per-and Polyfluoroalkyl Substances (PFASs) in Aqueous Film-Forming Foam (AFFF) with UV-Sulfite Photoreductive Treatment. Environ Sci Technol 54, 6957–6967. https://doi.org/10.1021/acs.est.0c00961

Toms, L.M.L., Bräunig, J., Vijayasarathy, S., Phillips, S., Hobson, P., Aylward, L.L., Kirk, M.D., Mueller, J.F., 2019. Per- and polyfluoroalkyl substances (PFAS) in Australia: Current levels and estimated population reference values for selected compounds. Int J Hyg Environ Health 222, 387–394. https://doi.org/10.1016/j.ijheh.2019.03.004

Trojanowicz, M., Bartosiewicz, I., Bojanowska-Czajka, A., Kulisa, K., Szreder, T., Bobrowski, K., Nichipor, H., Garcia-Reyes, J.F., Nałęcz-Jawecki, G., Męczyńska-Wielgosz, S., Kisała, J., 2019a. Application of ionizing radiation in decomposition of perfluorooctanoate (PFOA) in waters. Chemical Engineering Journal 357, 698–714. https://doi.org/10.1016/j.cej.2018.09.065

Trojanowicz, M., Bartosiewicz, I., Bojanowska-Czajka, A., Kulisa, K., Szreder, T., Bobrowski, K., Nichipor, H., Garcia-Reyes, J.F., Nałęcz-Jawecki, G., Męczyńska-Wielgosz, S., Kisała, J., 2019b. Application of ionizing radiation in decomposition of perfluorooctanoate (PFOA) in waters. Chemical Engineering Journal 357, 698–714. https://doi.org/10.1016/j.cej.2018.09.065

Trojanowicz, M., Bartosiewicz, I., Bojanowska-Czajka, A., Szreder, T., Bobrowski, K., Nałęcz-Jawecki, G., Męczyńska-Wielgosz, S., Nichipor, H., 2020. Application of ionizing radiation in decomposition of perfluorooctane sulfonate (PFOS) in aqueous solutions. Chemical

Engineering Journal 379, 122303.
https://doi.org/10.1016/j.cej.2019.122303

Trojanowicz, M., Bojanowska-Czajka, A., Bartosiewicz, I., Kulisa, K., 2018. Advanced Oxidation/Reduction Processes treatment for aqueous perfluorooctanoate (PFOA) and perfluorooctanesulfonate (PFOS) – A review of recent advances. Chemical Engineering Journal 336, 170–199. https://doi.org/10.1016/j.cej.2017.10.153

Trudel, D., Horowitz, L., Wormuth, M., Scheringer, M., Cousins, I.T., Hungerbühler, K., 2008. Estimating consumer exposure to PFOS and PFOA. Risk Analysis 28, 251–269. https://doi.org/10.1111/j.1539-6924.2008.01017.x

Tseng, N.S., 2012. Feasibility of Biodegradation of Polyfluoroalkyl and Perfluoroalkyl Substances. eScholarship 23, 401–516.

Turner, L.P., Kueper, B.H., Jaansalu, K.M., Patch, D.J., Battye, N., El-Sharnouby, O., Mumford, K.G., Weber, K.P., 2021. Mechanochemical remediation of perfluorooctanesulfonic acid (PFOS) and perfluorooctanoic acid (PFOA) amended sand and aqueous film-forming foam (AFFF) impacted soil by planetary ball milling. Science of the Total Environment 765, 142722. https://doi.org/10.1016/j.scitotenv.2020.142722

Vecitis, C.D., Park, H., Cheng, J., Mader, B.T., Hoffmann, M.R., 2009. Treatment technologies for aqueous perfluorooctanesulfonate (PFOS) and perfluorooctanoate (PFOA). Frontiers of Environmental Science and Engineering in China 3, 129–151. https://doi.org/10.1007/s11783-009-0022-7

Vedagiri, U.K., Anderson, R.H., Loso, H.M., Schwach, C.M., 2018. Ambient levels of PFOS and PFOA in multiple environmental media. Remediation 28, 9–51. https://doi.org/10.1002/rem.21548

Wang, S., Yang, Q., Chen, F., Sun, J., Luo, K., Yao, F., Wang, X., Wang, D., Li, X., Zeng, G., 2017. Photocatalytic degradation of perfluorooctanoic acid and perfluorooctane sulfonate in water: A critical review. Chemical Engineering Journal 328, 927–942. https://doi.org/10.1016/j.cej.2017.07.076

Wang, Y., Yu, N., Zhu, X., Guo, H., Jiang, J., Wang, X., Shi, W., Wu, J., Yu, H., Wei, S., 2018. Suspect and Nontarget Screening of Per- and Polyfluoroalkyl Substances in Wastewater from a Fluorochemical

Manufacturing Park. Environ Sci Technol 52, 11007–11016.
https://doi.org/10.1021/acs.est.8b03030

Wang, Z., Buser, A.M., Cousins, I.T., Demattio, S., Drost, W., Johansson,
O., Ohno, K., Patlewicz, G., Richard, A.M., Walker, G.W., White, G.S.,
Leinala, E., 2021. A New OECD Definition for Per- And
Polyfluoroalkyl Substances. Environ Sci Technol 55, 15575–15578.
https://doi.org/10.1021/acs.est.1c06896

Wang, Z., Cousins, I.T., Scheringer, M., Buck, R.C., Hungerbühler, K.,
2014a. Global emission inventories for C4–C14 perfluoroalkyl
carboxylic acid (PFCA) homologues from 1951 to 2030, part II: The
remaining pieces of the puzzle. Environ Int 69, 166–176.
https://doi.org/10.1016/j.envint.2014.04.006

Wang, Z., Cousins, I.T., Scheringer, M., Buck, R.C., Hungerbühler, K.,
2014b. Global emission inventories for C4-C14perfluoroalkyl
carboxylic acid (PFCA) homologues from 1951 to 2030, Part I:
Production and emissions from quantifiable sources. Environ Int 70,
62–75. https://doi.org/10.1016/j.envint.2014.04.013

Wang, Z., Cousins, I.T., Scheringer, M., Buck, R.C., Hungerbühler, K.,
2014c. Global emission inventories for C4-C14 perfluoroalkyl
carboxylic acid (PFCA) homologues from 1951 to 2030, Part I:
Production and emissions from quantifiable sources. Environ Int 70,
62–75. https://doi.org/10.1016/j.envint.2014.04.013

Wang, Z., Jin, X., Hong, R., Wang, X., Chen, Z., Gao, G., He, H., Liu, J.,
Gu, C., 2023. New Indole Derivative Heterogeneous System for the
Synergistic Reduction and Oxidation of Various Per-/Polyfluoroalkyl
Substances: Insights into the Degradation/Defluorination Mechanism.
Environ Sci Technol. https://doi.org/10.1021/acs.est.3c05940

Weiner, B., Yeung, L.W.Y., Marchington, E.B., D'Agostino, L.A., Mabury,
S.A., 2013. Organic fluorine content in aqueous film forming foams
(AFFFs) and biodegradation of the foam component 6:2
fluorotelomermercaptoalkylamido sulfonate (6:2 FTSAS).
Environmental Chemistry 10, 486–493.
https://doi.org/10.1071/EN13128

Yan, S., Liu, Y., Lian, L., Li, R., Ma, J., Zhou, H., Song, W., 2019.
Photochemical formation of carbonate radical and its reaction with
dissolved organic matters. Water Res 161, 288–296.
https://doi.org/10.1016/j.watres.2019.06.002

Yang, L., He, L., Xue, J., Ma, Y., Xie, Z., Wu, L., Huang, M., Zhang, Z., 2020. Persulfate-based degradation of perfluorooctanoic acid (PFOA) and perfluorooctane sulfonate (PFOS) in aqueous solution: Review on influences, mechanisms and prospective. J Hazard Mater. https://doi.org/10.1016/j.jhazmat.2020.122405

Yeung, L.W.Y., Mabury, S.A., 2013. Bioconcentration of aqueous film-forming foam (AFFF) in juvenile rainbow trout (oncorhyncus mykiss). Environ Sci Technol 47, 12505–12513. https://doi.org/10.1021/es403170f

Yi, S., Harding-Marjanovic, K.C., Houtz, E.F., Gao, Y., Lawrence, J.E., Nichiporuk, R. v., Iavarone, A.T., Zhuang, W.Q., Hansen, M., Field, J.A., Sedlak, D.L., Alvarez-Cohen, L., 2018. Biotransformation of AFFF Component 6:2 Fluorotelomer Thioether Amido Sulfonate Generates 6:2 Fluorotelomer Thioether Carboxylate under Sulfate-Reducing Conditions. Environ Sci Technol Lett 5, 283–288. https://doi.org/10.1021/acs.estlett.8b00148

Yi, S., Zhu, L., Mabury, S.A., 2019. First Report on in Vivo Pharmacokinetics and Biotransformation of Chlorinated Polyfluoroalkyl Ether Sulfonates in Rainbow Trout. Environ Sci Technol. https://doi.org/10.1021/acs.est.9b05258

Yu, K., Li, X., Chen, L., Fang, J., Chen, H., Li, Q., Chi, N., Ma, J., 2018. Mechanism and efficiency of contaminant reduction by hydrated electron in the sulfite/iodide/UV process. Water Res 129, 357–364. https://doi.org/10.1016/j.watres.2017.11.030

Zacs, D., Bartkevics, V., 2016. Trace determination of perfluorooctane sulfonate and perfluorooctanoic acid in environmental samples (surface water, wastewater, biota, sediments, and sewage sludge) using liquid chromatography – Orbitrap mass spectrometry. J Chromatogr A 1473, 109–121. https://doi.org/10.1016/j.chroma.2016.10.060

Zhang, Y., Liu, J., Ghoshal, S., Moores, A., 2021. Density Functional Theory Calculations Decipher Complex Reaction Pathways of 6:2 Fluorotelomer Sulfonate to Perfluoroalkyl Carboxylates Initiated by Hydroxyl Radical. Environ Sci Technol 55, 16655–16664. https://doi.org/10.1021/acs.est.1c05549

Zhang, Y., Liu, J., Ghoshal, S., Moores, A., n.d. Density functional theory calculations decipher complex reaction pathways of 6 : 2 fluorotelomer

sulfonate to perfluoroalkyl carboxylic acids initiated by hydroxyl radical, in: American Chemical Society Conference Spring 2021.

Zhang, Z., Chen, J.J., Lyu, X.J., Yin, H., Sheng, G.P., 2014. Complete mineralization of perfluorooctanoic acid (PFOA) by γ-irradiation in aqueous solution. Sci Rep 4, 1–6. https://doi.org/10.1038/srep07418

Appendix C

Table C1 Abbreviations of PFAS according to carbon chain length and PFAS chemical group.

Group Name		Perfluorocarboxylic Acid	Perfluorosulfonic Acid	Perfluorosulfonamide	Fluorotelomer Sulfonate	Fluorotelomer Sulfonamido Betaine	Fluorotelomer Betaine	Fluorotelomer Thioether Amido Sulfonate
Abbreviation		PFCA	PFSA	PFSAm	FTS	FtSaB	FtB	FtTAoS
General Structure		$(CF_2)_{n-1}COOH$	$(CF_2)_nSO_3H$	$(CF_2)_nSO_3NH_2$	$(CF_2)_n(CH_2)_2 SO_3H$	$(CF_2)_n(CH_2)_2SO_2NHC_3H_6N(CH_3)_2COOH$	$(CF_2)_n(CFH)_x(CH_2)_yN(CH_3)_2COOH$	$(CF_2)_n(CH_2)_2S(CH_2)_2CONHC(CH_3)_2(CH_2)SO_3H$
Carbon Chain Length (n)	1		TFMS					
	2	TFA	PFES					
	3	PFPrA	PFPrS					
	4	PFBA	PFBS		4:2 FTS	4:2 FtSaB		
	5	PFPeA	PFPeS				5:3 FtB, 5:1:2 FtB	
	6	PFHxA	PFHxS	PFHxSAm	6:2 FTS	6:2 FtSaB		6:2 FtTAoS
	7	PFHpA	PFHpS	PFHpSAm			7:3, 7:1:2 FtB	
	8	PFOA	PFOS	PFOSA, FOSA	8:2 FTS	8:2 FtSaB		8:2 FtTAoS
	9	PFNA	PFNS	PFNSAm			9:3, 9:1:2 FtB	
	10	PFDA	PFDS		10:2 FTS	10:2 FtSaB		10:2 FtTAoS
	11	PFUdA	PFUdS				11:3, 11:1:2 FtB	
	12	PFDoDA	PFDoDS					